Functional integration in the cortical neuronal network of conscious and anesthetized animals

Jeannette A. Vizuete
Marquette University

FUNCTIONAL INTEGRATION IN THE CORTICAL NEURONAL NETWORK OF CONSCIOUS AND ANESTHETIZED ANIMALS

by

Jeannette A. Vizuete

A Dissertation Submitted to the Faculty of the Graduate School,
Marquette University,
in Partial Fulfillment of the Requirements for
the Degree of Doctor of Philosophy

Milwaukee, Wisconsin

December 2012

ABSTRACT
FUNCTIONAL INTEGRATION IN THE CORTICAL NEURONAL NETWORK OF CONSCIOUS AND ANESTHETIZED ANIMALS

Jeannette A. Vizuete

Marquette University, 2012

General anesthesia consists of amnesia, analgesia, areflexia and unconsciousness. How anesthetics suppress consciousness has been a mystery for more than one and a half centuries.

The overall goal of my research has been to determine the neural correlates of anesthetic-induced loss of consciousness. I hypothesized that anesthetics induce unconsciousness by interfering with the functional connectivity of neuronal networks of the brain and consequently, reducing the brain's capacity for information processing. To test this hypothesis, I performed experiments in which neuronal spiking activity was measured with chronically implanted microelectrode arrays in the visual cortex of freely-moving rats during wakefulness and at graded levels of anesthesia produced by the inhalational anesthetic agent desflurane. I then applied linear and non-parametric information-theoretic analyses to quantify the concentration-dependent effect of general anesthetics on spontaneous and visually evoked spike firing activity in rat primary visual cortex.

Results suggest that desflurane anesthesia disrupts cortical neuronal integration as measured by monosynaptic connectivity, spike burst coherence and information capacity. This research furthers our understanding of the mechanisms involved with the anesthetic-induced LOC which may facilitate in the development of better anesthetic monitoring devices and the creation of effective anesthetic agents that will be free of unwanted side effects.

ACKNOWLEDGEMENTS

Jeannette A. Vizuete

First and foremost, I'd like to thank my mentor at the Medical College of Wisconsin, Dr. Anthony Hudetz, for his time, guidance and exceptional dedication to my success. Especially for all the hours spent discussing ideas, data results, and the countless emails. Through his guidance I have learned how to be resourceful, to open my mind to new and challenging views and to effectively communicate my findings. Secondly, I'd like to thank my advisor at Marquette University, Dr. Kristina Ropella, for all her patience and encouragement throughout the years. I am eternally grateful to her for giving me the opportunity to join Marquette University and making my dreams a reality. Both my advisors have been an integral part of shaping me, as a person and as a professional. I'd also like to thank the rest of my committee members, Dr. Scott Beardsley, Dr. Ted DeYoe, Dr. Olga Imas, Dr. Michael Johnson and Dr. Andrew Tyrba for their invaluable advice and input to my research. Also, a very special thanks to Dr. Kamran Diba for his instrumental contribution to the analysis of my first published manuscript and to Dr. Gabor Juhasz for sharing the LED design and implantation techniques with us.

Next, I'd like to thank my parents Julio and Haydee for all their love and never-ending support. Their advice and encouragement has been essential in helping me overcome any obstacle and to continually push forward. They have taught me the power of hard work, determination and faith in God. They have been my inspiration and motivation to reach for the stars, to never give up, and to always believe in myself. Also, a special thanks to my brothers and sisters, Annette, Steve, Lisa and Michael for always being by my side with words of comfort, love and reassurance. Achieving this goal has only been possible because of each and every one of you in my life, thank you forever.

I would also like to thank my friends, Sivesh, Xiping, Bruce, Jimmy, Matt, Reema, and Brinda for all their help and contribution in my research. Thank you for sharing ideas, for your helpful advice, and above all your friendship. Knowing that someone can relate to all the emotions, successes and hurdles I faced in graduate school has been central to helping me rise above and succeed.

And finally, above all a special thanks to my grandparents, Angelica, Bernardo, Susana and Edilberto for coming to this country from South America with dreams of success and the willpower to achieve their goals for the prosperity of our family. They have laid the foundation and strong family support system of which has been my rock throughout the years. Many thanks to my family, friends and colleagues!

TABLE OF CONTENTS

LIST OF TABLES

LIST OF FIGURES

GLOSSARY

CCG	Cross-Correlogram
CI	Interaction Complexity
CSD	Current Source Density
E/I	Excitatory-Inhibitory
EEG	Electroencephalography
ERP	Event-Related Potential
FF	Feedforward
FB	Feedback
GABA	Gamma-Aminobutyric Acid
GLM	Generalized Linear Model
IIH	Interspike Interval Histogram
K-S	Kolmogorov-Smirnov
LED	Light Emitting Diode
LFP	Local Field Potential
LOC	Loss Of Consciousness
LORR	Loss Of Righting Reflex
M1	Motor Cortex
MAP	Maximum-A-Posteriori
ML	Maximum Likelihood
M-W	Mann-Whitney
PCA	Principal Component Analysis
PFC	Prefrontal Cortex
PowerNAP	Power Neuroshare Analysis Program
PSP	Post-Synaptic Potential
PSTH	Peri-Stimulus Time Histogram
PtA	Parietal Association Area
RM-ANOVA	Repeated Measure Analysis Of Variance
SNR	Signal-to-Noise Ratio
T-K	Tukey-Kramer
UA	Unit Activity
V1	Primary Visual Cortex
V1M	Primary Visual Monocular Cortex
V2	Secondary Visual Cortex

SYNOPSIS

The general goal of my research has been to determine the neural correlates of anesthetic-induced loss of consciousness. *I hypothesize that anesthetics induce unconsciousness by interfering with the functional connectivity of neuronal networks of the brain and consequently, reducing the brain's capacity for information processing.* To test this hypothesis, I performed experiments in which neuronal spiking activity was measured with chronically implanted microelectrode arrays in the visual cortex of freely-moving rats during wakefulness and at graded levels of anesthesia produced by the inhalational anesthetic agent desflurane.

In Aim 1, I examined how excitatory and inhibitory functional connectivities in the neuronal network were altered at various desflurane concentrations from wakefulness (0%) to unconsciousness (6%). The excitatory-inhibitory (E/I) balance of neurons has been thought to influence neural computation and information processing. Monosynaptic excitatory and inhibitory spike transmission probabilities were determined using pairwise cross-correlogram (CCG) analysis of spontaneous extracellular unit activity. Anesthesia decreased the number of active units, the number of functional connections, and the strength of excitatory connections. The ratio of excitatory and inhibitory connection probabilities (number of connections per number of active unit pairs) significantly increased at the deepest anesthesia level associated loss of consciousness. The elevated E/I balance was accounted for by an increase in excitatory connections, suggesting paradoxical anesthetic-induced hyperexcitability of active neuronal units.

In Aim 2, I investigated whether neuronal hyperexcitability developed gradually at relatively shallow levels of anesthesia. Electroencephalographic (EEG) burst-suppression is known to occur in deep anesthesia and to indicate hyperexcitability. Spike bursts, representing brief periods of increased spike firing, were identified at each anesthetic condition using a threshold value obtained from the duration-weighted interspike interval histogram (IIH). Unit

activity was continuous (unimodal IIH) during wakefulness, and was gradually transformed into bursting (bimodal IIH). Anesthesia increased the intraburst spike rate and decreased burst duration; the reverse was observed for the interburst periods. Bursting was also indicated by an increase in peak height of the spike autocorrelogram. The burst periods of various units were temporally correlated in wakefulness; this correlation was diminished during anesthesia, suggesting a gradual disruption of coordination across the neuronal network as a result of increasing hyperexcitability. Moreover, a concentration-dependent reduction of synchronized bursts across cortical depths was observed, suggesting anesthetics impede interlaminar functional interactions.

In Aim 3, I compared the effect of anesthesia on three measures of neuronal information capacity based on information entropy. In a leading theory, anesthesia is thought to suppress consciousness by blocking the brain's ability to process and integrate information. Therefore, I examined the concentration-dependent effect of desflurane on the cortical information capacity during the units' response to flash stimuli. In general, information capacity was higher for the stimulus-related response compared to spontaneous activity. Desflurane decreased the overall repertoire of coincident spike patterns (decreased integration) upon loss-of consciousness. Most, but not all, of the observed changes were accounted for by a change in spike rate.

Taken together, the results suggest that desflurane anesthesia disrupts cortical neuronal integration as measured by monosynaptic connectivity, spike burst coherence, and information capacity. The anesthetic suppression of consciousness is associated with altered functional connectivity in localized cortical areas before global effects in the brain are present. Consciousness may be ablated by altering the excitatory-inhibitory balance, reducing spike burst synchrony and functional integration. Furthermore, the anesthetic-induced unconsciousness may be associated with diminution of functional interactions across cortical depths indicating a suppression of laminar dependent local processing. Future studies investigating how anesthetics

alter functional neuronal interactions between remote cortical regions and layers should yield insight into the directional and lamina-specific cortico-cortical neuronal communication underlying large-scale information integration for sensory perception.

BACKGROUND AND SIGNIFICANCE

I. CURRENT UNDERSTANDING OF THE ANESTHETIC-INDUCED UNCONSCIOUSNESS

General anesthesia consists of amnesia, hypnosis, analgesia and areflexia. Of these, the mechanism of hypnosis, a.k.a. loss of consciousness, has been the most elusive, yet fascinating problem. How anesthetics suppress human consciousness has been a mystery since the first demonstration of ether anesthesia in 1946. Numerous studies have been dedicated to understanding specifically what happens to the working brain when anesthetics are applied and consciousness is lost. Studying neural mechanisms of general anesthesia also provides a way to better understand the neurobiological mechanisms of consciousness itself. Finding the neural mechanism of consciousness represents one of the most fundamental problems of neuroscience. Anesthetics provide us with a unique tool to investigate the neural mechanisms involved in the loss and return of consciousness in a systematic and reversible manner.

Anesthetics have numerous molecular effects, targeting various excitatory and inhibitory receptors, neurotransmitter release, voltage-gated and ion-gated ion channels (Alkire, Hudetz, & Tononi, 2008; Antkowiak & Kirschfeld, 2000; Franks, 2008). In general, the dominant effect of most anesthetics is an enhancement of gamma-aminobutyric acid (GABA-ergic) synaptic transmission, by prolonging the postsynaptic inhibitory chloride currents (Table 1). This is complemented by the anesthetics' direct suppressive effect on various excitatory amino acid receptors, therefore enhancing inhibition and suppressing excitation. These molecular effects of general anesthetics contribute to the general slowing, hypersynchronization, and eventual silencing of electrocortical activity.

Although the cellular-molecular effects of anesthetics are well known, this knowledge does not directly answer the question of how consciousness is suppressed by anesthetics. The molecular targets of anesthetics are widespread in the central nervous system and it is unclear

how anesthetic modulation of these targets leads to specific cognitive-behavioral effects, especially amnesia and unconsciousness. In other words, the molecular and systems level effects of anesthesia have not been bridged. A better understanding of the neural mechanism of anesthesia now requires a systems neuroscience approach.

A recognized difficulty in the study of the mechanism of anesthetic-induced unconsciousness is the lack of an objective measure of the state of consciousness. The presence or absence of consciousness is clinically assessed by surrogate measures, mainly behavioral and autonomic responses, such as purposeful response to verbal command or an abrupt change in heart rate. Obviously, these measures are indirect, are not anesthetic invariant and are confounded by the use of muscle relaxants and cardiovascular drugs. Another surrogate measure of the state of consciousness is the encephalogram, which under anesthesia, the measure of anesthetic depth generally undergo similar changes to those observed in slow wave sleep. There is ongoing research to validate EEG as a measure of anesthetic depth and the state of consciousness. Following the practice in both clinical anesthesia and anesthesia research, we operationally define consciousness as the patient's ability to respond to verbal and/or tactile commands. The loss of righting reflex (LORR) in rats was found to be analogous to the loss of verbal commands in humans (Franks, 2008) and is used here as an indicator of loss of consciousness. Below, I summarize current evidence and theories of anesthetic-induced unconsciousness.

A. Thalamic Switch Theory

There are several ways conscious sensation may, in principle, be abolished. Sensory stimuli may be suppressed peripherally, blocked en-route to the brain or to the cerebral cortex, or the brain may be incapacitated to receive or interpret the sensory information. Several general anesthetic agents, for example, suppress nociceptive stimuli at the level of the spinal cord (Antognini & Carstens, 1999, 2002; Antognini, Carstens, Sudo, & Sudo, 2000; Rampil & King,

1996; Rampil, Mason, & Singh, 1993). Sensory transmission may also be suppressed in the thalamus. Based on work in the somatosensory system *in vivo*, Angel (Angel, 1991) proposed that the anesthetic state may be due to thalamic block of sensory information. Moreover, isoflurane attenuates the thalamic transfer of somatosensory signals *in vitro* (Detsch, Vahle-Hinz, Kochs, Siemers, & Bromm, 1999) through hyperpolarization of neurons and shunting voltage gated Na^{2+} and Ca^{2+} currents (Ries & Puil, 1999b, 1999c). Evidence from human functional brain imaging also suggests the preferential suppression of thalamic activity, although not with all anesthetic agents (Alkire et al., 1995; Alkire, Haier, Shah, & Anderson, 1997; Alkire et al., 1999; Bonhomme et al., 2001; Fiset et al., 1999; Reinsel et al., 2000; R. A. Veselis et al., 1997). This has led to the theory of a "thalamic switch" of consciousness (Alkire, Haier, & Fallon, 2000). It is yet to be determined, however, whether the thalamus is inactivated directly or indirectly due to cortical suppression. Hentschke et al., proposed the neocortex as the primary target of general anesthetics (Hentschke, Schwarz, & Antkowiak, 2005).

B. Integration Theory

There are several reasons why a simple blockade of sensory information transfer, at the thalamus, may not suffice as an explanation of anesthetic-induced unconsciousness. First, in most studies, the thalamic block was implied almost exclusively based on studies in the somatosensory modality. Previous evidence shows that somatosensory cortical activation is depressed at relatively low levels of anesthetic concentration with preserved consciousness (Bonhomme et al., 2001; Disbrow, Buonocore, Antognini, Carstens, & Rowley, 1998; Lahti, Ferris, Li, Sotak, & King, 1999). The enhanced sensitivity of the somatosensory system may in part be due to the agents' peripheral effects. Antognini (Antognini et al., 2000) showed that isoflurane administered preferentially to the brain did not block the thalamic, reticular and cortical responses to nociceptive stimuli unless the torso and spinal cord were also anesthetized.

Second, electrophysiological, cognitive and functional imaging studies suggest that the

anesthetized brain continues to process auditory and visual information that is likely to get through the thalamus. A number of studies in animals have shown that cortical auditory and visual middle latency evoked potentials can be elicited under deep anesthesia (Imas, Ropella, Ward, Wood, & Hudetz, 2005b; Rabe, Moreno, Rigor, & Dafny, 1980; Santarelli et al., 2003). Plourde (Plourde & Boylan, 1991) showed that sufentanyl anesthesia in patients differentially blocked the long latency auditory evoked potential P3b, but not P3a, suggesting continued cortical processing at possibly diminished awareness. Furthermore, at isoflurane concentrations that produced EEG burst suppression, both auditory and visual stimuli produced cortical activation (Hartikainen et al., 1995; Makela, Hartikainen, Rorarius, & Jantti, 1996). Other anesthetic agents, for example ketamine, do not suppress the EEG or sensory evoked potentials at all (Plourde, Baribeau, & Bonhomme, 1997) and allow continued cortical information processing (Schwender, Klasing, Madler, Poppel, & Peter, 1993). Several recent studies using functional brain imaging demonstrate focal cortical activation to adequate stimuli (Alkire, Haier, Fallon, & Barker, 1996; Dueck et al., 2005; Heinke & Koelsch, 2005; Kerssens et al., 2005; Plourde et al., 2006; R. Veselis, Reinsel, Feshchenko, Beattie, & Akhurst, 2004).

Third, numerous studies revealed that at anesthetic concentrations high enough to produce unresponsiveness, patients still processed auditory information to form implicit memories (Alkire et al., 1996; Andrade, 1995, 1996; Deeprose & Andrade, 2006; Ghoneim & Block, 1997; Haas, 1998; Iselin-Chaves et al., 1998; Iselin-Chaves et al., 2005; Kiviniemi, 1994, 1997; Smith & Zapala, 1998; Van Hooff et al., 1995). If meaningful (semantic) information can be encoded in the cerebral cortex of an anesthetized patient, then this information presumably must have passed through the thalamus to the cerebral cortex. Moreover, implicit emotional learning may not need cortical mediation (Phelps & LeDoux, 2005) compared to semantic memory in humans as demonstrated by implicit memory tests even when free recall of intraoperative events is absent.

Taken together, the investigations so far suggest that a subcortical blockade of

information transfer is inconsistent with cortical information processing under anesthesia and lead us to an alternative theory: a cortical integrative hypothesis of unconsciousness.

C. Synchronization

Specialized areas in the cerebral cortex are thought to differentially process sensory information. The specialized areas then integrate to form coherent, unified representations of the external world that are consciously perceived. Evidence has shown that selective synchronization of distributed cortical neuronal activity contributes to visual perception (A. Engel, Konig, Kreiter, & Singer, 1991; A. K. Engel, Konig, Gray, & Singer, 1990; Gray, 1999). Synchronized activity among cortical neurons is thought to be important for cognitive functions like perception, memory, language, or consciousness (A. K. Engel, Fries, Konig, Brecht, & Singer, 1999b; A. K. Engel & Singer, 2001; Melloni et al., 2007).

Bursts are defined as brief periods of highly synchronized firing activity, followed by prolonged silence. Bursts have been observed in high anesthetic levels (Amzica, 2009; Hudetz & Imas, 2007) and associated with slow-wave sleep (Steriade & Timofeev, 2003). While most studies indicate that bursting inhibits information transmission (Brown, Lydic, & Schiff, 2010), others suggest that bursts may carry information (Sherman, 2001). Within localized areas, Erchova et al. showed that anesthetics alter synchronization of bursts at light to deep surgical levels (Erchova, Lebedev, & Diamond, 2002). Thus, anesthetics may impair cognition and consciousness by interfering with the temporal relationships among cells, suppressing synchronization and information processing.

D. Excitatory-inhibitory (E/I) balance

The balance between excitation and inhibition in local networks is considered to be of significant importance for neural computation, cognitive function and regulation of global firing activity (Bartho et al., 2004; Buzsaki, 2007; Buzsaki, Kaila, & Raichle, 2007). It has been suggested that information capacity and transmission are maximized at an intermediate E/I

balance (Shew, Yang, Yu, Roy, & Plenz, 2011). Deviation from this balance, specifically elevated E/I, leads to information processing deficits and has been observed in psychiatric diseases such as schizophrenia and autism (Yizhar et al., 2011) and suppressed memory recall and retrieval (Wang & Zochowski, 2012). Elevated E/I balance may be due to either increased excitation or decreased inhibition. The breakdown of effective connectivity observed during slow wave sleep was also found to be associated with a shift in the balance between synaptic excitation and inhibition toward inhibition, determined by increased GABA release (Esser, Hill, & Tononi, 2009; Ferrarelli et al., 2010). Lower doses of anesthetics were associated with a tilt in the balance of E/I towards excitation, whereas the reverse was observed in higher doses (Populin, 2005). EEG burst suppression commonly observed in deep anesthesia is generally associated with hyperexcitability of cells through reduced inhibition and may also contribute to the alteration of the E/I balance (Amzica, 2009). Hence, anesthetics may work by altering the balance between excitation and inhibition.

E. Subcortical Targets of Anesthetics

Other studies have shown that unconsciousness may also be produced by the inactivation of various subcortical structures. Microinjection of carbachol into the medial pontine reticular formation of rats produced an anesthesia-like state (Bonhomme et al., 2001). Microinjection of pentobarbital into the mesopontine tegmentum produced antinocicpetion, atonia and loss of righting reflex (Devor & Zalkind, 2001). Moreover, inactivation of the medial septum or the hippocampus by local injection of a $GABA_A$ receptor agonist, muscimol, in freely behaving rats decreased the dose of halothane and isoflurane needed to ablate the righting reflex and response to tail pinch (Ma, Shen, Stewart, Herrick, & Leung, 2002). Dose-dependent sedation in rats can also be achieved by microinjection of muscimol into the tuberomamillary nucleus (Nelson et al., 2002). Reverse effects of anesthetics by microinjection of norepinephrine into the Nucleus Basalis of Meynert were observed in rats with desflurane (Pillay, Vizuete, McCallum, & Hudetz,

2011). Furthermore, focal injuries to specific paramedian structures of the brainstem and thalamic intralaminar nuclei lead to immediate and permanent loss of consciousness (Laureys, 2005; Schiff et al., 2002) but this has not been shown with anesthetic agents. These studies confirm that numerous subcortical regions are necessary to enable consciousness but they do not explain the mechanism of anesthetic-induced unconsciousness when the agents are applied systemically.

II. Extracellular Neuronal Activity

Evidence suggests a direct link between neuronal firing patterns and network oscillations observed in electrophysiological recordings (Buzsaki, 2006; Deco, Jirsa, & McIntosh, 2011). Functional interactions among various neuronal cell groups in localized areas are thought to be responsible for information processing and modulation of global activity. To investigate this complex process, the microelectrode array has been increasingly applied in neuroscience research to understand localized functional properties of neuronal networks. Microelectrode arrays have the ability to simultaneously record extracellular neuronal activity, also known as spikes, and local field potentials (LFP) within small neuronal populations. Furthermore, numerous variations to the design of the neural probes can be customized to record from various horizontal and vertical depths. The signals acquired from the electrodes reflect the input-output system dynamics in the cerebral cortex.

The action potential or spike response from a neuron is recorded from a microelectrode pin positioned near the extracellular space of its cell membrane. This signal emerges from movement of ions along their electrochemical gradient as a result of ion channel openings. The opening of these ion channels causes the membrane resistance to lower therefore permitting ions to flow inward or outward across the membrane and thus resulting in a small voltage that can be recorded with microelectrode tips. The voltage produced by the ion exchange process produces a

very characteristic action potential waveform appearing as a short, large-amplitude event for a duration of about one millisecond (Buzsaki, 2006).

Since however, the voltage is small and the signal rapidly decreases with an increase in spatial distance, the electrode must be positioned relatively close to the neuron to maintain a high signal-to-noise ratio (SNR) (Bartho et al., 2004). Spike signals, however, may come from the soma and dendrites of the same neuron and therefore it is possible for each electrode pin to record from several neurons at once; ~1000 neurons in the rat cortex within a 140 μm radius can essentially be recorded via a microelectrode array (Buzsaki, 2004). Movement from the animal, electrical noise and high electrode impedance contribute to artifacts commonly observed in the neuronal signal (Csicsvari et al., 2003). As such, post-processing methods such as spike sorting are necessary to identify single units and reduce artifacts and noise (Brown, Kass, & Mitra, 2004; Lewicki, 1998).

Although very useful, the damaging process caused by invasive insertion of the electrode into the brain leads to inflammation which in return causes astrocytes and microglia to proliferate and form a glial scar which encapsulates the implant (Seymour & Kipke, 2007; Winslow, Christensen, Yang, Solzbacher, & Tresco, 2010), hence degrading neuronal recording over time. Various types of microelectrodes are now available in adjustable sizes, substrates, spacing, length and geometries, each having certain advantages over the other. The functional relationship of cells at various cortical layers as well as intercortically can now be investigated while minimizing the amount of cortical tissue injury.

III. ELECTROPHYSIOLOGICAL STUDIES OF CONSCIOUSNESS

Sensory information processing is believed to involve bi-directional recurrent communication among neurons within a cortical network and is suggested to play a key role for conscious perception. Feedforward (FF) connections are associated with low-level processing of the stimulus, whereas feedback (FB) connections contribute to higher level processing required

for conscious awareness (Lamme, Zipser, & Spekreijse, 2002). The temporal components of a visual evoked response observed in electrophysiological studies such as electroencephalography (EEG), evoked local-field potentials and induced spike responses are thought to reflect these bidirectional processes.

Peri-stimulus time histograms (PSTHs) of stimulus-induced neuronal activity in the visual cortex revealed various temporal components in which a series of sharp peaks of high firing rate were followed by silent intervals of suppressed spiking activity (Hudetz, Vizuete, & Imas, 2009). Berry et al. showed similar results with rabbit retinal ganglion cell responses to repeated stimuli (Berry, Warland, & Meister, 1997). These studies demonstrate that the response to a visual stimulus is characterized by several bursts of increased firing.

Other studies described a relationship between the positive peaks detected in stimulus-induced electrophysiological data and bi-directional information processing. In a masked paradigm human study, Del Cul et al. demonstrated that a mask stimulus presented at a delay time of less than 50 ms after the initial stimulus reduced visibility and conscious perception of the first stimulus (Del Cul, Baillet, & Dehaene, 2007). Furthermore, the initial event-related potential (ERP) response (<250 ms) correlated with increased activity in the occipital-temporal pathway and was insensitive to decreasing masked delay times, whereas activation in the fronto-parieto-temporal network correlated with the secondary ERP peak (>270 ms) and conscious perception of the stimuli. Significant suppression of the secondary peak was observed when masking delay times decreased to less than 50 ms (Del Cul et al., 2007). The same results were observed with EEG recordings of macaque monkeys using a mask paradigm (Fahrenfort, Klooster, Sjoerdsma, & Kamermans, 2005) and indicate that conscious information processing may involve two linked but differentially affected components.

A. Anesthetics and cortical neuronal activity

Few studies have been devoted to the concentration-dependent effect of volatile anesthetics on visual cortical neuronal responses. Ikeda and Wright (Ikeda & Wright, 1974a) found that halothane increased from 0.2 to 2.2 % reduced the sensitivity of cat striate cortex neurons to stimulus orientation, spatial frequency and contrast. Halothane suppressed the sustained component of firing more than the initial component. Tigwell and Sauter (Tigwell & Sauter, 1992) found reliable neuron responses in monkey striate cortex at isoflurane concentrations 0.5 to 0.9 %. Villeneuve and Casanova (M. Y. Villeneuve & Casanova, 2003) found that isoflurane produced greater suppression of neuronal response to stimuli than halothane at 0.4 to 1.4 equi-MAC concentrations but neither anesthetic influenced orientation and direction sensitivity and receptive field organization.

Recently we found a preferential suppression of the late component or secondary peak after ~150 ms in spike activity during administration of desflurane around the LORR in the rat (Hudetz et al., 2009). The late or sustained response component has been thought to be generated at least in part by feedback pathways from hierarchically higher to lower level cortex. Also, Forget et al., (Forget, Buiatti, & Dehaene, 2010) and Lamme et al., (Lamme, Super, & Spekreijse, 1998) suggest that feedforward pathways serve in the analysis of stimulus properties, whereas feedback pathways are required for perceptual analysis. The results of neuronal computation along the feedforward information stream alone remain unconscious in the absence of feedback. Thus, these studies demonstrate that both feedforward and feedback projections in the cortex are essential in producing the normal visual evoked response. If anesthetics selectively interfere with the function of feedback projections, this may partially explain how they ablate perceptual consciousness. Supporting evidence to this theory has in fact been found in rats (Imas, Ropella, Ward, Wood, & Hudetz, 2005a; Imas, Ropella, Wood, & Hudetz, 2006), and subsequently in

humans (Ku, Lee, Noh, Jun, & Mashour, 2011), demonstrating a decrease in fronto-parietal connectivity and specifically a reduction of feedback.

Although the fronto-parietal feedback theory of unconsciousness is gaining popularity, there are also arguments against it. In particular, patients with extensive frontal lobe injury remain conscious, thus refuting the necessary role of the frontal lobes for consciousness. It is possible the function of local recurrent loops (e.g. within modality-specific cortex and parieto-temporal association cortex) are sufficient for conscious perception and may refocus the target of future studies to anesthetic-induced changes in regional neuronal interactions.

Two main features of neuronal firing patterns in the brain have been extensively investigated: frequency and timing. It is thought that the frequency, temporal pattern or both of neuron activity are important for coding of sensory information (Berry et al., 1997; Izhikevich, 2002). Coding of individual neurons itself, however, is not sufficient to represent a unified description of the environment. As such, it is the functional connections among neuronal groups that are essential for representation of environmental context. Considerable evidence demonstrates that neuronal firing patterns and their functional connections are modulated by brain state. Understanding how neuronal firing properties and functional connections are altered during various states of consciousness is important in elucidating the state-dependent effects on neuronal computation and information processing.

IV. THE RAT VISUAL SYSTEM

In this study, the rat visual system was used as a model to study anesthetic-suppression of cortical sensory processing. Although rodents have a limited acuity of vision, they can discriminate a wide range of patterns and figures and this function is dependent on the visual cortex (Dean, 1990). A relatively large volume of the rat neocortex (10-12 % or 8 mm^2) is devoted to vision and consists of at least seven visuotopically organized areas (Olavarria & Montero, 1981, 1984). The primary visual area (striate cortex, area 17, Oc1, V1) consists of

medial and lateral divisions representing monocular (V1M), responding mainly to central field stimuli, and binocular (V1B) vision, which responds to peripheral field stimuli. V1 is surrounded by visual areas V2M (Oc2M or 18b) medially and V2L (Oc2L or 18a) laterally; these are further subdivided into medial vs. lateral and anterior vs. posterior regions, respectively.

The visual areas are also surrounded by association regions. In Paxinos' atlas (Paxinos & Watson, 1998), the rostral part of V2L is delineated as the posterior parietal association area (PtA). It is defined by its transitional myelination in-between somatosensory and visual cortex (Kolb, 1990). This area is important in the perception of visual transients, visual navigation tasks and contains neurons similar to hippocampal place cells (Dean, 1990).

Connections of visual areas with the prefrontal cortex have been suggested to be important for conscious perception. The rat prefrontal cortex (PFC) is identified by its reciprocal connections with the mediodorsal thalamic nucleus (Mitchell & Cauller, 2001). According to Zilles (Zilles & Wree, 1995), the rat PFC is formed by the transition zone of anterior cingulate, agranular insular and orbitofrontal cortices. The PFC is distinct from the frontal eyefields (FEF) contained by caudal medial secondary motor cortex (M2 or Fr2). The medial orbital PFC has predominantly limbic connections whereas the ventral and ventrolateral orbital divisions have more sensory and premotor connections (Mitchell & Cauller, 2001). Visual areas and the PFC are reciprocally connected both directly and indirectly. The posterior part of V2M is connected with PFC (Sanderson, Dreher, & Gayer, 1991). V2L is connected with perirhinal and temporal association (TeA) areas (Miller & Vogt, 1984) that connect with PFC. An indirect connection also exists via the PtA (Kolb, 1990).

V. Functional Connectivity Measures of Spike Trains

There has been a recent surge of interest in measures of functional integration as it may be a key component for conscious awareness. Increased neuronal synchrony among different regions of the brain was found to be associated with performance of complex tasks (A. Engel et

al., 1991; von Stein, Chiang, & Konig, 2000). Decreased functional connectivity has been demonstrated in neuropathological conditions such as Alzheimer's (de Haan et al., 2009; Stam, Jones, Nolte, Breakspear, & Scheltens, 2007), sleep (Vyazovskiy, Cirelli, & Tononi, 2011), coma, vegetative state (Boly et al., 2011; Landsness et al., 2011) and anesthesia (Boly et al., 2012; Hudetz & Hemmings, 2012; Imas et al., 2005a; Imas et al., 2006; Liu, Lauer, et al., 2012; Liu, Li, Yang, Hudetz, & Li, 2012). A loss of cortical effective connectivity in humans at midazolam concentration levels known to induce loss of consciousness (LOC) and preferential suppression of feedback communication at LOC (Alkire et al., 2008; Ferrarelli et al., 2010; Judge, Hill, & Antognini, 2009) was observed. Therefore, reliable methods are needed to putatively identify functional connections within a neuronal network. It is important first, however, to characterize what is meant by functional connectivity and how this differs from other measures currently being investigated today.

Three main types of brain connectivity have been described as structural, functional and effective connectivity (Fingelkurts & Kahkonen, 2005; Rubinov & Sporns, 2010). Structural connectivity heavily relies on physical anatomical connections among cells found within the brain. Functional connectivity, defined as an increase in the spatio-temporal relationship between neurons based on their firing activity, can be examined by methods such as cross-correlation. Effective connectivity differs from functional connectivity such that the influence of one neuronal cell has on another cell is assessed. In other words, effective connectivity is a measure of the causal relationship between cells.

The increasing application of microelectrode probes for neuroscience research has enabled investigators to simultaneously record from a larger number of cells therefore allowing us to explore how cells within a network work together to process information and perform complex tasks. Yet, recording from elements in a neuronal network using microelectrode arrays encompasses only a small fraction of the brain and therefore all true connections cannot be realistically determined. Aertsen et al., explains that, although it is not possible to reveal all

possible connections due to unobserved elements within the network, the measure of the dependencies among active cells within a neuronal network are an approximate description of how the network functions (Stevenson, Rebesco, Miller, & Kording, 2008). The methods used for evaluating functional connectivity are therefore only an estimate of how neuronal interactions give rise to behavior.

In order to better understand how neuronal cells communicate and process information, appropriate measures are therefore needed to effectively analyze and interpret extremely large data sets. Numerous approaches have been proposed, each with its own advantages and disadvantages, yet no specific method has been unanimously agreed upon (Brown et al., 2004; Le Van Quyen & Bragin, 2007). While some investigations focus on neuroanatomical analysis, here we focus on functional and causal relationships among the cells within a network. Next, I discuss some of the current methods used to measure functional connectivity focusing on those pertaining to neuronal spiking activity from microelectrode arrays.

A. Linear Measures

Cross-Correlation

The classical approach to measure functional connections within a neuronal network is cross-correlation. Cross-correlation is based on a linear model and is a statistical measure of the spike transmission probability between a pair of neuronal cells. It can be used to determine the time shift necessary to obtain the highest relationship between the two signals, therefore providing a measure of causality and directionality.

Several studies have implemented the use of cross-correlograms (CCG) to putatively identify direct monosynaptic pyramidal-interneuron connections between pairs of neuronal cells (Bonhomme et al., 2001; Csicsvari, Hirase, Czurko, & Buzsaki, 1998). Results from CCG analysis were then used to construct a directed spatial mapping of the inferred functional connections in the hippocampus, frontal and motor cortex (Bartho et al., 2004; Fujisawa,

Amarasingham, Harrison, & Buzsaki, 2008). The type of monosynaptic connection can also be putatively classified as either inhibitory or excitatory based on the causal effect within a short-latency interval in the CCG histogram. A significant correlation between remote regions of the cortex (hippocampus and prefrontal cortex) was also detected using CCG on extracellular multi-unit activity (S. E. Fujiwara, Akema, & Izaki, 2008).

Inferred functional connections using CCG has several drawbacks. First, common input and indirect influences from unrecorded cells are not fully accounted by pairwise linear measures. Hence, third-party contributions to short-latency discharges are unknown. Second, an early study evaluating CCG analysis in the detection of excitatory and inhibitory connections showed that CCG analysis is less sensitive in the detection of inhibitory connections compared to excitatory connections (Aertsen & Gerstein, 1985) due to the high variability in the cross-inter-spike interval histogram of inhibitory connections. Third, CCG analysis was also shown to effectively identify functional connections in simplistic network models containing only excitatory connections, but failed in complex simulated networks that included inhibitory as well as excitatory connections (Garofalo, Nieus, Massobrio, & Martinoia, 2009).

Pairwise analysis however, may be sufficient to represent the correlated states within a network. Using an Ising model, >95% of the correlated states were accounted for by pairwise measures (Schneidman, Berry, Segev, & Bialek, 2006). Similar results were found in cortical slices (~88%) (Tang et al., 2008) and visual cortex of the rat (~93%) (Yu, Huang, Singer, & Nikolic, 2008). These results suggest that, indeed, pairwise correlations capture most of the patterns found within the cortex and may be a sufficient representation of the cortical network.

Several studies have investigated the effects of anesthetics in spike and synaptic transmission probabilities. CCG analysis between single-unit and multi-unit neuronal activity recorded from the same electrode in the rostral ventromedial medulla in rats determined that under anesthetics (light or deep levels) their interaction in response to a noxious stimulus was not altered and remained highly synchronized (McGaraughty & Reinis, 1993; McGaraughty, Reinis,

& Tsoukatos, 1995). Bartho et al. also showed that the proportion of putatively identified excitatory to inhibitory cells is not altered with anesthetics (Bartho et al., 2004). The pyramidal-interneuron relationship however, was shown to be state dependent and lowest during slow-wave sleep-like spike patterns (Csicsvari et al., 1998). Furthermore, the discharge rate of pyramidal cells to its target interneuron was found to be frequency-dependent; highest in active cells (5-25 Hz firing rate) (Marshall et al., 2002). These studies demonstrate that the efficacy of spike transmission within a neural network may depend on brain state, as delineated by patterns of cortical synchrony, and consequently the animal's level of consciousness.

The studies conducted using CCG analysis have been mainly performed in intact cortical neuronal networks during wakefulness, sleep or deep anesthetic levels (Bartho et al., 2004; Csicsvari et al., 1998; Fujisawa et al., 2008; S. E. Fujiwara et al., 2008; McGaraughty & Reinis, 1993). A systemic measure of spike transmission probabilities at multiple graded levels of anesthesia from wakefulness to unconsciousness has not been investigated.

Network Likelihood Model

Higher-order measures that combine neuronal firing properties such as ensemble spiking history and external influences are crucial factors that affect spiking behavior and hence functional connectivity. Methods that incorporate these factors simultaneously into modeling spiking activity may allow better interpretation of results, thereby, enhancing our understanding of information processing in the cerebral cortex. As such, several studies have been dedicated to creating methods that can simultaneously analyze multiple interactions to infer functional connectivity within a neuronal network (Okatan, Wilson, & Brown, 2005; Pillow et al., 2008; Stevenson et al., 2009; Stevenson et al., 2008; Truccolo, Eden, Fellows, Donoghue, & Brown, 2005). Trucculo et al. described modeling the instantaneous firing rate of a neuron using a statistical analysis of point processes observations based on discrete likelihood functions (Truccolo et al., 2005). A generalized linear model (GLM) was used to model spike train firing

activity (Pillow et al., 2008; Truccolo et al., 2005) of the entire population. To determine the optimal values for the parameters in this model, a maximum-likelihood (ML) approach was applied. Parameter estimations are determined by maximizing the probability of obtaining the observed sample. The ML method has the advantage of simultaneously incorporating information from the population of neuronal cells to infer functional connectivity and has been applied in hippocampal place cells and in the primary motor cortex (M1) (Stevenson et al., 2009; Truccolo et al., 2005). In very large data sets, however, the ML method tends to overfit the data and is hence a poor fit with real data (Stevenson et al., 2008). Overfitting is caused by a larger number of parameters that need to be estimated, of which increases quadratically with the number of neuronal units (e.g., with 100 neurons, 10,000 connections are possible).

In order to overcome this limitation, several assumptions based on previous empirical evidence, on the type of connectivity within the network have been incorporated into the model such as sparse connectivity and smooth time-varying interactions within the network. Connectivity measures are then calculated using the maximum-a-posteriori (MAP) approach based on Bayesian statistics (Stevenson et al., 2008). MAP has the advantage of including these *a-priori* assumptions to estimate functional connectivity within the network. Stevenson et al. demonstrated the superiority of Bayesian estimation of functional connectivity over ML, especially in large data sets with relatively short recording lengths (Stevenson et al., 2008). These measures have only recently been applied to binary networks and hence give no information on the types of connections that are present in the system.

B. Information-Theoretic Measures

Shannon's Information Entropy and variants

Entropy, first described by Claude E. Shannon in 1948, is a non-parametric measure of the degree of statistical dependences between two random variables and is estimated in terms of a non-parametric probabilistic model concept. Entropy is commonly defined as the amount of

"disorder" in the system. In a highly complex system such as that observed during consciousness, entropy is high. Sleigh states that disorder can instead be described as the amount of possible "choices (or states)" within the system (J.W. Sleigh, Olofsen, Dahan, de Goede, & Steyn-Ross, 2001). When entropy is high, the brain must decide upon the appropriate path from many choices, i.e. neuronal connections, whereas when entropy is low, the number of choices is reduced. Spectral entropy, a measure based on the frequency components of the electroencephalography (EEG), is a recently introduced method for assessing consciousness in humans (Vanluchene, Struys, Heyse, & Mortier, 2004; Vanluchene, Vereecke, et al., 2004). This method, however, is measured in one or more areas of the brain independently and does not incorporate the effects of functional interactions within these areas to assess consciousness.

Various information-theoretic variants of information entropy such as multi-information, interaction entropy, transfer entropy, cross-approximate entropy, complexity and mutual information have been used to study functional connectivity within local and remote areas of the brain (Garofalo et al., 2009; Hudetz, Wood, & Kampine, 2003; Pillay et al., 2011; Tononi & Edelman, 1998b). Comparison of pairwise information-theoretic measures demonstrated superiority of entropy measures over cross-correlation in the estimation of functional connectivity in simulated cortical networks (Garofalo et al., 2009). Furthermore, highly distributed and specialized connectivity was found to be associated with high measures of complexity (Tononi & Edelman, 1998b; Tononi, McIntosh, Russell, & Edelman, 1998).

Several studies have used entropy to measure local and remote information transfer during anesthetics. These studies showed that feedback communication between remote regions of the cortex is suppressed at the LORR in rats (Hudetz et al., 2003; Imas et al., 2005a). Microinfusion of norepinephrine into the Nucleus Basalis of Meynert increased information capacity in anesthetized rats (Pillay et al., 2011). Furthermore, intracerebroventricular infusion of a cholinergic agonist returned frontal bihemispheric cross-approximate entropy in the rat cortex

during light anesthesia (Hudetz et al., 2003). Hence, alterations of information integration as measured by entropy may be useful for understanding loss and return of consciousness.

Information Integration and consciousness

Numerous studies in humans and animals have indicated that inter-regional recurrent processing is essential in cognitive information processing and conscious awareness. While studies have shown that the brain is composed of functionally specialized neuronal groups in distinct areas, information at these various cortical loci must be effectively and rapidly integrated to achieve a subjective conscious experience. Tononi hypothesized that rapid integration of distributed functionally neuronal groups is achieved through the process of recurrent parallel communication within and among brain regions and essential for conscious experience (Tononi, 2004, 2005, 2010; Tononi & Edelman, 1998b).

Recent studies with simulated networks, demonstrated that the capacity of a system to effectively integrate information, explained by Tononi's integration theory of consciousness, is associated with complex systems consisting of highly specialized and integrated neuronal groups, thought to be associated with consciousness (Gamez, 2010; Gamez & Aleksander, 2011; Tononi, 2004; Tononi & Edelman, 1998b). Recently, this theory has been applied to EEG data in human subjects and revealed that in patients under propofol anesthesia was correlated with a decrease in the capacity for neural information integration (Lee, Mashour, Kim, Noh, & Choi, 2009). Moreover, Tononi's theory has also been extended to dynamical properties of the system and promises further insight into the time-varying changes of integrated information (Balduzzi & Tononi, 2008). Applying this theory to cortical neuronal networks may provide useful insight into the extent of functional integration present at conscious and unconscious states.

VI. SIGNIFICANCE

Although anesthetic agents have been used for more than one and half century, how they produce unconsciousness remains a mystery. Nearly 60,000 patients per day are given general

anesthesia for surgery in the United States alone (Brown et al., 2010). General anesthetics are used to assist in operations where a patient must be unconscious, free of pain and unable to recall the events of the surgery. Decades of research ranging from microscopic to macroscopic studies of the brain have shed light on what neuronal properties are affected by various anesthetics yet identifying the neuronal mechanisms involved with anesthetic-induced unconsciousness remains unanswered and to date no model of the loss of consciousness has emerged. Currently accepted methods for monitoring anesthetics based on neuronal activity recorded from the brain such as bispectral index or spectral entropy of the encephalogram have been used to guide anesthetic administration in the operating room but these indices are empirical and not fully reliable to predict the presence or absence of consciousness. These current methods cannot be used alone as a measure of consciousness and therefore other behavioral and physiologic measures are required to ensure the safety of the patient while anesthetized. Yet, even with anesthetic monitoring devices and the expertise of an anesthesiologist, in several instances patients have reported mild to severe post-operative side effects and in extreme rare cases intra-operative awareness. In this work, I seek to determine the neural correlate of the anesthetic-induced loss of consciousness (LOC) in neuronal networks. The purpose of this research is to further our understanding of the mechanisms involved with the anesthetic-induced LOC. On the long term, the benefits of these investigations will facilitate in the development of better monitoring devices and lead to the creation of effective anesthetic agents that will be free of unwanted side effects.

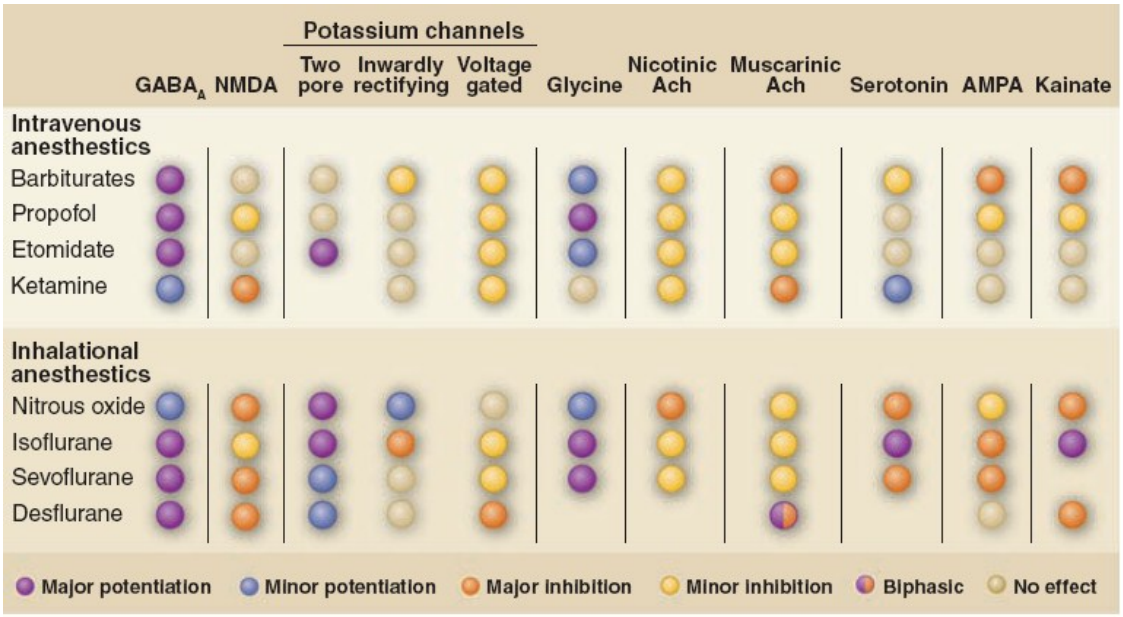

Table 1. Ionic mechanisms and targets of current clinical anesthetics
Abbreviations: Ach, acetylcholine; AMPA, a-amino-3-hydroxy-5-methyl-4-isoxazolepropionic acid; GABAA, g-aminobutyric acid, type A; NMDA, N-methyl-D-aspartate. Figure from (Alkire et al., 2008).

EXPERIMENTAL PROCEDURES

ELECTRODE IMPLANTATION

The proposed experimental procedures and protocols were reviewed and approved by the Institutional Animal Care and Use Committee (Medical College of Wisconsin, Milwaukee, WI). All procedures conform to the *Guiding Principles in the Care and Use of Animals* of the American Physiologic Society and are in accordance with the *Guide for the Care and Use of Laboratory Animals* (National Academy Press, Washington, D.C., 1996). All efforts were made to minimize the number of animals used and their suffering.

Sprague-Dawley rats were kept on a reversed light-dark cycle in dedicated rooms of the Animal Resource Center for at least one week prior to physiological experiments. On the day of the aseptic surgery, the rat (260-440 gm) was anesthetized using isoflurane (Abbott Laboratories, Chicago, IL) in an anesthesia box. The animal's head was then secured in a rat stereotaxic apparatus (Model 900, Kopf Instruments, Tujunga, CA) and a gas anesthesia adaptor (Stoelting Co., Wood Dale, IL) was placed over the snout to continue anesthesia at ~2.0% isoflurane. Body temperature was rectally monitored via temperature controller (model 73A, YSI, Yellow Springs, OH) and maintained at 37° C via an electric heating pad (TC-1000, CWE Inc., Ardmore, PA). The antibiotic, Enrofloxacin (10mg/kg s.c.), was administered prior to surgery onset (Bayer Healthcare LLC. Shawnee Mission, KS). The dorsal surface of the head was prepared for sterile surgery with betadine (VWR, Radnor, PA) and alcohol. Sterile 0.5% Bupivicaine (Hospira Inc. Lake Forest, IL), a local anesthetic, was injected under the skin prior to surgery (~0.1ml). A midline incision was then made and the skin was laterally reflected. The exposed cranium was gently scraped of connective tissue and any bleeding was cauterized.

A multishank, 64-contact microelectrode array (5 mm length, 200 μm electrode spacing, 200 μm shank spacing, Neuronexus Technologies, Ann Harbor, MI) was chronically implanted

stereotaxically within the monocular region of the visual cortex, V1M (7.0 mm posterior, 3-3.5mm lateral, relative to bregma) as illustrated in Figure 1. To implant the microelectrode array, a craniotomy of rectangular shape of approximately 2x4 mm was prepared using a low speed, compressed air-driven dental drill and bur No. FG 1 (Sullivan/Schein Dental, Melville, NY). The exposed dura mater was resected and the electrode array was inserted using a micromanipulator. The array was subsequently advanced at increments of 10 μm to a depth of approximately 2.1 mm below the brain surface. To secure the neural probe, the perimeter surrounding the electrode probe was covered with silicone gel (Kwik-Sil, World Precision Instruments, Sarasota, FL). A reference wire attached to the neural probe was wrapped around a cranial steel screw located between bregma and lambda (~4.0 mm posterior, ~2.0 mm lateral, relative to bregma) in the opposite hemisphere. An illustration of the electrode implantation is displayed in Figure 2.

For visual stimulation which is not dependent on field of view (FOV) in the rat, one light-emitting diode (LED), with a peak wavelength of ~650nm and 8 mm diameter, was subcutaneously implanted behind the contralateral eye between the skull and tissue (Szabo-Salfay et al., 2001). This wavelength allows the intensity of the light to penetrate the tissue and directly stimulate the retina. Prior to implantation, the legs of the LED were soldered into a 2-pin socket connector. Once positioned, the LED was secured with dental resin/cement (Dentsply Caulk, Milford, DE).

In addition to the implanted electrode, sterilized stainless steel screws (MX-080-2, #0-80 x 1/8", Components Supply Co Inc., Fort Meade, FL) were placed in the cranium as anchors. The whole assembly was embedded into a nontoxic skull fixture adhesive, Cerebond (MyNeurolab, Saint Louis, MO), with only the IC connectors protruding from the skull fixture adhesive cap. The analgesic, carprofen (Pfizer Animal Health, New York, NY), 5 mg/kg subcutaneously, was administered post-surgery. The animal was then returned to the housing cage in the animal facility. Carprofren, 5 mg/kg s.c. once daily, was administered for 2 days and enrofloxacin

(10mg/kg s.c. once daily) for 7 days. The animal was then observed for 7-10 days for any infection or other complications.

Desflurane was chosen for this study because it is a modern, and commonly used anesthetic with favorable pharmacokinetic and pharmacodynamic properties and minimal cardiovascular side effects (Eger & Johnson, 1987). The anesthetic actions of desflurane are in most respects similar to those of isoflurane (Murrell, Waters, & Johnson, 2008; Rehberg, Bouillon, Zinserling, & Hoeft, 1999), with the exception of its rapid equilibration, which makes desflurane a preferred choice for experiments to be performed at multiple steady-state anesthetic depths in the same experimental setting.

We referred to anesthesia at 6% desflurane as a state of unconsciousness. Arguably, consciousness cannot be directly assessed; we can only measure a behavioral surrogate. In rats, the righting reflex is a widely used behavioral index of consciousness because it is abolished at equivalent anesthetic concentrations to those that abolish response to commands in human subjects (Franks, 2008). The desflurane concentration that suppresses the righting reflex has been previously determined as 4.6±0.45% (Imas et al., 2005b). The experiments were conducted starting with the anesthetized condition and finishing with the wakeful condition. We chose this order of conditions to the initial threshold selection for spike detection under anesthesia, when signal-to-noise ratio was optimal. Thus, strictly speaking, we investigated the neuronal events associated with regaining as opposed to losing consciousness. During emergence from anesthesia, the threshold for righting reflex may be slightly lower than during induction (Friedman et al., 2010), indicating hysteresis or "neuronal inertia". Because our experiments were conducted under steady-state conditions with relatively long equilibration periods before each recording, a hysteresis effect was very unlikely. In preliminary studies with similar equilibration periods, we observed no significant difference in spike rate or interspike intervals between induction and emergence conditions at the same anesthetic concentration (Figure 3).

Therefore, 4%-6% is a good estimation of range of desflurane concentration at which a reversible transition between consciousness and unconsciousness occurred.

EXPERIMENTAL PROTOCOL

Following recovery, the rat was placed in a cylinder anesthesia chamber (Figure 4). The chamber was then sealed and ventilated with a heated, humidified gas mixture of 30% O_2, balance N_2. The room was then darkened and the rat was allowed to freely move around in the box for about one hour to accommodate to the environment. After the accommodation period, the electrode array was then connected to a headstage with its wire bundles connected to a preamplifier (Blackrock Microsystems, Salt Lake City, UT) outside the anesthesia chamber.

Extracellular unit activity (UA) and local field potentials (LFP) were recorded using a 128-channel neural acquisition system (Blackrock Microsystems, Salt Lake City, UT). UA was auto-thresholded using a root mean square multiplier of -6.25 and kept constant throughout the experiment. Spiking activity was analog filtered from 250 – 7500 Hz and digitally sampled at 30 kHz. LFPs were analog bandpass-filtered at 1-250 Hz, analog notch-filtered at 60 Hz and digitally sampled at 1000 Hz.

Recording was performed first under anesthetized conditions and then in wakefulness. Four anesthetic concentrations were used at which rats were either deeply anesthetized (8%), unconscious (6%), moderately anesthetized (4%), or lightly sedated (2%). At each anesthetic condition, spontaneous unit activity was recorded for ten minutes. After spontaneous acquisition, 110-120 discrete flashes (~5ms) were delivered randomly with an interstimulus interval of 5-15 seconds (Figure 5). Continuous monitoring of the anesthetic concentration was performed using a POET II monitor (Criticare Systems, Waukesha, WI). Since monitoring accuracy is 0.1%, an indication of the target or target ±0.1% concentration was accepted. An equilibration time of 15-20 minutes after a decrease in concentration was allowed before recording of extracellular activity. The time marker of the flash was also recorded using 128-channel neural acquisition

system (Blackrock Microsystems, Salt Lake City, UT). Before the start of neural acquisition, the righting reflex was tested by tilting the anesthesia chamber by 30 degrees. Righting was considered intact if the rat stood on all four feet. In case of absent righting, the tilt was repeated three times.

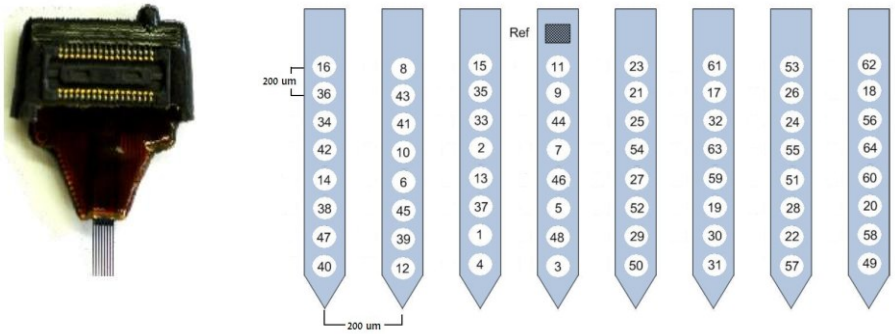

Figure 1. Neuronexus Zif neuronal probe
Multi-shank 8x8 silicon probe (left). Electrode mapping of customized 64-channel probe (right). Figure not drawn to scale. Figure extracted from NeuroNexus Technologies, Inc. Ann Harbor, MI website

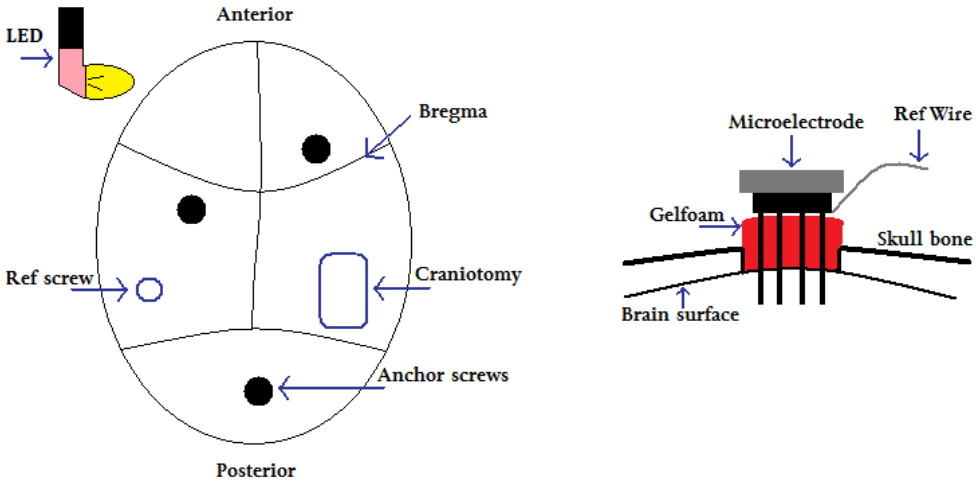

Figure 2. Electrode implantation
Example of electrode placement location in rat visual cortex (left). Craniotomy in right hemisphere behind bregma where electrode was inserted (center location – AP: -7.00 mm, L: +3.0-3.5 mm) with reference wire wrapped around reference screw in opposite hemisphere; LED placed between skin tissue and skull on left hemisphere behind left eye. Example of electrode insertion into brain (left). Gelfoam, an absorbable gelatin, or silicon gel is placed in area surrounding the electrode shanks.

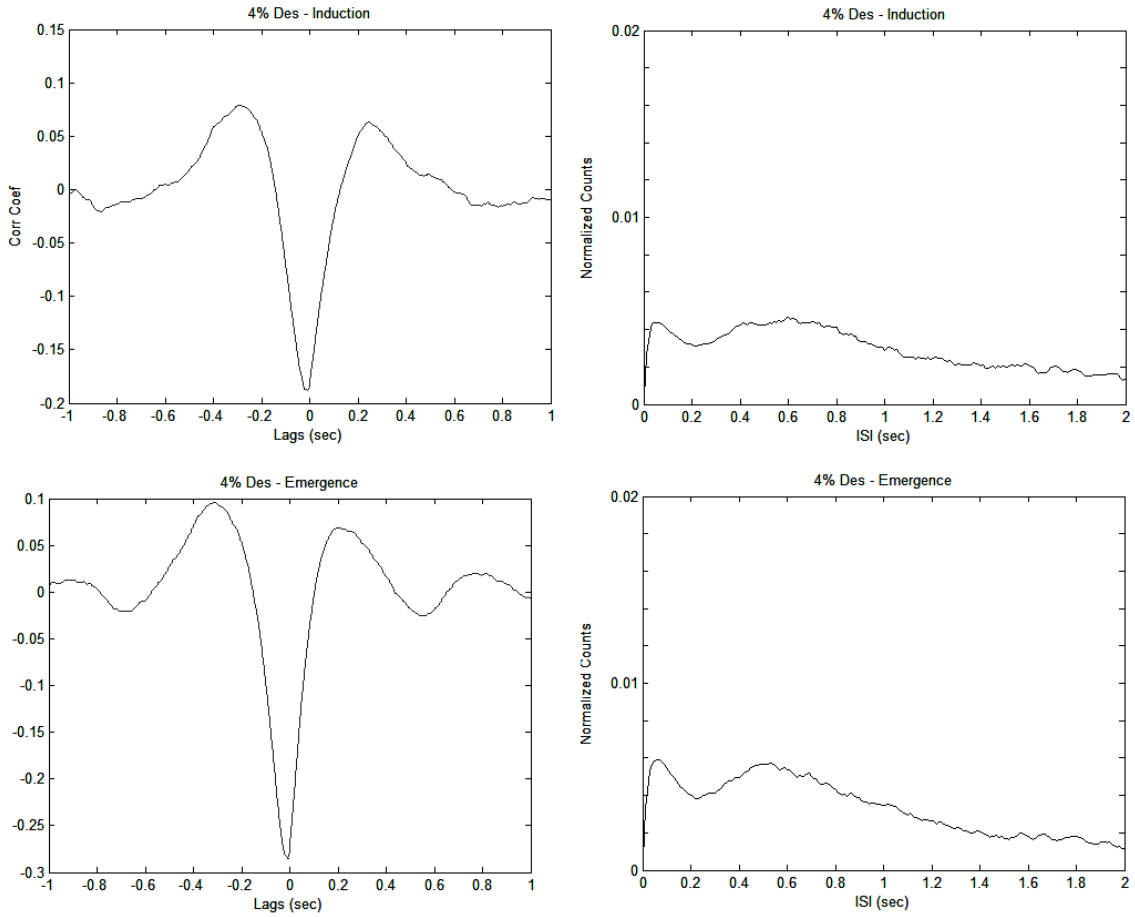

Figure 3. Comparison between induction and emergence
Left panels display average correlation between unit activity and local-field potential during induction (top) and emergence at 4% desflurane level. Right panels display average weighted-interspike intervals at 4% during induction (top) and emergence (bottom). No difference was observed.

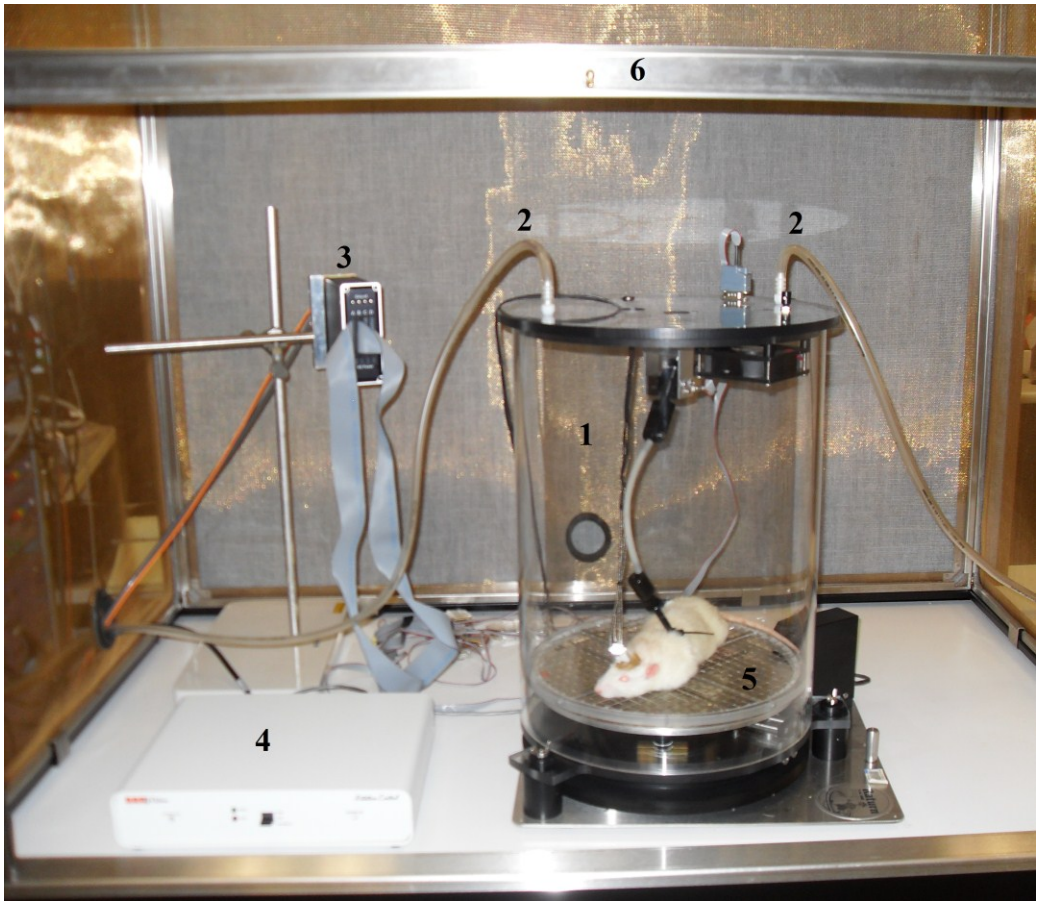

Figure 4. Experimental recording chamber
Anesthesia chamber built in MCW machine shop (1) air-tight chamber, (2) gas inlet/outlet lines, (3) 64-channel preamplifier, (4) Raturn motor, (5) rotating, heated shock floor, (6) Faraday shielded cage.

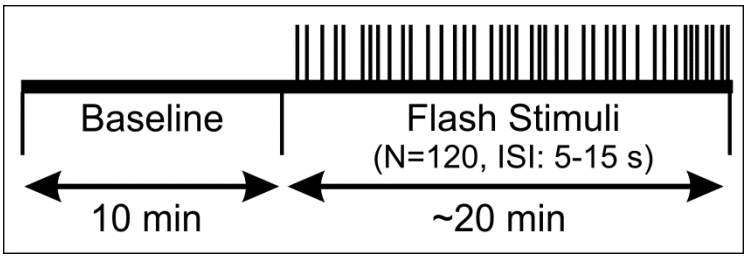

Figure 5. Experimental protocol
At each anesthetic condition, 10 minutes of spontaneous activity followed by stimulus induced activity from 120 flashes presented at random inter-stimulus interval of 5-15 sec was acquired.

CHAPTER 1

MONOSYNAPTIC FUNCTIONAL CONNECTIVITY IN CEREBRAL CORTEX DURING WAKEFULNESS AND UNDER GRADED LEVELS OF ANESTHESIA

INTRODUCTION

Local computations within neuronal networks constitute the foundation for information processing that ultimately leads to conscious experience and behavior (Buzsaki, 2006, 2007; Buzsaki et al., 2007). The balance between excitation and inhibition in local networks is also considered to be of significant importance for neural computation, cognitive function, and regulation of global firing activity (Bartho et al., 2004; Buzsaki, 2006; Buzsaki et al., 2007). Parallel recording of extracellular activity using microelectrodes is the principal technique to investigate neuronal communication within localized areas. Accordingly, there has been a strong interest in reliable approaches to extract neuronal connectivity from multichannel unit recordings in both awake and anesthetized animals. How the derived neuronal interactions depend on the level of consciousness including waking, sleep and anesthesia, is a principal question that may shed light on the neuronal mechanisms underlying neuronal computations that support cognitive functions. To date, relatively little is known about the nature of anesthetic dose-dependent changes in functional interactions in intact neuronal networks. The modulation of neuronal communication by anesthetic agents is of particular interest because anesthetics can be applied to investigate the emergence and breakdown of consciousness in a controlled manner.

Several studies suggest that the brain's ability to process and integrate information across remote and local areas in the cerebral cortex gives rise to conscious experience (Alkire et al., 2008; Tononi & Edelman, 1998b). We suggested that remote (long-range) functional communication within the cerebral cortex is disrupted during loss of consciousness as produced

by various anesthetics (Hudetz, 2002; Hudetz et al., 2003; Imas et al., 2005a, 2005b; Imas et al., 2006). Likewise, a loss of cortical effective connectivity has been demonstrated in humans at an anesthetic depth associated with unconsciousness(Alkire et al., 2008) (Ferrarelli et al., 2010; Kelly, Smith, Kass, & Lee, 2010; Langheim, Murphy, Riedner, & Tononi, 2011). Furthermore, a recent study using local field potential recordings found a concentration-dependent effect of several anesthetics on intracortical functional connections, suggesting that anesthetics modulate neuronal communication in local circuits (Kreuzer et al., 2010). Thus, functional communication in neuronal networks may be a primary target of anesthetics.

Anesthetic agents have been shown to exert graded suppressive effects on both spontaneous and evoked neuronal activity (Detsch, Kochs, Siemers, Bromm, & Vahle-Hinz, 2002; Hudetz et al., 2009; J. W. Sleigh et al., 2009; M. Y. Villeneuve & Casanova, 2003). Moreover, most common anesthetics suppress excitatory and facilitate inhibitory synaptic transmission (Pearce, Stringer, & Lothman, 1989; Pittson, Himmel, & MacIver, 2004). Whereas the effect of anesthesia on single unit activity has been studied extensively, how the observed synaptic changes influence communication in the intact neuronal network remains unclear. Elucidation of the latter requires an estimation of functional neuronal connectivity from the simultaneous recording of a large number of active units, *in vivo,* across multiple states of arousal.

Numerous techniques have been recently applied to estimate functional connectivity in intact neuronal networks (Brown et al., 2004; Kass, Ventura, & Brown, 2005). Putative monosynaptic connections can be identified in local networks of extracellularly recorded units by estimating spike transmission probabilities from cross-correlogram (CCG) analyses (Bartho et al., 2004; Csicsvari et al., 1998; Fujisawa et al., 2008). Results showed that spike transmission probabilities were state-dependent in rat hippocampal cells: highest during exploration and rapid-eye movement (REM) sleep, as observed by the presence of theta waves, and lowest during sharp-waves bursts associated with slow-wave sleep (Csicsvari et al., 1998). Fujisawa et. al.

further demonstrated behavior-dependent changes in short-term functional connectivity as measured by monosynaptic interactions in the medial prefrontal cortex (Fujisawa et al., 2008). These studies demonstrate that the efficacy of spike transmission within a neural network may depend on brain state, and consequently, the animal's level of consciousness.

The studies conducted using CCG analysis have been mainly performed in intact cortical neuronal networks during wakefulness, sleep or deep anesthetic levels (Bartho et al., 2004; Csicsvari et al., 1998; Fujisawa et al., 2008; S. E. Fujiwara et al., 2008; McGaraughty & Reinis, 1993). However, deep anesthesia associated with nociceptive immobility (Antognini & Kien, 1995; Rampil, 1994), does not inform us about dose-dependent changes associated with the loss and return of consciousness (Gugino et al., 2001). To understand the critical changes in network function associated with loss of consciousness, there is a need to determine, in a controlled manner, how spike transmission probabilities are altered at multiple graded levels of anesthesia. In this study, I compared excitatory and inhibitory spike transmission probabilities in rat cerebral cortex during wakefulness and under graded levels of anesthesia. ***I hypothesized that desflurane anesthesia suppresses monosynaptic functional connectivity at loss of consciousness.***

DATA ANALYSIS

Spike Train Analysis

Movement artifacts were identified as synchronous time segments across all channels and manually removed. On average, 4.9±1.3% of the data contained signal artifacts due to chewing, twitching, or grooming. An 8-10 minute segment of artifact-free spontaneous extracellular unit activity was extracted from the recordings at each state for post-processing and further analysis.

At each concentration, PowerNAP (OSTG, Inc., Fremont, CA), an open-source software, was used to sort the spike waveforms at each contact into individual neuronal units. This offline spike sorter software applies principal component analysis (PCA) along with various clustering methods for sorting. PCA determines the linearly dependent factors in the spike waveform data

and transforms them into an ordered set of orthogonal basis vectors that capture the direction of the largest variation (Fee, Mitra, & Kleinfeld, 1996; Hudetz et al., 2009). A scatterplot using the first two principal components was then constructed, and K-means clustering analysis was used to define the cluster boundaries of individual units. Occasional remaining outliers were removed manually, if necessary.

Cross-Correlogram Analysis

Cross-correlogram (CCG) analysis is a linear statistical assessment of the interdependencies between two signals and represents how two signals relate with one another as a function of time displacement. It has been applied to indirectly classify monosynaptic connections as either excitatory or inhibitory based on the functional interaction dynamics between neuronal cell pairs (Bartho et al., 2004; Csicsvari et al., 1998; Fujisawa et al., 2008). CCG is calculated as the time difference of spike occurrences (cross-interspike interval) between a reference spike and the target spike train. Here we used a time window interval of [-20, +20] ms with a 1.3 ms bin size to produce a count histogram of the calculated cross-interspike intervals.

In order to eliminate short-time scale chance correlations while retaining larger-time scale (i.e., spike rate) information, a jitter resampling method was performed (Fujisawa et al., 2008; Quilichini, Sirota, & Buzsaki, 2010). A simulated randomized spike train was produced by independently and randomly "jittering" or shifting the occurrence time of each spike in the target spike train within a small uniformly distributed time interval of -5 to +5 ms. CCG analysis was then performed on the reference spike train and the jittered spike train. The jittering method was performed 1000 times, yielding 1000 surrogate data sets. The variation produced by the jittered CCG data sets provided the confidence intervals for the number of counts in each bin. Global thresholds of 97% confidence interval were determined from the maximum and minimum of each jittered surrogate CCG and used for classification of significant monosynaptic connections.

Monosynaptic connections were identified by the presence of a significant CCG peak height or trough observed within the delay interval of [+1.3, +5.2] ms. Significance was determined with respect to the global thresholds (Bartho et al., 2004; Csicsvari et al., 1998; Fujisawa et al., 2008). The count values in the original CCG histogram that surpassed or fell below twice the global threshold within this short latency interval indicated a direct excitatory or inhibitory monosynaptic connection, respectively. For the units that were recorded from the same electrode contact, the time zero bin was excluded from the analysis due to the built in blanking period of the spike detection system. CCG was calculated using the sigTool toolbox (Lidierth, 2009) in MATLAB R2007b (Mathworks, Natick, MA).

The effect of desflurane anesthesia on excitatory and inhibitory connections was determined as the total number of putatively identified monosynaptic connections normalized to the total number of possible connections at each anesthetic concentration. The Euclidean distance of the connected neuronal pairs was determined based on their electrode locations. A histogram of the distance lengths for each connection type was then created and normalized to the total count of excitatory and inhibitory connections. The vertical distance from the source to the target cell, representing the connection depth, was also calculated for excitatory and inhibitory connections at each concentration and a histogram was produced.

Connection strength represents the efficacy of spike transmission between each pair of cells and was defined as the standardized peak height in the CCG. Specifically, the absolute difference between the number of spikes in the peak or trough of the CCG histogram and the jittered mean was taken and divided by the jittered standard deviation (Fujisawa et al., 2008). Based on the type of connections revealed by the CCG analysis, each presynaptic cell was indirectly classified as a putative pyramidal cell or interneuron. The majority of pyramidal cells fire at lower frequencies than do interneurons (Csicsvari et al., 1998). The distribution of spike rates of the two putatively classified cell types was compared.

Statistical assessment

The effects of desflurane on baseline firing rates and number of active units, excitatory and inhibitory connections were estimated using the repeated measures analysis of variance (RM-ANOVA) test with the anesthetic concentration as a fixed factor and the subject (rat) as a random factor. The concentration-dependent effects of desflurane on the percentage and strength of connections was tested using the same method as mentioned above with the percentage of connections or connection strength as the response variable. When the interaction term was significant, the component effects were further examined using Tukey-Kramer Multiple-Comparison test (T-K) or a Bonferroni test. Statistical analyses were performed using NCSS 2007 (NCSS, Kaysville UT).

RESULTS

Behavioral observations

Experiments were performed in seven rats at three levels of inhaled desflurane anesthesia (6%, 4%, and 2%) and wakefulness. At the 6% level, spontaneous movement was absent. As the anesthetic was withdrawn, rats exhibited a gradual increase in their level of alertness. At moderate depth of anesthesia (4%), they displayed sporadic and brief behaviors such as, temporary whisker twitching or chewing, but for the most part, they remained immobile. During light sedation (2%), most rats displayed head and limb movements, and postural changes that lasted for several seconds. Finally, during wakefulness (0%), rats displayed typical intermittent grooming and exploratory behaviors as well as quiet (absence of movement) alertness. The return of righting reflex suggested that consciousness was regained at 4% anesthetic concentration.

Unit activity and monosynaptic connections

Spontaneous extracellular spikes were recorded using 64-contact multishank neural probes chronically implanted in the primary visual cortex (Figure 6A). Each electrode shank spanned the entire depth of the cortex, recording from eight equally-spaced depths and eight equally-spaced positions. Spikes were detected at approximately half of the electrode contacts (54%±16%). Spike sorting yielded one to three units from each electrode contact (Figure 6B). In seven rats during wakefulness, 434 active units with spike rates of at least 1 s^{-1} were recorded. Deviation from the zero slope was tested using a linear trend planned comparison test. The number and spike rate of units decreased with the anesthetic concentration ($p<0.05$, linear trend, Table 2).

Putative excitatory and inhibitory monosynaptic connections were identified by cross-correlogram (CCG) analysis from the counts of correlated spiking between each possible pair of units at various time lags. Examples of CCG corresponding to excitatory, inhibitory and reciprocal functional connections are illustrated in Figure 6C. The mappings of classified monosynaptic connections found between and within electrode contacts in wakefulness and at the deepest anesthesia level are illustrated in Figure 6D and Figure 6E. In wakefulness, a total of 94 connections were found. This number represents approximately 0.5% of all possible unit pairs. The majority of connections were excitatory (ratio: 1.82±0.71). Anesthesia reduced the number of all connections ($p<0.05$, linear trend, Table 2).

The CCG analysis also classifies the presynaptic unit as a putative pyramidal cell or interneuron depending on whether it forms an excitatory or inhibitory connection. A non-normal distribution of spike rates for classified pyramidal cells was observed (Kolmogorov-Smirnov, $p<0.05$). As such, the spike rate distribution of classified pyramidal cells and interneurons at waking across all rats was compared using a Kolmogorov-Smirnov (K-S) test. A significant difference in the spike rates of putative pyramidal cells and interneurons was tested using a

Mann-Whitney (M-W) test. Putative pyramidal cells fired at a lower rate (median: 3.76, 95% CI: 3.25-5.48) than interneurons (median: 6.27, 95% CI: 4.87-7.91) during wakefulness, and their spike rate distributions were significantly different ($p<0.01$, K-S, Figure 7). In addition, a significant difference ($p<0.05$, M-W) between the spike rates of putative pyramidal cells and interneurons was present after one outlier was removed (> 3SD). The number of both cell types was reduced with deepening anesthesia (Table 2).

Spatial distribution of monosynaptic connections

During wakefulness, most connections were short-range, within 200 μm (Figure 8A), and most inhibitory and excitatory connections were confined to the same electrode contact at 73% and 64%, respectively (Figure 8B). This was similar at the deepest anesthetic level (6% desflurane, Figure 8E), where short-range excitatory and inhibitory connections were present at 81% and 69%, respectively. However, the number of long-range connections was noticeably smaller than in wakefulness (Figure 8D). During wakefulness, most excitatory connections projected from deeper to more superficial layers, whereas inhibitory connections were widespread, spanning nearly all cortical layers (Figure 8C). During anesthesia, the connections were limited to a shorter intralaminar span (Figure 8F).

To investigate if a reduction in active units contributed to the paucity of long-range connections, we compared the statistical distribution of the Euclidean distance of all possible connections among the measured units in wakefulness and anesthesia (Figure 9). We found that the distributions were essentially identical ($p=0.74$, K-S) implying that the reduction in connection distances was not due to a reduction in the number of active units.

Connection probability and connection strength

An unbiased measure of functional connectivity is connection probability, defined as the number of observed monosynaptic connections relative to the number of all possible pairs of the recorded units (Figure 10A). Anesthesia exerted a differential effect on excitatory and inhibitory

connection probabilities, as indicated by a significant interaction term ($p<0.05$, RM-ANOVA). This effect was due to a significantly higher probability of excitatory vs. inhibitory connections (ratio: 2.95, $p<0.01$, T-K) at the 6% desflurane level. The higher excitatory to inhibitory connection probability at 6% resulted from a significant increase in the excitatory connection probability at 6% from the 4% concentration level ($p<0.05$, Bonferroni). There was no difference in connection probability between wakefulness and the two lighter levels of anesthesia.

We also examined connection strength, measured by the normalized height of the CCG peaks (Figure 10B). This quantity characterizes the efficacy of monosynaptic spike transmission. Anesthesia reduced excitatory connection strength in a dose-dependent manner ($p<0.05$, linear trend). There was no change in the strength of inhibitory connections.

We considered the possibility that excitatory connection strength might decrease because of the reduced spike rate, reducing the height of the correlation peaks in the CCG. We examined this by constructing a correlation plot of the connection strength and the corresponding spike rate of each connected unit or unit pair (Figure 11). The results showed a very low correlation between connection strength and spike rate (source: $R^2=0.07$, target: $R^2=0.05$, combined: $R^2=0.08$).

To examine this question further, we sought to determine if a decrease in spike rate of either the presynaptic (source) or the postsynaptic (target) unit alone or both could alter the detectability of excitatory connections. To this end, we chose 13 classified excitatory connections of highly spiking source or target units, and decimated the number of spikes in the source, target or both units by 0, 50, 80, 90, or 95%. The CCG analysis was then repeated on all decimated data. The results showed that even at relatively low spike rates (<10 spikes/sec), the range of connection strength remained large (5 to 35, standardized peak height) suggesting an independence of the connection strength from spike rate (Figure 12).

DISCUSSION

This study applied CCG analysis for the first time to investigate the concentration-dependent effects of desflurane anesthesia on putatively classified monosynaptic excitatory and inhibitory functional connections *in vivo*. We found that anesthesia decreased the number of active units and the absolute number of functional connections they formed. Anesthesia also reduced excitatory connection strength that reflects the efficacy of synaptic transmission. Nevertheless, at a depth of anesthesia that purportedly corresponds to unconsciousness, a significant increase in the ratio of excitatory and inhibitory connection probabilities occurred. The latter change suggests an imbalance of excitatory and inhibitory functional connectivity that may indicate abnormal synaptic communication patterns in the state of suppressed consciousness.

The effect of anesthesia on spike transmission probabilities in intact cortical neuronal networks, *in vivo*, has not been investigated. Previous studies using *in vitro*, whole cell or single-channel recordings have established that most anesthetics enhance inhibitory and suppress excitatory synaptic transmission by modulating ligand-gated ion channels (Pearce et al., 1989; Pittson et al., 2004; Ries & Puil, 1999b). Our results are consistent with these observations in that inhibitory connection strength was resistant to desflurane, whereas excitatory connection strength was decreased in a concentration-dependent manner. Minor differences with the *in vitro* data, such as the lack of enhancement of inhibitory connection strength, is understandable due to the recurrent nature of excitatory and inhibitory interactions in local circuits *in vivo*.

In contrast, the significantly higher excitatory to inhibitory connection probability (E/I balance) at 6% desflurane anesthesia was unexpected. This effect could be due to a change in spike patterns or circuit properties, perhaps due to a reduced absolute number (but not strength or efficiency) of inhibitory connections. The difference between the changes in excitatory connection probability and excitatory connection strength is understandable given the different nature of the two parameters. Connection probability measures the frequency of occurrence of

functional connections relative to the number of all possible pairs of active units. Connection strength, on the other hand, characterizes the efficacy of spike transmission for each identified functional connection. Thus, it is possible to encounter higher connection probability at lower transmission efficiency.

We also found that the decrease in connection strength could not be directly accounted for by the decrease in spike rate of either the source or the target cells. One explanation for the decreased connection strength may be the change in firing pattern of the presynaptic cell. Short interspike-intervals between pairs of spikes in the presynaptic cells have been shown to more robustly discharge their postsynaptic target (Kara & Reid, 2003; Usrey, Reppas, & Reid, 1998). Anesthetic modulation of spike pattern variability and its consequent effect on connection strength and connection probability may be investigated in the future.

The change in E/I balance observed at 6% desflurane concentration is important. It has been suggested (Shew et al., 2011) that information transmission and information capacity are maximized at intermediate E/I. An alteration of the E/I balance, in particular elevated E/I, may impair information processing as observed in psychiatric disorders (Yizhar et al., 2011), suppress memory retrieval and recall (Wang & Zochowski, 2012) and reduce sensory-motor integration as observed in evoked responses with lower doses of anesthetics (Populin, 2005). An elevation of E/I from its optimal value may represent insufficient suppression of excitation by inhibition, and was shown to result in excessive correlation, also referred to as hypersynchrony, between neurons (Shew et al., 2011). In fact, our results revealed an increase in excitatory connection probability at the deepest anesthetic level. As suggested by Buzsaki and colleagues, the lack of inhibition could create an unstable system resulting in an avalanche of excitation (Buzsaki, 2006; Buzsaki et al., 2007) that is incompatible with meaningful information processing. Stereotypic hypersynchronous activity is commonly observed in deep anesthesia characterized by electroencephalography (EEG) burst-suppression and is thought to have limited information capacity (Alkire et al., 2008). In burst-suppression, the cortex displays brief periods of increased

activity followed by electrically silent periods. It is accompanied by cortical hyperexcitability through reduced inhibition, therefore causing a shift in the E/I balance (Amzica, 2009; Ferron, Kroeger, Chever, & Amzica, 2009; Hudetz & Imas, 2007). In our experiments at desflurane concentrations up to 6%, there was no burst-suppression in recorded local field potentials, suggesting that the state of hyperexcitability was not attained. It is possible that neuronal firing may have acquired a bursting pattern - as another form of hyperexcitability, although this was previously observed under deep urethane anesthesia only (Erchova et al., 2002). This possibility should be tested in additional studies in the future.

The present results demonstrate that CCG analysis can extract putative monosynaptic connections of functionally interacting neuron pairs at distances up to 1200 μm in the rat visual cortex in both wakefulness and under anesthesia. We also observed a more pronounced deflection in the jittered CCG histogram of inhibitory than excitatory connections. This is consistent with previous *in vivo* and *in vitro* studies and reflects the slower time course of inhibitory post-synaptic potentials (PSP) relative to excitatory PSPs (Bartho et al., 2004; Fujisawa et al., 2008; Tamas, Buhl, & Somogyi, 1997; Thomson, West, Hahn, & Deuchars, 1996). Similar to previous studies (Bartho et al., 2004; Fujisawa et al., 2008), most functional connections were close-range (< 200 μm) and found within the same electrode contact. During wakefulness, most excitatory connections projected upward toward more superficial layers consistent with that seen in the auditory cortex of identified pyramidal cells (Crochet & Petersen, 2009; Sakata & Harris, 2009). In the anesthetized condition, the spread of excitatory activation was confined to smaller cortical depths suggesting a reduction in information transmission across cortical layers. The reduction in the spatial dispersion of monosynaptic connections may therefore be another indication of reduced cortical communication and integration associated with the anesthetic induced unconsciousness.

In general, anesthetic drugs target various ligand-gated and voltage-gated ion channels that regulate synaptic transmission (Alkire et al., 2008; Franks, 2006; Rudolph & Antkowiak,

2004) and it is difficult to extrapolate the effect of one agent to that of another. Depression of neuronal excitability has been observed with various anesthetics (Hentschke et al., 2005; Schumacher, Schneider, & Woolley, 2011), thought to be primarily caused by enhanced synaptic inhibition at γ-aminobutyric acid A ($GABA_A$) receptors (Banks & Pearce, 1999; Bieda & MacIver, 2004) producing hyperpolarization. A suppression of inhibitory neurotransmitter release (Maclver, Mikulec, Amagasu, & Monroe, 1996) and the anesthetic modulation of sodium and potassium channels (Hemmings et al., 2005) may also contribute to reduced excitability. Previously, we showed a suppression of baseline and long-latency cortical neuronal responses to stimuli under desflurane *in vivo* (Hudetz et al., 2009). Inhalational anesthetics such as isoflurane and sevoflurane, as well as intravenous anesthetics propofol and midazolam, and perhaps alpha-chloralose (Garrett & Gan, 1998), primarily $GABA_A$ potentiators similar to desflurane, may produce comparable results. Generalization to other types of anesthetics, such as ketamine or urethane, with substantially different ionic mechanisms and targets (Hara & Harris, 2002; Harrison & Simmonds, 1985; Sceniak & Maciver, 2006) is not straightforward.

As with all similar studies, a recognized technical limitation is the undersampling of the neuronal population. Although we were able to simultaneously record approximately 70 units during wakefulness in each experiment, this number represents a small percentage of active neurons in the sampled region. Because recorded spike amplitudes are attenuated exponentially with distance, 60-100 neurons could be reliably recorded within a 60 μm radius in the rat hippocampus and medial pre-frontal cortex (Buzsaki, 2004; Fujisawa et al., 2008). Assuming similar spike amplitude attenuation in the visual cortex, under optimal conditions, we were able to isolate 1 to 3 units per electrode contact, representing 1-3% of the total possible units. Possible reasons for the relatively low number of recorded cells in our experiments include the potential damage to cells by insertion of the electrode and the possible insulated nature of silicon probe shank that reduces the number of observable neurons (Moffitt & McIntyre, 2005). Furthermore, the spike rate decreased in a concentration-dependent manner, thus reducing the number of active

units (>1s^{-1}) used for CCG analysis. The limited number of recorded cells and concentration-dependent change in spike rate may also account for the relatively low percentage of classified monosynaptic connections relative to all possible connected cell pairs as identified by CCG analysis, consistent with previous findings (Csicsvari et al., 1998; Fujisawa et al., 2008). Another limitation of the pairwise CCG analysis is that it cannot account for the effects of possible indirect connections (Gerstein & Perkel, 1969) although the time scale of interactions (~1 to 5 ms) make the contribution of multi-synaptic effects unlikely. Recent studies have shown that pairwise analysis may represent the correlated states of a network surprisingly well both *in vitro* (Schneidman et al., 2006; Shlens et al., 2006; Tang et al., 2008), and *in vivo* (Yu et al., 2008). Therefore, the pairwise CCG method should represent a reasonable first approximation of population activity.

In summary, our results demonstrate that general anesthesia by desflurane at a concentration that induces unconsciousness alters the excitatory/inhibitory balance of monosynaptic interactions in rat visual cortex neurons *in vivo*. The elevation of the excitatory-inhibitory balance may result from altered spike firing variability, therefore reducing the efficacy of excitatory transmission among the neurons. Overall, elucidating the effect of general anesthesia on functional communication between cortical neuronal cells should help better understand how changes in spikes modulate population activity as a function of cortical state and awareness.

Figures

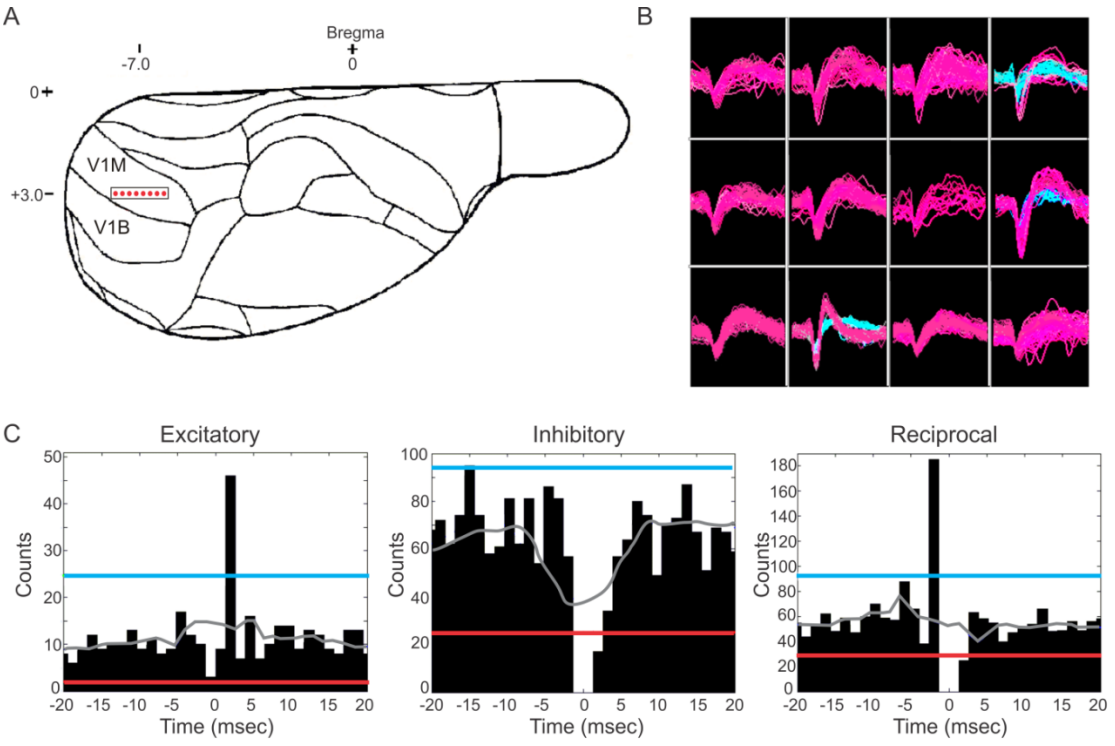

E

E,I	E,I	E,I	E,I	E,I	E,I	E,I	E,I
5,0	2,0	2,2	0,0	0,0	1,0	1,0	0,0
1,0	2,0	0,0	0,0	1,0	0,0	1,2	0,0
3,0	2,1	1,3	1,1	1,0	0,0	2,0	0,0
0,3	1,0	1,0	0,1	1,0	2,0	0,0	1,0
2,0	0,0	2,0	0,0	0,2	0,3	0,2	1,0
1,0	2,1	1,0	2,0	1,0	0,0	0,1	0,1
0,0	0,0	0,0	0,0	0,0	0,0	1,0	0,0
0,0	0,1	0,0	0,0	0,0	0,1	0,0	0,0

E,I	E,I	E,I	E,I	E,I	E,I	E,I	E,I
1,0	1,1	1,0	1,0	0,0	2,0	0,0	0,0
1,1	0,0	0,0	0,0	0,0	0,0	1,0	0,0
0,0	1,0	0,0	2,0	2,0	0,0	0,0	1,2
2,2	0,0	0,0	1,0	0,0	0,1	2,0	0,0
0,0	0,0	1,0	1,0	1,0	0,0	0,0	0,0
0,0	0,0	0,0	0,0	1,0	0,1	1,0	0,0
0,1	0,0	0,0	0,0	0,0	0,0	0,0	0,0
0,0	0,0	0,0	0,0	0,0	0,0	1,0	0,0

Figure 6. Schematic of Electrode Placement and Examples of Recorded Units and Connection Types.

(A) Electrode placement of the 64-contact neural probe in the rat primary visual cortex monocular region (V1M) in the right hemisphere. Each dot represents the approximate location of an electrode shank. Schematic is overlaid on a stereotaxic drawing obtained from the Paxinos rat brain atlas. (B) Example of recorded spike waveforms from 12 channels in one experiment. Color waveforms represent online sorting of units during acquisition. (C) Spike cross-correlograms for excitatory, inhibitory and reciprocal connections. Thresholds are represented for excitatory connections (blue line), inhibitory connections (red line) and jittered mean displayed as gray trace. Bin size is 1.3 ms. The gap in the center bin reflects the blanking period of spike sampling

for connections observed within the same electrode contact. (D) Illustration of excitatory (blue) and inhibitory (red) connections superimposed on a map of electrode contacts during wakefulness (0% desflurane) and unconsciousness (6% desflurane) from all experiments. Presynaptic cell putatively defined as pyramidal cell (blue triangle), interneurons (red circle), or unclassified (gray square). In some cases multiple units are shown at the same contact. For greater clarity, connections between electrode contacts only are shown. (E) Number of classified within-contact excitatory and inhibitory (E, I) connections during wakefulness (left) and unconsciousness (right).

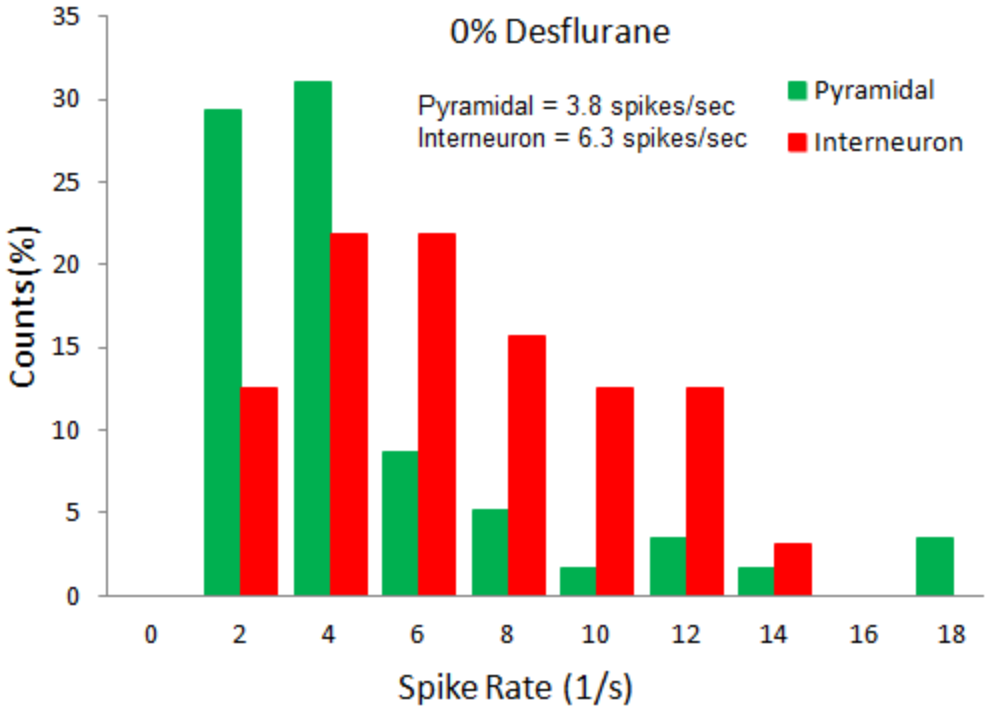

Figure 7. Spike rate distribution of putative pyramidal cells and interneurons at wakefulness

Kolmogorov-Smirnov (K-S) test reveals different distributions for pyramidal cell and interneurons ($p<0.01$). Spike rates for interneurons are higher for interneurons (6.3 spikes/sec) than pyramidal cells (3.8 spikes/sec) ($p<0.05$, M-W).

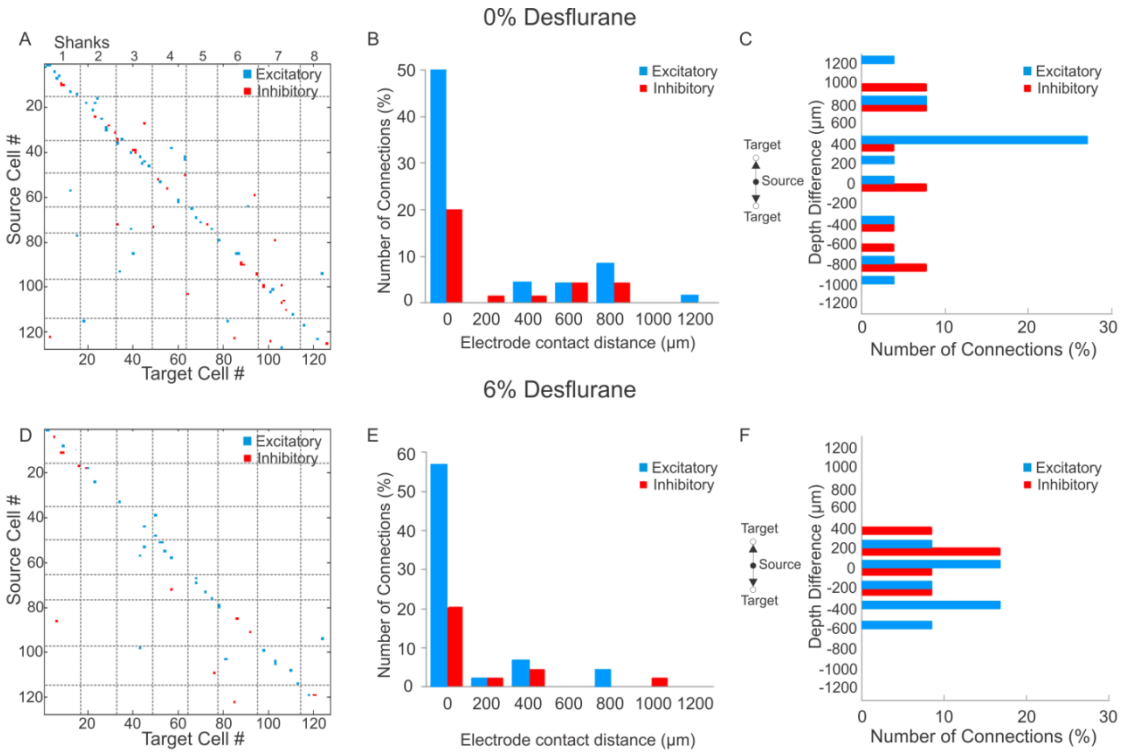

Figure 8. Excitatory and Inhibitory Connections at Wakefulness and Under Anesthesia. (A) Matrix of observed excitatory and inhibitory connections for all rats combined at wakefulness arranged by order of mapping. Cells were numbered from 1 to 127 based on their position of their electrode contact within the array, and arbitrarily within electrode contacts, with the result that consecutive numbers are mapped to neighboring cells. Points on the diagonal represent within-electrode connections, points near the diagonal represent within-shank connections, and points far off the diagonal represent between-shank connections. Most excitatory (blue) and inhibitory (red) connections are found along the diagonal representing connections within or near the same contact. (B) Distribution of distance between source and target units during wakefulness. The number of connections in each bin is normalized to the total number of observed connections (excitatory + inhibitory). Most excitatory and inhibitory connections are found within the same electrode contact (73% and 64%, respectively) (C) Distribution of depth (source depth – target depth) of excitatory and inhibitory connections from different electrode contacts at wakefulness, corrected for angle of insertion. Excitatory connections project to superficial layers. (D) Connection matrix during unconsciousness. (E) Distance distribution of functionally connected neuron pairs at unconsciousness normalized to total number of connections. Similar to the wakeful condition, both excitatory and inhibitory connections are mainly found within the same electrode contact (81% and 69%, respectively). (F) During unconsciousness the connection depth was limited to shorter distances.

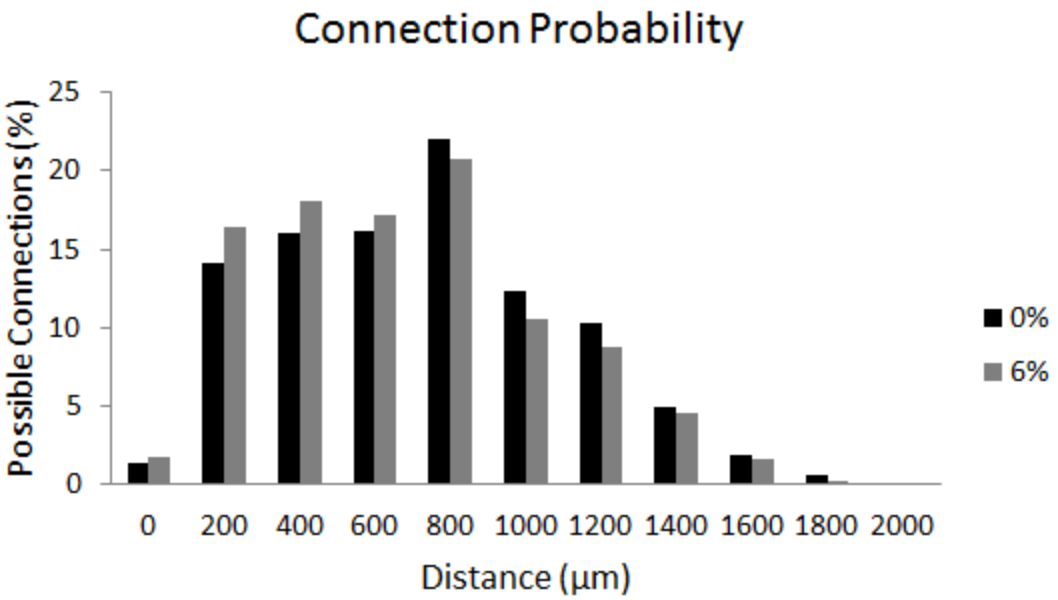

Figure 9. Connection probability as a function of distance at 0% and 6%.
The potential short and long range connections are not affected by anesthetic level (p=0.74, K-S). Desflurane normalized to total counts at each concentration.

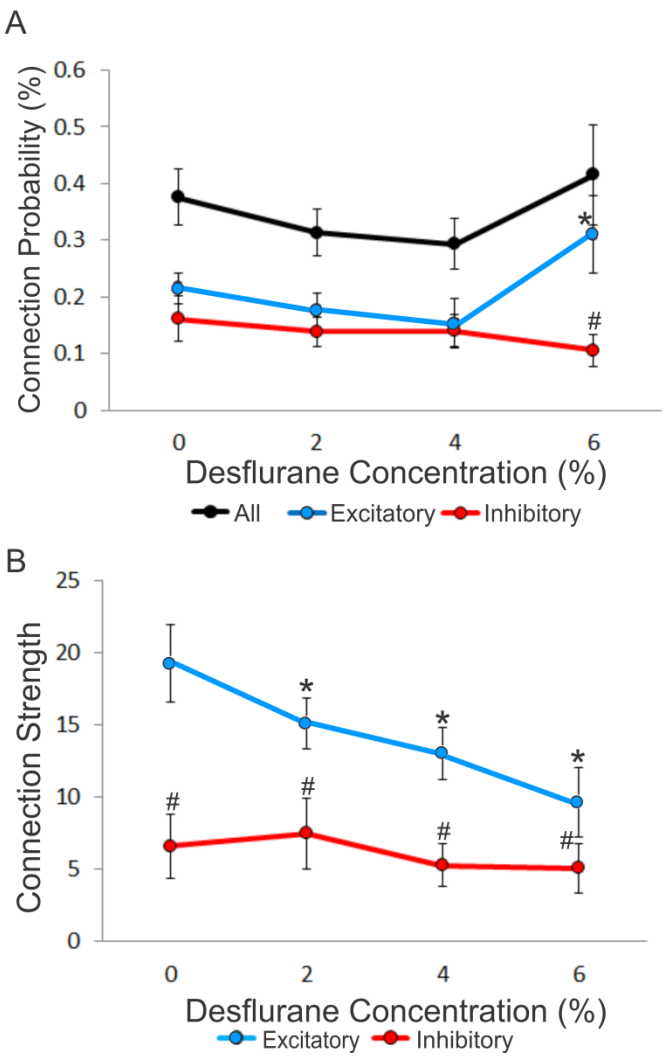

Figure 10. Concentration-dependent Effect of Desflurane on Connection Probability and Connection Strength.
(A) Effect of desflurane concentration on the percent connected over all possible connections. A significant difference on excitatory and inhibitory connections at 6% desflurane is observed, 3:1 (#$p<0.01$, Tukey-Kramer). At 6% desflurane, significant increase in excitatory connection probability is observed from the 4% concentration level (*$p<0.05$, Bonferroni). Data are represented as mean +/- SEM. (B) Desflurane effect on connection strength. A significant linear decrease in excitatory connections strength (*, $p<0.05$, linear trend) with desflurane is present. A significant difference between the strength of excitatory and inhibitory connections is present at all desflurane concentrations (#, $p<0.001$, RM-ANOVA). Data are represented and mean +/- SD.

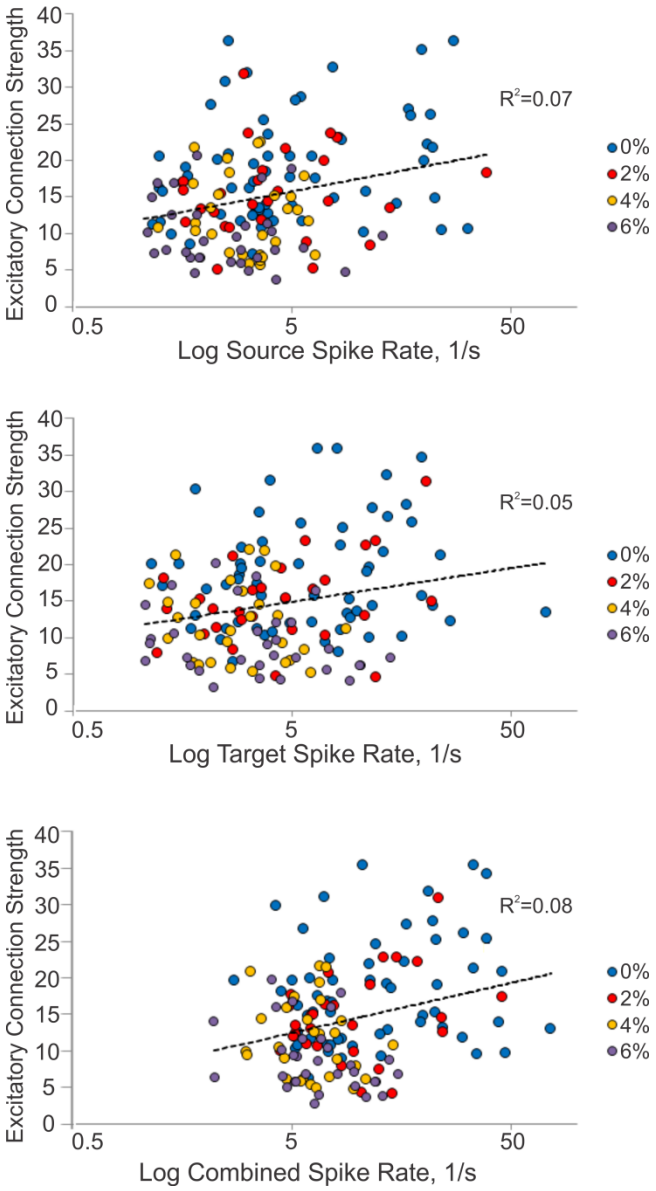

Figure 11. Relationship between Connection Strength and Spike Rate.
Scatterplot of excitatory connection strength and source (top), target (middle) and combined (bottom) spike rates from all experiments. Source spike rate (R2=0.07), target spike rate (R2=0.05), or combined spike rate (R2=0.08) is not an indicator of connection strength.

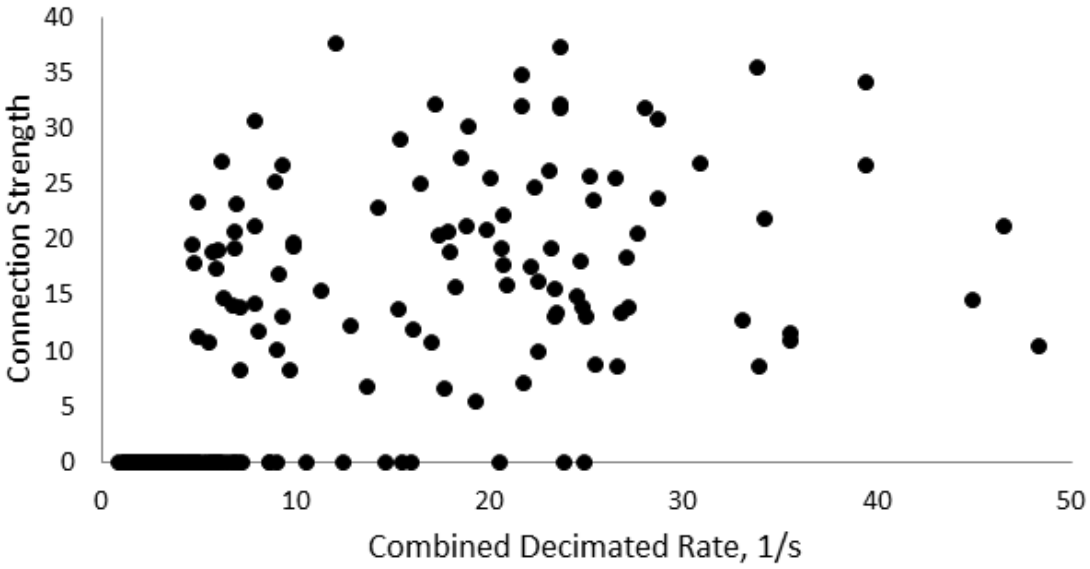

Figure 12. Scatterplot of connection strength and combined spike rate
Combined spike rate was incrementally decimated by 0, 80, 90, or 95% for all combinations. As shown in the figure, even at low spike rates (~10 spikes/sec) there is a relatively wide range of excitatory connection strength (5-35). Connection strength of zero indicates no connection was found.

	Desflurane Concentration			
	0%	2%	4%	6%
All				
Units *	434	309	346	271
Spike Rate, 1/s *	5.5 (4.9,6.5)	4.2 (3.6,4.8)	3.3 (2.9,3.7)	2.8 (2.4,3.2)
Classified				
Connections, all *	94	67	53	44
Excitatory	60 (64%)	39 (58%)	28 (53%)	31 (71%)
Inhibitory	34 (36%)	28 (42%)	25 (47%)	13 (30%)
Putative cells, all	90	47	50	42
Pyramidal cell	58 (64%)	28 (60%)	27 (54%)	31 (74%)
Interneuron	32 (36%)	19 (40%)	23 (46%)	11 (26%)
Pyramidal Spike Rate, 1/s	3.8 (3.3,5.5)**	3.5 (2.5,6.2)	3.5 (2.2,3.9)	2.6 (1.7,3.4)
Interneuron Spike Rate, 1/s	6.3 (4.9,7.9)	3.4 (1.6,5.8)	4.0 (2.5,5.2)	3.6 (1.4,5.2)

Table 2. Properties of classified units and connections used for CCG analysis from 7 experiments.
Number in parentheses indicates percent of all connections and cells. Spike rates are median with 95% confidence intervals. A significant linear decrease in the number of units and unclassified spike rates with desflurane was present. A significant difference in the spike rates of putative pyramidal cells and interneurons was observed at wakefulness.
*$P < 0.05$, linear trend, ** $P < 0.05$, Mann-Whitney.

CHAPTER 2

SPATIAL SYNCHRONIZATION OF NEURONAL SPIKE BURSTS IN THE CEREBRAL CORTEX OF AWAKE AND ANESTHETIZED RATS

INTRODUCTION

Information processing in the brain is thought to be modulated by the spatio-temporal dynamics of cell firing activity. Two distinct patterns of spiking activity are generally described as, burst firing and regular spiking, although several others have also been identified (Buzsáki, 2006; Klausberger & Somogyi, 2008). Neuronal bursts are thought to be a signature of slow-wave sleep, (Amzica & Steriade, 1998; Steriade, 2004; Steriade, Contreras, & Amzica, 1994) drowsiness and epileptic seizures (Kim & McCormick, 1998; McCormick & Feeser, 1990). Recently, neuronal spike bursts were observed in localized areas during prolonged wakefulness (Nir et al., 2011; Vyazovskiy, Olcese, et al., 2011). As such, burst patterns are thought to reflect an impairment of information processing (Brown et al., 2010). Others, however, suggest that bursts carry information (Balduzzi & Tononi, 2012; Ramcharan, Gnadt, & Sherman, 2000; Sherman, 2001).

Anesthetic agents have been shown to exert graded suppressive effects on both spontaneous and evoked neuronal activity (Detsch et al., 2002; Hudetz et al., 2009; J. W. Sleigh et al., 2009; C. Villeneuve et al., 2009). Whereas bursting activity has been detected in sleep, burst patterns have also been observed at the neuronal level in deep anesthetic levels with various inhalational and intravenous general anesthetics (N. Fujiwara et al., 1988; Luczak, Bartho, Marguet, Buzsaki, & Harris, 2007).

During deep surgical anesthesia, bursting patterns in the electroencephalogram (EEG) and local field potentials (LFP) are commonly observed (Amzica, 2009; Ferron et al., 2009;

Hudetz & Imas, 2007). They can also present in coma, hypothermia, cerebral hypoxia and ischemia, early infantile encephalopathy (Ching, Purdon, Vijayan, Kopell, & Brown, 2012; Jirsa, 2008) etc. It has been postulated that burst-suppression in the EEG may be due to decreased brain metabolism through activation of ATP-activated potassium channels leading to suppressed neuronal firing (Ching et al., 2012). Several other studies have suggested that burst suppression may be due to enhanced excitability in cortical networks caused by either diminished activation of cortical interneurons leading to suppressed inhibition (Detsch et al., 2002; Ferron et al., 2009; Kroeger & Amzica, 2007), or persistent glutamate-mediated excitatory synaptic transmission (Lukatch, Kiddoo, & Maciver, 2005). Hence, burst-suppression patterns observed in the EEG and LFP may be produced by changes at the neuronal level, through reduced inhibition or increased excitability.

Burst suppression patterns are generally accompanied by increased excitability of neuronal cells, displaying bistable firing patterns (Amzica, 2009; Destexhe, Contreras, & Steriade, 1999). Recent evidence, however, suggests that neuronal bursts may be observed in localized areas without global effects (Nir et al., 2011; Vyazovskiy, Olcese, et al., 2011). Moreover, in the absence of burst-suppression in the local-field, we observed a paradoxical anesthetic-induced hyperexcitability of active neuronal units associated with the loss of unconsciousness (Vizuete, Pillay, Diba, Ropella, & Hudetz, 2012). Hence, whereas burst-suppression may be associated with neuronal bursts, it is also possible to observe neuronal bursts without an accompanying global phenomenon.

Spike bursts may occur independently or synchronously in the neuronal network. A link between neuronal synchronization and consciousness has been widely demonstrated (Crick & Koch, 1990; A. K. Engel et al., 1999b; Fries, 2005; Melloni et al., 2007; Singer, 1999; Tononi & Massimini, 2008). Increased activation from specialized areas in brain are thought to "bind" together by synchronous firing during consciously perceived visual stimuli (A. K. Engel et al., 1999b). When consciousness is lost, synchronization is suppressed (Imas et al., 2006). Another

signature of neuronal synchronization can be measured by spike bursts, which reflect periods of increased excitability. Synchronization of bistable firing patterns among neuronal populations has been observed in naturally sleeping animals (Luczak et al., 2007). Furthermore, periods of suppressed neuronal firing was found to synchronize with increasing sleep pressure in awake rats, indicating that burst synchrony may be a signature of local sleep (Vyazovskiy, Olcese, et al., 2011). Burst-suppression is thought to reflect hypersynchronized activity among populations of neurons (Yoshitani, Kawaguchi, Takahashi, Kitaguchi, & Furuya, 2003). In the only relevant study I am aware of, Erchova et. al., found that bursts become more synchronized with deepening anesthesia (Erchova et al., 2002). However, only light to deep surgical anesthetic levels were examined, whereas the critical anesthetic dose associated with loss of consciousness was not investigated. Whether burst synchronization correlates with the increase or fading of consciousness remains controversial.

The goal of this study was to determine the concentration-dependent effects of anesthesia on spike bursts in the local neuronal network of the rat cerebral cortex *in vivo*. In particular, I examined whether bursts were present at wakefulness and shallow levels of desflurane anesthesia. Next, I investigated whether desflurane altered the synchronization of spike bursts in the cortical neuronal network. Finally, I tested the concentration-dependent effects of desflurane on the spatial organization of bursts. ***I hypothesized that the spatiotemporal synchronizations of neuronal spike bursts diminished at anesthetic levels associated with loss of consciousness.***

DATA ANALYSIS

In all experiments, burst analysis was performed from a 2- to 5-min segment of data free from motion artifacts. Extracellular activity from each electrode contacts was independently sorted into individual units using the public domain offline spike sorter PowerNAP (OSTG, Inc., Fremont, CA).

Weighted interspike interval and threshold selection

In general, the interspike intervals between spike occurrences were used to differentiate between bursting and non-bursting epochs. Although visual inspection of a burst in the spike train is easily recognized, the histogram of the interspike interval may not reflect this pattern. The distribution of interspike intervals consists of mainly the rapid intervals between spikes and therefore scarcely occurring slow periods are suppressed. In order to augment the sporadically occurring long durations between spikes, we applied a duration weighted-interspike histogram (IIH) in order to enhance the off periods. To this end, a vector of weights, representing the number of counts for each inter-spike interval, was created. Assuming a 1 ms minimum duration between firing of a subsequent spike, the number of counts was determined by multiplying the inter-spike interval duration by 1000. The inter-spike interval between two spike onsets was then placed in each bin. A histogram of the binned interspike intervals was produced and normalized to the total number of counts. An example is illustrated in Figure 13. Next, we determined an optimal binsize for the generation of the weighted IIH histogram based on the minimization of mean integrated squared error (MISE) with variable binsizes (Shimazaki et al, Neural Computation, 2007). A histogram of the weighted IIH was then produced for each active unit, normalized to the total count and smoothed using a 9-point moving average. The distribution of slower intervals between spikes is therefore enhanced typically producing a bimodal IIH for a spike train that includes both rapid and slow firing patterns. Thus, the differentiation between spike firing patterns is more easily detected as illustrated in Figure 14.

Spike burst identification

To objectively identify bursts within the spike train of an active unit, an averaged weighted IIH was calculated at each anesthetic level across all rats. At the deepest desflurane level (8%), the minimum between the two peaks in the average weighted IIH from all rats was determined (Figure 16B). The corresponding time point located at the minimum was used as a threshold to detect bursts in spike trains. The threshold represents the time between short

intervals within a burst and longer intervals from non-bursting epochs. Spike burst intervals, representing periods of high firing activity with inter-spike intervals less than the threshold, was then identified for each active unit. A minimum of three spikes within a burst was also used an additional constraint. The threshold determined at the deepest anesthetic level was used for all other anesthetic levels and wakefulness.

Spike burst properties and synchronization

At each condition, the duration and spike rate of the intraburst and interburst intervals was calculated for each unit. Burst in spike trains have also been identified using the autocorrelogram (ACG) of the spike train. As such, the ACG histogram of each unit was fit with an inverted Mexican hat function between the interval of -50 to +50 ms (Figure 17A, red trace). The initial peak in the ACG histogram signifies a period of increased probability of a subsequent spike to fire after each previous spike. The burst magnitude was defined as the peak of the ACG fit between 0 – 50 ms minus the peak at +50 ms (Figure 17A, yellow arrow). A scatterplot of the percent of spikes observed in bursts and the intraburst spike rate versus and the ACG peak height was produced to determine a correlation between the bursting properties and the firing probability at each anesthetic level.

The binary time series representing the bursting intervals was used to examine the temporal correlation or synchrony of bursts in the neuronal network. The correlation coefficient was calculated from binary sequences of 0 and 1, where 1 marked the time points within burst and 0 marked time points between bursts at 1 ms time bins. The correlation coefficient calculated by Pearson's formula from binary data was equivalent to the sum of within-burst time points coincident between a pair of units, normalized to the geometric mean of within-burst time points of the two units. If more than one unit was found in the electrode contact, the average was used. Specifically we inspected the within and across layer correlation dependency of spike bursts at each anesthetic condition.

And finally, we performed a spatial correlation to determine the anesthetic effect of desflurane on the co-varying properties of bursting patterns of cells located in neighboring channels. As such, the correlation for each channel and its corresponding eight neighbors were averaged. In order to remove random correlation among channels, we shuffled the arrangement of channels and once again calculated the spatial correlation. The correlation in each channel above the shuffled average was used to calculate the average spatial correlation at each anesthetic condition.

Statistical assessment

Initially, distributions of spike rate and intra- and inter-burst properties were tested for normality using K-S test. If normality was rejected then appropriate statistical tests were applied to test for a significance difference in medians. The within and across layer correlation dependence of bursts was tested using a two-way ANOVA with the desflurane concentration and depth (or shank) as a fixed factor. The concentration-dependent effects of desflurane on the spatial correlation was tested with repeated measures analysis of variance (RM-ANOVA) with type (burst and non-burst) as between-factor, desflurane concentration as within-factor, the subject (rat) as random variable, and the correlation coefficient as the response variable. When the interaction term was significant, the component effects were further examined using Tukey-Kramer Multiple-Comparison test (T-K). Statistical analyses were performed using NCSS 2007 (NCSS, Kaysville UT) or MATLAB R2007b (Mathworks, Natick, MA).

RESULTS

Behavioral observations

Experiments were performed in eight rats at four concentration levels of inhaled desflurane anesthesia (8%, 6%, 4%, and 2%) and wakefulness. From 8-6% level, spontaneous movement was absent. As the anesthetic was withdrawn, rats exhibited a gradual increase in their

level of alertness. At moderate depth of anesthesia (4%), sporadic and brief behaviors such as, temporary whisker twitching or chewing was observed, but mainly they remained immobile. During light anesthesia (2%), most rats displayed head and limb movements, and postural changes that lasted for several seconds. Finally, during wakefulness (0%), rats displayed typical intermittent grooming and exploratory behaviors as well as quiet (absence of movement) alertness. The return of righting reflex suggested that consciousness was regained at 4% anesthetic concentration.

Unit activity

Spikes were detected in approximately half of the electrode contacts (58%±12%) and spanned multiple cortical layers (Figure 15A). Spike sorting yielded one to three units from each electrode contact (Figure 15B). In one experiment for one rat, at 2% desflurane, the headstage was accidently removed and therefore the data at that concentration was not included in the analysis. In eight rats during wakefulness, 485 active units with spike rates of at least 1 s^{-1} were recorded. A linear concentration-dependent reduction in the number and total spike rate of units was observed ($p<0.05$, linear trend, Table 3).

Spike firing pattern in conscious (0%) and unconscious (6%) levels along with their corresponding local field potential can be viewed in Figure 15. During wakefulness, a continuous firing pattern is observed (Figure 15C, left panel) and negatively correlated with the negative deflections of the LFP (Figure 15C, right panel). In the unconscious state, a burst firing pattern was typical with periods of firing followed by silent intervals which corresponded to longer interspike intervals (Figure 15D, left panel). Increased negative correlation with LFP signal was also observed (Figure 15D, right panel).

Weighted interspike interval

The optimal binsize calculated at 8% desflurane using the MISE method was found to be approximately 10 ms (9±4 ms). Examples of the duration-weighted IIH distributions from

wakefulness to deep anesthesia from one experiment are displayed in Figure 16A. Initially, during wakefulness, on average, a unimodal distribution was observed with an initial peak around 100 ms. Beginning at light anesthesia, we observed a secondary peak, reflecting a bimodal distribution indicating a separation between bursting and non-bursting epochs in the spike train. On average, the time point located at the minimum between the two peaks at the highest anesthetic level (8%) was 20 ms (20 ± 5 ms). Therefore, we used a threshold of 200 msec to identify bursts within the spike train (Figure 16B). Burst intervals were identified as those spikes with an interspike interval of less than the threshold and a minimum of three spikes within an interval (Figure 16C).

We also tested the dependence of the threshold selection on the intraburst duration for several units with low and high firing rates. As expected we found that intraburst duration depended on the spike rate. A positive correlation between spike rate and interburst duration was found for thresholds of 200, 400, and 600 ms for units with spike rates less than $15s^{-1}$. In units with high spike rates the intraburst duration was independent of the threshold selection. By decimating the spike rate by 50%, we found a similar positive correlation for all threshold selections. Thus, although intraburst durations increased with increasing threshold selection, similar trends were observed in decimated data sets indicating that spike burst detection depended more on the spike rate and not the selection of the threshold.

Spike burst properties and synchronization

Examples of identified bursts at the five conditions from one experiment are displayed in Figure 16D. Distributions of the burst and non-burst duration and spike rates were non-normal (K-S, $p<0.05$). Hence, the effects of desflurane on the baseline spike rate and the intra- and inter-burst spike rate and durations were estimated using the Kruskal-Wallis one-way analysis of variance (KW-ANOVA) test with the anesthetic concentration as the factor variable and the rate as the response variable. If the term was found significant, the post-hoc Dunn's test was

performed to determine a significant difference from the conscious control level (0%). Deviation from the zero slope was also tested using a linear trend planned comparison test. During wakefulness, longer burst intervals were observed. As the anesthesia level increased, the burst intervals became shorter and the intraburst spike rate increased ($p<0.05$, linear trend) displayed in Figure 16E-F (blue trace). The opposite effect was observed for interburst intervals; duration increased and spike rate decreased ($p<0.05$ linear trend) as shown in Figure 16E-F (red trace).

We also wanted to compare our results to a commonly used measure of spike burst firing patterns. As such, the height of the initial peak of the autocorrelogram histogram has been shown to indicate the presence of bursts. A negative correlation ($R^2=0.45$) between the percent of spikes observed within a burst and the ACG peak height was observed (Figure 17B) whereas, the intraburst spike rate and ACG peak height was found to be positively correlated ($R^2=0.62$) and displayed in Figure 17C.

Next we sought to examine the depth-dependent synchronization among the identified burst intervals in the cortical neuronal network. To this end, we measured the dependence of burst intervals within and across layers. The burst correlation for each rat at each concentration at each depth is displayed in Figure 18A. At most desflurane concentrations and wakefulness, intralaminar correlation was highest between 600-800 μm compared to deep layers ($p<0.01$, T-K) (Figure 18B and Table 4). When consciousness was lost (6%), the correlation across most layers (200-1200 μm) significantly decreased to a minimum ($p<0.005$, T-K). Then, at the deepest anesthetic level, the correlation once again increased across most layers from the 6% concentration level ($p<0.005$, T-K) indicating hypersynchronization among the neuronal network (Table 4). Finally, we compared the within-shank (interlaminar) correlation and found no significant difference in correlation across shanks at most concentrations (Figure 19). Once again a concentration dependent decrease in correlation was observed in most shank from 0-6%, with an increase at 8% from the 6% concentration level ($p<0.005$, T-K).

Finally, we investigated the concentration-dependent effects of desflurane on the spatial correlation of identified bursts among neighboring cells. Figure 20A displays the average spatial correlation for each rat at each concentration level arranged by the electrode contact mapping. At the 8% desflurane level, we found two typical LFP traces consisting of bursting and non-bursting patterns (Figure 20B). Therefore, we compared the spatial correlation of identified burst intervals for the two patterns. A concentration-dependent decrease was observed for non-bursting patterns ($n=4$, $p<0.05$, linear trend), whereas an initial decrease from 0-6%, followed by an increase at 8% was found ($n=4$, $p<0.05$, quadratic trend). Furthermore, a significant difference between the spatial correlation of non-bursting and bursting intervals, beginning in the unconscious level (6%) was observed ($p<0.01$, T-K).

DISCUSSION

This study for the first time investigated the concentration-dependent effects of desflurane anesthesia on spike bursts detected from spontaneous extracellular activity. We observed a gradual transformation of spike firing patterns from a unimodal to bimodal distribution commencing at low levels of desflurane anesthesia, indicating the presence of spike bursts before burst suppression in the corresponding local field is observed. Anesthesia also produced a concentration-dependent decrease in the synchronization of bursts from wakefulness to the anesthetic-induced unconscious level, signifying disconnection of the neuronal network. At the deepest anesthetic level, a significant increase in spike burst correlation was observed associated with burst-suppression pattern in the local-field, suggesting hypersynchronization due to hyperexcitability of neuronal firing patterns. This suggests that disconnection among neuronal cells is associated with the anesthetic-induced loss of consciousness, whereas hypersynchronization may be an indicator of burst-suppression found in deep anesthesia.

Methodological considerations

Several methods have been proposed to identify bursts in spike trains. The most widely used method of burst detection is the Poisson-surprise method (Legendy & Salcman, 1985; Palm, 1981). The Poisson-surprise method extracts significant bursts in a spike train by comparing the observed interspike intervals to that produced by a randomized Poisson process. Alternative methods have also been proposed using a nonparametric approach (Gourevitch & Eggermont, 2007) or a self-adaptive technique. The burst detection methods mentioned above, however, detect bursts in spike trains assuming that the train also contains spontaneous activity. While this may be favorable under active states, it is not applicable in the absence of high spontaneous activity as commonly observed during deep anesthesia, where brief periods of burst firing is observed followed by long silent intervals. In that case, applying the commonly used burst detections methods would only further segment the sparsely occurring bursts. Therefore, in this study we identified bursts by determining a critical time point between two peaks, similar to Cocatre-Zilgien and colleagues (Cocatre-Zilgien & Delcomyn, 1992), using for the first time, a the weighted interspike interval distribution.

Spike burst properties

Using a weighted interspike interval technique to enhance the occurrence of slow intervals between spikes, we have shown that anesthesia alters the firing pattern of spikes in a concentration-dependent manner, beginning at light anesthetic levels (2%). The percent of spikes found in bursts decreased from wakefulness to deep anesthesia. This suggests that anesthetics reduced the overall firing rate of the cell, which in turn suppressed the ability of spikes to form bursts. Therefore, as the results showed, the interval between spikes increased while the interburst rate decreased with anesthesia, consistent with the general idea that anesthetics work by hyperpolarizing the cell membrane potential through increased inhibition or reduced excitation (Ries & Puil, 1999a, 1999c).

Nevertheless, although the percent of spikes found in bursts decreased in a concentration-dependent manner, the firing rate of the spikes found in bursts increased. The increase in the intraburst rate was positively correlated with change in the peak height of the autocorrelogram, another indicator of bursts in spike trains (Bartho et al., 2004). Spike burst patterns have also been observed in the awake state, although at higher frequencies and irregular patterns (Destexhe et al., 1999; Greenberg, Houweling, & Kerr, 2008; Luczak et al., 2007). In all anesthetic conditions, we found that the increased firing of cells was associated with the negative component of the local-field and increased with deepening anesthesia levels, consistent with previous findings (Amzica, Neckelmann, & Steriade, 1997; Detsch et al., 2002; Nir et al., 2011; Shew, Yang, Petermann, Roy, & Plenz, 2009; Steriade, Amzica, & Contreras, 1996; Vyazovskiy, Olcese, et al., 2011). The results suggest that the administration of general anesthetics rapidly converts the temporal firing pattern of spikes to bursts as previously demonstrated with various anesthetics (Alkire et al., 2008; Amzica, 2009; Pearce et al., 1989).

Spike burst synchronization

Two typical trends associated with increasing anesthetic levels on the burst correlation of cells in neighboring channels were observed. From wakefulness to unconsciousness (0-6%), spatial correlation in the neuronal network decreased in a concentration-dependent manner. Other the hand, Erchova et al. found increasing synchronization with deepening urethane levels (Erchova et al., 2002). The lightest level of urethane in that study however was well beyond LOC and by our terminology considered deep anesthesia. We examined the anesthetic effect from wakefulness to unconsciousness and found a significant decrease in synchronization associated with LOC. At the deep anesthetic level (8%), the correlation among neighboring channels was either significantly augmented or suppressed contingent on the presence of burst suppression patterns in the LFP.

Synchronization among cortical cells has been suggested to be associated with conscious awareness (A. K. Engel et al., 1999b; Fries, 2005; Singer, 1999). Previous studies demonstrated an increase in synchronous activity associated with encoding of sensory stimuli (Berry et al., 1997; Melloni et al., 2007). Reduced synchronization was observed with several anesthetic concomitant with LOC (Imas et al., 2006; Munglani, Andrade, Sapsford, Baddeley, & Jones, 1993). In a previous study, increased 'off' periods, representing cessation of population neuronal firing, was observed in local areas of sleep-deprived animals (Vyazovskiy, Olcese, et al., 2011). Likewise, localized slow wave activity (< 1Hz) was found to be associated with alternating active and inactive neuronal states (Nir et al., 2011) . We also observed an increase in interburst durations from wakefulness to deep anesthesia. Whereas Vyazovskiy et al., looked at population off periods (Vyazovskiy, Olcese, et al., 2011), we measured interburst durations for each individual neuronal cell. The difference in the calculation may account for the larger interburst durations observed in this study.

Two possible mechanisms for loss of consciousness have been proposed. Anesthetics may produce unconsciousness by producing a possible disconnection among cortical areas (Hudetz et al., 2009; Imas et al., 2006; Tononi & Massimini, 2008). Anesthetics may also produce unconsciousness by transforming the system to a hyperexcitable state as commonly observed in epileptic induced LOC and deep anesthesia (Alkire et al., 2008). Here, we found that disconnection as observed by reduced synchrony is associated with LOC. At deep anesthetic levels, hypersynchronous activity is associated with global burst-suppression. Hence, our results are more consistent with disconnection as a mechanism of LOC. Although local correlations were investigated here, future work may focus on the anesthetic effect on spike burst synchronization between remote regions.

In general, a higher probability of recorded active units at the superficial compared to deeper cortical depths was found. As such, the average correlation was normalized to the total number of active units observed at each depth. Results demonstrated that synchronization of

bursts among neuronal pairs was depth-dependent indicating preferential within layer correlation, consistent with results from several studies that demonstrated preferential within compartment coherence associated with functional differences between cortical laminae (Maier, Adams, Aura, & Leopold, 2010; Maier, Aura, & Leopold, 2011; Sakata & Harris, 2009). Moreover, during wakefulness the correlation of synchronized bursts was highest in middle layers (600-800 μm) with a sharp decrease observed around 1200 μm depth (layer 5/6). Similarly relevant results were found with LFPs and spike correlation; enhanced activity in superficial middle layers with a sharp transitional reduction in deeper layers (Maier et al., 2010; Sakata & Harris, 2009) possibly reflecting separate functional processes for controlling propagation and directionality of information. Anesthetics reduced the intralaminar spike burst correlation in a concentration-dependent manner. At the highest concentration level increased correlation was observed in all depths, suggesting hypersynchronization concomitant with burst-suppression of the local field.

Spike burst mechanisms

Anesthetic-induced bursts are thought to be generated by the synchronized burst firing of neurons in close temporal relation to the electroencephalography (Hudetz & Imas, 2007; Steriade, Amzica, & Contreras, 1994). Burst suppression observed in EEG or LFP signals is generally accompanied by cortical hyperexcitability resulting from reduced inhibition, therefore causing a shift in the excitatory-inhibitory (E/I) balance (Amzica, 2009; Hudetz & Imas, 2007). An alteration of the E/I balance, in particular elevated E/I, may impair information processing and result in excessive correlation, also referred to as hypersynchrony, between neurons (Buzsáki, 2006; Buzsaki et al., 2007; Shew et al., 2011). We recently found evidence of elevated E/I balance in the neuronal network at anesthetic levels absent of burst suppression activity in the local-field (Vizuete et al., 2012). Furthermore, we found a concentration-dependent reduction of burst synchronization associated with loss of consciousness. Previous studies postulated that only

a subset of neurons may be responsible for the initiation of burst-suppression observed in EEG (Lukatch et al., 2005; Steriade, Amzica, et al., 1994).

In summary, our results demonstrate that a decrease in burst synchronization is associated with the anesthetic-induced unconsciousness. The reduction of burst synchronization may represent disconnection within the neuronal network suggesting a gradual disruption of coordination across the neuronal network as a result of increasing hyperexcitability. Understanding the effects of anesthesia on the temporal patterns of neuronal cells should contribute to the elucidation of how local population activity modulates global patterns in the brain across various conscious states.

Figures

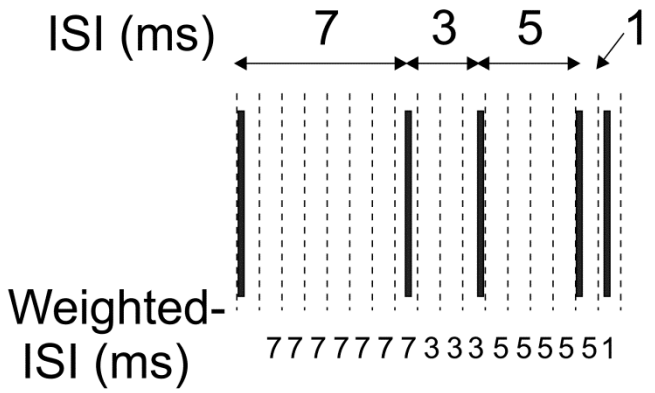

Figure 13. Illustration of duration-weighted interspike-interval calculation
Top displays the typical approach for attaining interspike interval between subsequent spike occurrences. Bottom displays duration-weighted interspike interval method. The spike train is binned by 1 ms and the time difference the between two spike onsets is placed in each 1 ms bin.

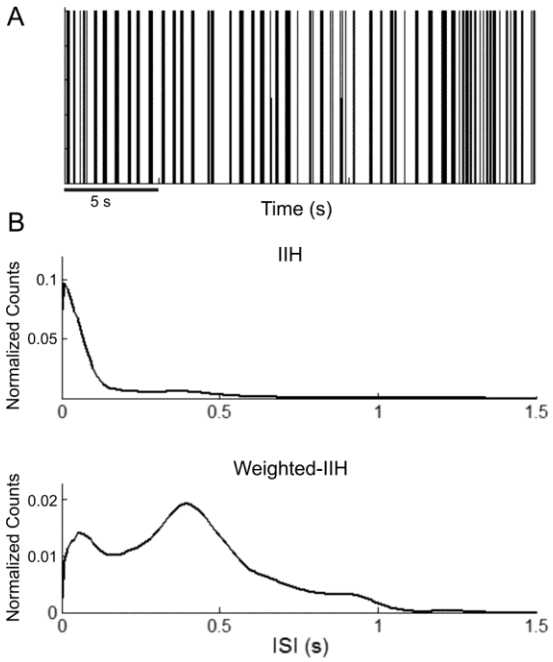

Figure 14. Inter-spike interval histogram
(A) Example of unit firing at 6% desflurane. Firing pattern displays period of increased firing followed by silent intervals. (B) Interspike interval histogram (IIH) of corresponding unit using general method (top) and duration-weighted calculation (bottom). Weighted-IIH augments slow intervals.

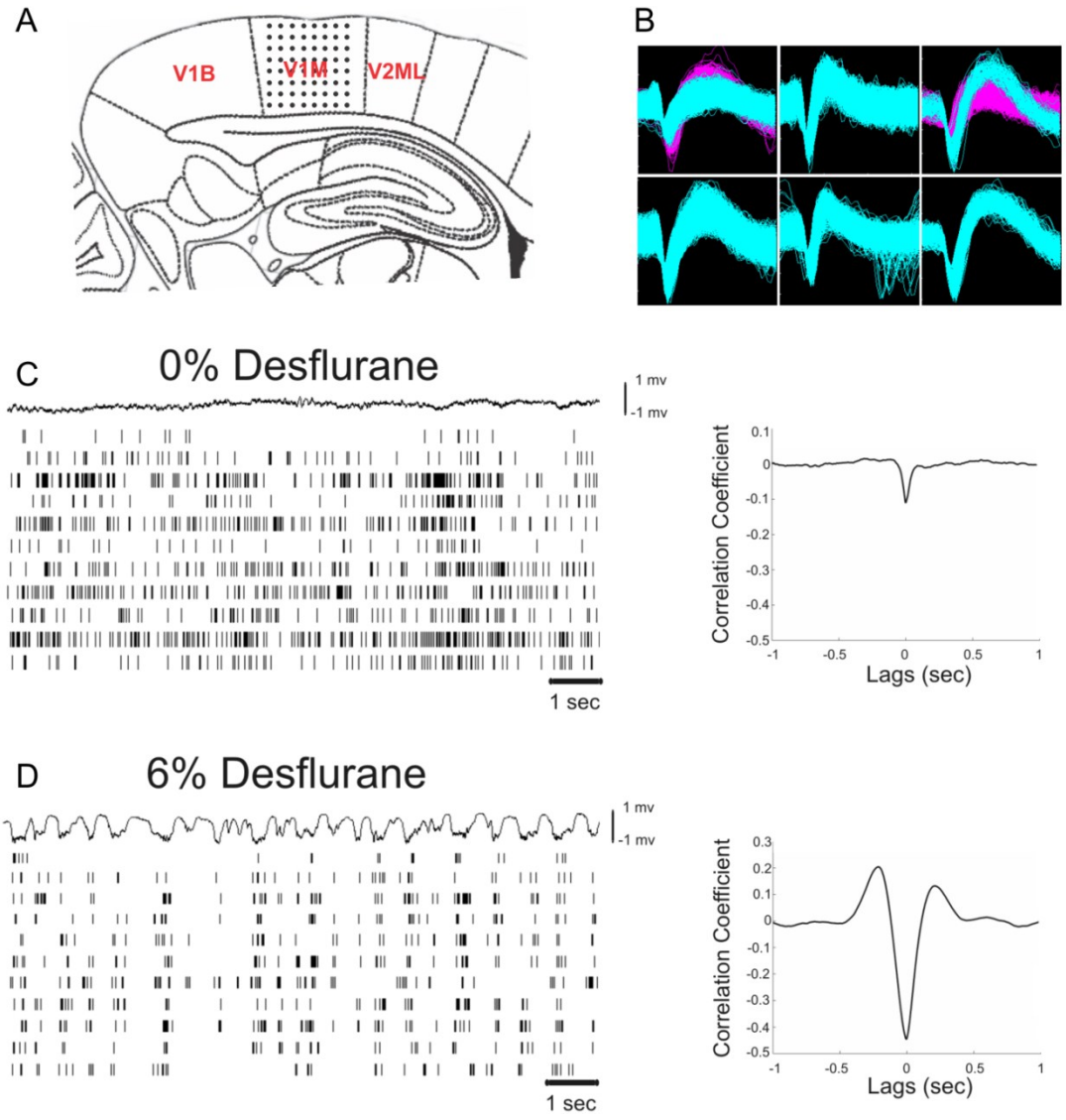

Figure 15. Schematic of Electrode Placement, Examples of Recorded Units, Raster plot with corresponding local field potential, and Spike-field correlation

(A) Electrode placement of the 64-contact neural probe in the rat primary visual cortex monocular region (V1M) in the right hemisphere. Each dot represents the approximate location of an electrode contact. Schematic is overlaid on a stereotaxic drawing obtained from the Paxinos rat brain atlas. (B) Example of recorded spike waveforms from 9 channels in one experiment. Color waveforms represent sorted units. (C) Raster plot of spontaneously responding active units along with a corresponding recorded local field potential (LFP) from a selected electrode contact at wakefulness. Continuous firing pattern during wakefulness is observed (left panel). Cross-correlogram between the population spike rate (of all active units) and the LFP in the conscious state (right panel) shows minimal correlation. (D) A burst firing pattern, displayed as brief periods of increased firing following by prolonged silent intervals, in the unconscious state is observed (left panel). A significant negative peak indicates that spike firing is maximum during the negative deflection of the LFP (right panel).

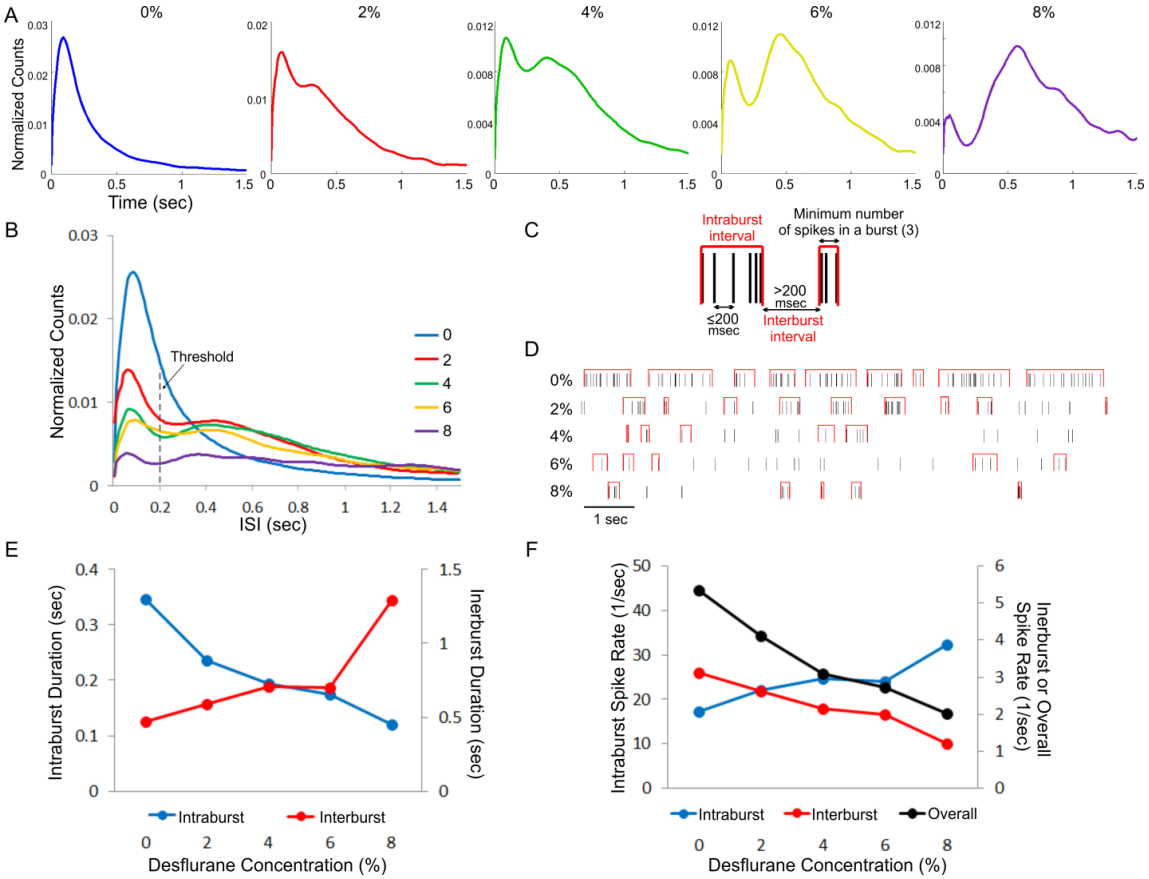

Figure 16. Weighted interspike histogram (IIH), examples of detected burst interval, and concentration-dependent properties of identified bursts and non-bursts intervals
(A) Examples of weighted interspike intervals at 5 anesthetic conditions from one experiment. A second peak at longer interspike intervals corresponding to the silent periods between the spike bursts is present in light anesthetic levels to deep anesthesia. (B) The averaged weighted IIH across all rats from 0-8%. Threshold, used to detect bursts in a spike train was determined at the deepest anesthetic level (8%) and found to be 200 ms (dashed line). (C) Demonstration of burst detection method. Intervals between spike occurrences below the threshold time and a minimum of 3 spikes classified bursts in a spike train. (D) Examples of detected burst (red trace) in a spike train (vertical black ticks) from at each anesthetic condition from one experiment. (E) Concentration-dependent effect on intraburst and interburst duration. A significant linear decrease in the intraburst duration ($p<0.05$, linear trend) and increase in interburst duration ($p<0.05$, linear trend) was observed. (F) Effect of desflurane anesthesia on the intraburst, interburst and overall spike rate. A concentration-dependent increase in the intrabust spike rate ($p<0.05$, linear trend) and decrease in interburst and overall spike rate was observed ($p<0.05$, linear trend). Data represented as median.

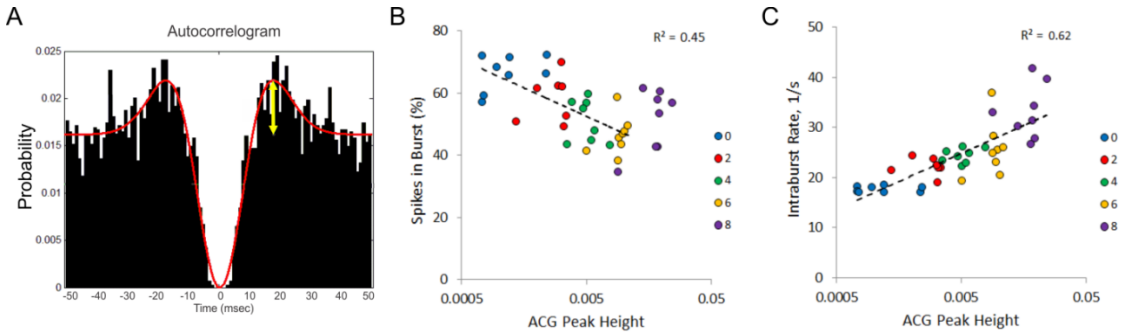

Figure 17. Relationship between Spike Burst properties and Peak Height of Autocorrelogram

(A) Example of autocorrelogram (ACG) histogram of active unit. Red trace represents inverted Mexican hat fit to the distribution. ACG peak height was measured as difference from initial peak to baseline (yellow arrow). (B) Scatter plot of percent spikes observed in bursts and ACG peak height from all rats. A negative correlation (R^2=0.45) is observed. (C) Scatter plot of the intraburst rate and ACG peak height. A positive correlation (R^2=0.62) is found indicating burst-like patterns in the spike associated with increased peak height in the autocorrelogram.

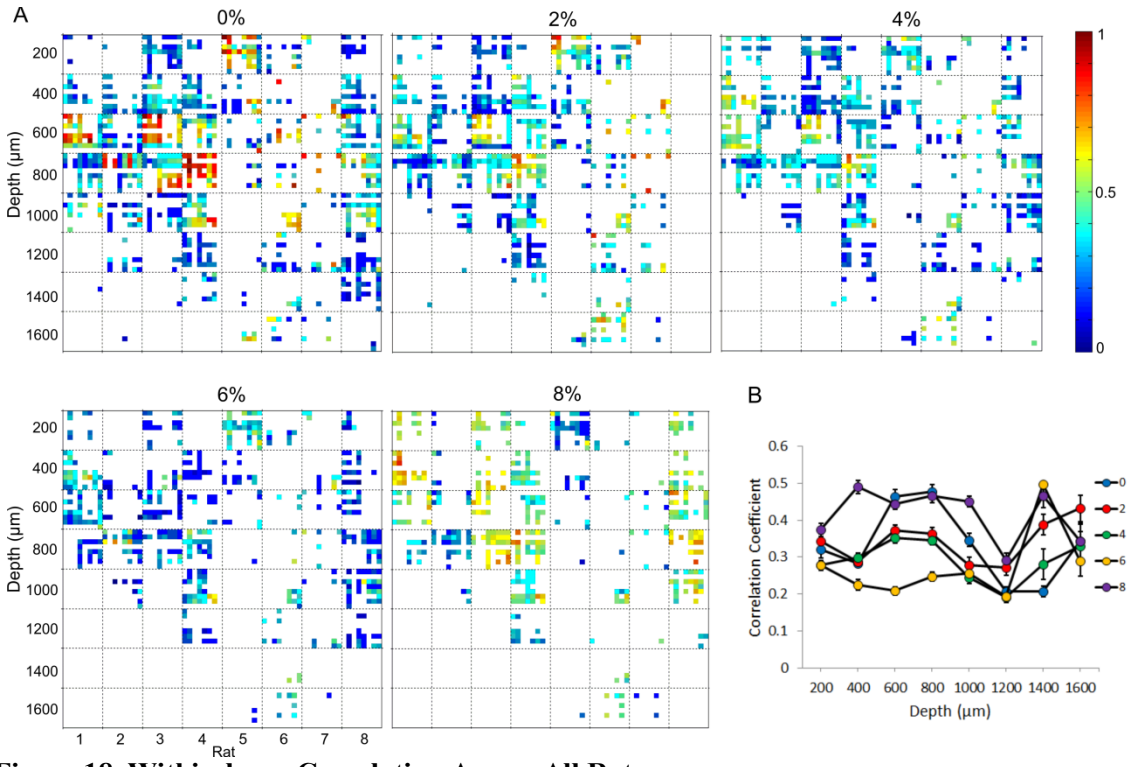

Figure 18. Within-layer Correlation Across All Rats

(A) Correlation of identified bursts between all possible unit pairs at each depth (row) for each rat (column) at the five anesthetic conditions. Colored squares within each larger square represents the correlation between all possible pairs at each depth. (B) Distribution of average correlation between neuronal pairs at each depth. During wakefulness, higher correlation was observed within 600-800 µm ($p<0.01$, T-K). At the highest anesthetic level, correlation increased ($p<0.005$, T-K) from 6% desflurane level across multiple layers (200-1000 µm).

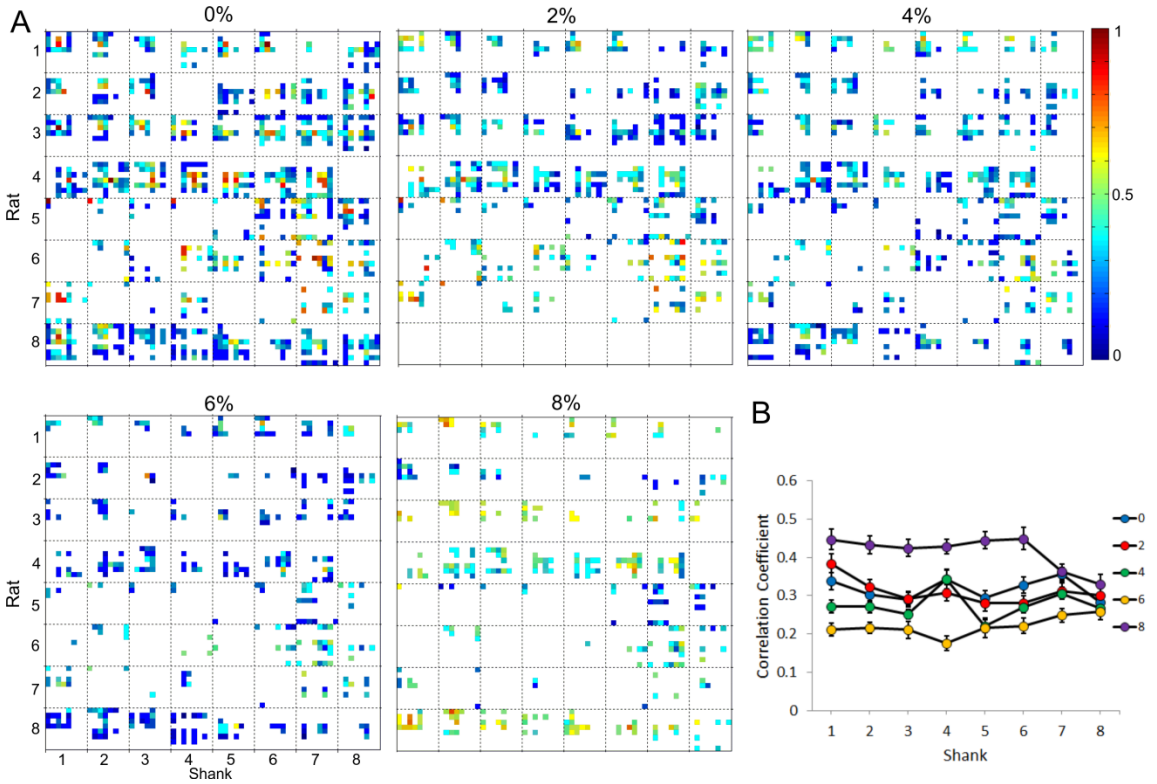

Figure 19. Within-shank correlation across all rats

(A) Correlation of identified bursts between all possible unit pairs within each shank (column) for each rat (row) at the five anesthetic conditions. Colored squares within each larger square represents the correlation between unit pairs at each shank. No difference in correlation between shanks was found. (B) Distribution of average correlation between neuronal pairs at each shank. No significant difference in correlation across shanks was found for most concentrations (0, 2, 6, 8% desflurane). Correlation within each shank decreased in a concentration-dependent manner across most shanks from 0-6% desflurane ($p<0.005$, T-K) and increased at 8% from the 6% concentration level ($p<0.005$, T-K).

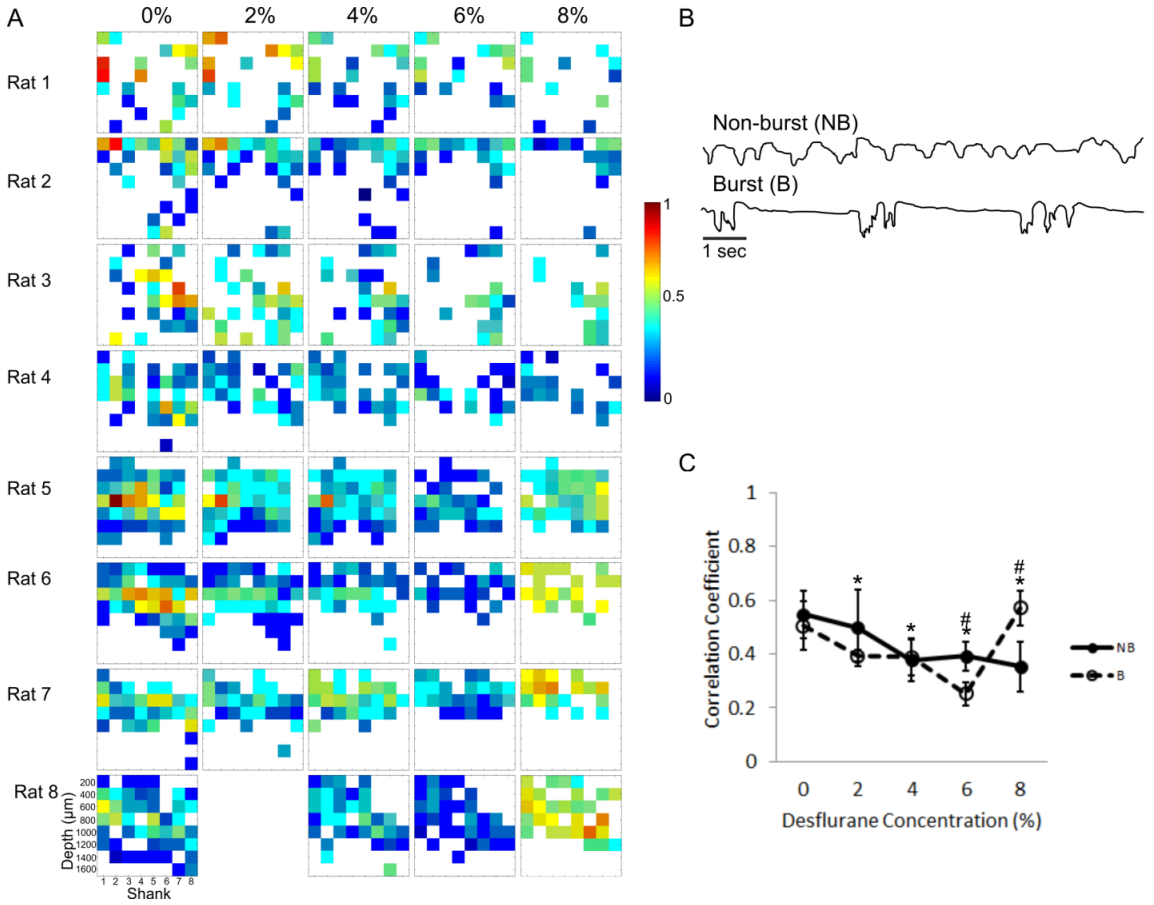

Figure 20. Concentration-dependent effects of desflurane on spatial correlation among neighboring channels

(A) Spatial correlation among neighboring channels arranged by order of electrode mapping for each rat at five anesthetic conditions. First four rats display a concentration-dependent decrease, whereas the last four rats demonstrate an increased correlation at the deepest anesthetic level (8%). The 2% concentration for rat 8 was not used in the analysis. (B) Examples of two typical patterns, representing slow-wave (NB) and burst-suppression (B) activity, observed in the local field potential (LFP) at 8% desflurane concentration level. (C) Average spatial correlation at each concentration separately for non-bursting and bursting LFP patterns. A concentration dependent decrease in spatial correlation is observed for non-burst (NB) trend (*$p<0.05$, linear trend), whereas a significant increase (*$p<0.05$, quadratic trend) at 8% is observed for burst (B) trend, indicating hypersynchronization among neighboring channels. A significant difference on the correlation of non-burst and burst types at 6-8% is observed (#$p<0.01$, T-K).

	Desflurane (%)				
	0	2	4	6	8
*Number of Units**	485	425	388	302	254
*Overall Rate, 1/s**	5.4 (4.8,6.2)	4.1 (3.6,4.7)	3.1 (2.8,3.4)	2.7 (2.4,3.1)	2.0 (1.8,2.2)
Intraburst					
*Rate, 1/s**	17.3 (17.0, 17.6)	22.2 (1.5,22.8)	24.7 (24.1,25.3)	23.9 (22.9,25.1)	32.4 (31.0,33.6)
*Duration, s**	0.35 (0.342,0.348)	0.24 (0.234,0.238)	0.19 (0.193,0.195)	0.17 (0.172,0.176)	0.12 (0.119,0.121)
Interburst					
*Rate, 1/s**	3.1 (2.8,3.5)	2.6 (2.4, 2.8)	2.2 (2.0,2.3)	2.0 (1.7,2.2)	1.2 (1.2,1.3)
*Duration,s**	0.47 (0.467,0.479)	0.59 (0.582,0.594)	0.70 (0.700,0.716)	0.70 (0.691,0.711)	1.29 (1.268,1.318)

Table 3. Properties of units and identified spike bursts from 8 experiments
A significant linear decrease in the number of active units and overall spike rates with desflurane was present. A concentration-dependent increase in the intraburst spike rate and decrease in the duration was observed. The reverse was observed for interburst intervals; significant decrease in interburst spike rate and increase in duration with increasing anesthetic levels. Data are represented as median with 95% confidence intervals. *$p < 0.05$, linear trend.

Desflurane (%)	Depth (µm) 200	400	600	800	1000	1200	1400	1600
0	0.32 (0.02)	0.28 (0.01)	0.46 (0.02)*	0.48 (0.02)*	0.35 (0.02)	0.21 (0.01)*	0.21 (0.01)*	0.34 (0.05)
2	0.34 (0.02)	0.29 (0.01)	0.37 (0.02)	0.36 (0.02)	0.28 (0.02)	0.27 (0.02)	0.39 (0.02)	0.43 (0.04)
4	0.28 (0.01)	0.30 (0.01)	0.35 (0.01)	0.34 (0.01)	0.24 (0.02)	0.19 (0.01)	0.28 (0.04)	0.33 (0.04)
6	0.28 (0.01)	0.22 (0.01)	0.21 (0.01)	0.25 (0.01)	0.26 (0.02)	0.19 (0.02)	0.50 (0.01)	0.29 (0.04)
8	0.37 (0.02)	0.49 (0.02)**	0.44 (0.02)**	0.47 (0.02)**	0.45 (0.02)**	0.29 (0.02)	0.47 (0.03)	0.34 (0.05)

Table 4. Desflurane effect on cortical depth correlation from 8 rats
At wakefulness, correlation is highest at depths 600-800 µm (*p<0.01, T-K), lowest at 1200-1400 µm (*p<0.01, T-K). Correlation increases from unconsciousness (6%) at deepest anesthetic level (**p<0.005, T-K). Data displayed as mean±SEM

CHAPTER 3

IMPAIRED NEURONAL INFORMATION INTEGRATION IN RAT CEREBRAL CORTEX ASSOCIATED WITH ANESTHETIC-INDUCED LOSS OF CONSCIOUSNESS

INTRODUCTION

How general anesthetics produce unconsciousness in humans and animals has been a fundamental and intriguing question of neuroscience (Alkire et al., 2008). Despite a substantial amount of accumulated knowledge regarding the interaction of anesthetic agents with specific receptor and molecular sites an understanding of exactly how the cellular and molecular effects of anesthetics translate to cognitive functional alterations remains unclear. In one prevailing theory (Tononi, 2004), loss of consciousness results from a failure of information and integration by neuronal networks, due to specific changes in synaptic transmission and a disruption of neuronal communication. Reduced functional integration has been observed under anesthesia (Schrouff et al., 2011), vegetative state (Boly et al., 2009; Zhou et al., 2011) and sleep (Tononi & Massimini, 2008).

Equally important, the capacity for information processing in the brain may be hampered under anesthesia by a diminution of the possible functional configurations of neuronal signaling. Consciousness has been characterized as requiring a large repertoire of cortical states (information) that can be functionally integrated (integration) (Alkire et al., 2008; Tononi, Edelman, & Sporns, 1998). When the number of discriminable patterns is diminished, information becomes less informative although it may still be highly integrated as in hypersynchronized burst-suppression patterns in deep anesthesia levels (Ferron et al., 2009; Hudetz & Imas, 2007) and generalized seizures (Tononi, 2004). Anesthetic agents may suppress

consciousness by reducing the number of available brain states and consequently diminishing information integration (Alkire et al., 2008; Tononi & Edelman, 1998a).

Various arousal levels and pharmacologic conditions are known to modulate spontaneous (Vizuete et al., 2012) as well as evoked firing activity (Hudetz et al., 2009) of neurons. Anesthetics were shown to suppress the long-latency (>100 ms) component of visual responses, possibly indicating a preferential suppression of feedback connections (Hudetz et al., 2009). Likewise, reduction of the late component was also observed in non-detected stimuli (Lamme & Roelfsema, 2000; Super, Spekreijse, & Lamme, 2001). Anesthetics were also shown to suppress spontaneous functional connectivity in the neuronal groups (Vizuete et al., 2012). Therefore, anesthetics may work by impairing recurrent functional connections and thus information integration.

Increasing evidence has shown that the temporal organization of spike firing among neuronal groups, specifically synchronized activity, may contribute to neural coding as opposed to firing rate (Berry et al., 1997; Grun, Diesmann, & Aertsen, 2002; Lawhern, Nikonov, Wu, & Contreras, 2011; Uzzell & Chichilnisky, 2004). Likewise, information flow is thought to be regulated by the synchronization of spiking activity in neuronal populations (Mainen & Sejnowski, 1995). Conscious awareness, language, memory encoding and retrieval are thought to involve synchronization among cortical neurons for information processing (A. K. Engel, Fries, Konig, Brecht, & Singer, 1999a; A. K. Engel et al., 1999b; Singer & Gray, 1995).

Previous investigations have focused on identifying coincident firing patterns in the neuronal network (Grun et al., 2002; Grun, Diesmann, Grammont, Riehle, & Aertsen, 1999) as they may contribute to behavior and sensory processing. Less is known about how spiking activity patterns of interacting neuronal populations are altered as a function of state, and how the altered dynamics may affect the capacity of the neuronal system for information processing. ***I hypothesized that the anesthetic-induced unconsciousness is associated with a reduction of information capacity in the cortical neuronal network.***

In this study, I examined the concentration-dependent effects of desflurane anesthesia on the flash evoked neuronal response of active neurons. To this end, I compared three measures of information capacity on coincident firing patterns from a local neuronal population in the waking state and at several graded steady-state desflurane concentrations levels. Specifically, we examined how altered states of consciousness affected information capacity in the cortical neuronal network.

DATA ANALYSIS

General surgical, experimental and neuronal recording methods follow those described for Chapters 1 and 2. At each condition, 110-120 discrete flashes (~5ms) were randomly delivered with an interstimulus interval of 5-15 seconds via an implanted LED. The neuronal response to flash was recorded first under anesthetized conditions at desflurane concentrations of 8, 6, 4 and 2%, and then at wakefulness.

Data segmentation

Each flash trial was segmented into a pre-stimulus component (-250 to 0 ms) and post-stimulus component (0 to 250 ms). All trial segments were then concatenated for each component separately to form one spike train for each active unit.

Unique patterns

Coincident spiking within the neuronal population was used as an estimate of the repertoire of available states within a neuronal population over time. As such, in order to measure the number of coincidence firing patterns, the timestamps of spike occurrences of each neuronal unit was transformed into a binary time series with a 1 ms bin size. Each bin received a 1 if a spike occurred within that time bin and 0 if no firing was observed. For N neurons, there are 2^N possible states that could be observed during a recording. The activities of the individual neurons i is then described by parallel binary sequences, $x_i(t)$. The simultaneous spiking activity of N neurons is described as a time sequence shown below:

$$\mathbf{x}(t) = \begin{bmatrix} x_1(t) \\ \vdots \\ x_i(t) \\ \vdots \\ x_N(t) \end{bmatrix}$$

where, $i = 1, \ldots N;\ t = 0, \ldots . T - 1;\ x_i(t) \in \{0,1\}$; and p_i is the firing probability of each neuron i.

A histogram (X) of the number of times each pattern, $\mathbf{x}(t)$, is observed in the time sequence across all units is then produced and normalized to the total number of unique patterns observed within the system.

To determine the information produced by the distribution of observed firing patterns within the cortical network across all recording sites, information capacity was measured using three non-linear information-theoretic measures, integration (Jordan, 1999; Watanabe, 1960), interaction entropy (Shew et al., 2011) and interaction complexity (Tononi & Edelman, 1998a).

Total Correlation (Integration)

Integration (I) measures the amount of redundancy among the neuronal groups in a system. Integration has also been referred to as total correlation (Watanabe, 1960) and multi-information (Jordan, 1999). It is expressed as:

$$I(X) = \sum_{i=1}^{N} H(x_i) - H(X)$$

where $H(x_i)$ is the information entropy of the firing probability of each unit in the system and $H(X)$ is the joint entropy of observed patterns across all units. $I(X)$ is zero if the elements in the system are statistically independent. As such, total correlation quantifies the information of the system shared among its units from that of the individual units if they were totally independent of one another.

Interaction Entropy (Entropy)

Interaction entropy is more specific as it measures the amount of redundancy in the system due to the correlation among the neuronal population [Shew, 2011; Abbot 2001]. To remove the contribution of uncorrelated spike events to the entropy measure, the time series were shuffled by a random time lag. The shuffling removes the correlation among the channels while maintaining the average spike rate of each channel. The shuffling was performed five times and

the average entropy of the shuffled surrogate dataset was calculated. Interaction entropy is calculated as the difference of entropy of the coincident spike patterns and that formed by random shuffling of the data, $H(X)$- $Hs(X)$. Interaction entropy estimates the information associated with nonrandom correlations in the neuronal population.

Interaction Complexity (Complexity)

Interaction complexity (CI) measures the amount of the entropy of a system that is accounted for by the interactions among its elements (Tononi, Edelman, et al., 1998). It is measured by computing amount of entropy between each element conditioned by the entropy of the rest of the system (Sporns, Tononi, & Edelman, 2000; Tononi, McIntosh, et al., 1998). The mathematical equation describing complexity is shown as:

$$CI(X) = H(X) - \sum_{j=1}^{N} H(X_j|X - X_j)$$

Here $H(X)$ is the entropy of the coincident spike patterns in the system and $H(X_j|X - X_j)$ is the conditional entropy of a subset of the system X_j with one unit removed, conditioned on its complement $X - X_j$, and the sum is over all possible subpatterns. The value of CI is high for complex systems and it is low both for random and completely regular systems. The contribution of uncorrelated spike events was removed using the same shuffling procedure described above.

The three measures of information capacity were calculated for pre and post stimulus trials at each anesthetic condition and wakefulness. Data analysis was performed using MATLAB 2011a (MathWorks).

Statistical assessment

The concentration-dependent effect of desflurane on overall firing rates, number of active units was estimated using the repeated measures analysis of variance (RM-ANOVA) test with the anesthetic concentration as a fixed factor, the subject (rat) as within factor. Deviation from the

zero slope was tested using a linear trend planned comparison test. The desflurane effect on number of unique patterns, the number of spikes, and the entropy measures for pre- and post-stimulus conditions was tested using the same method with the anesthetic condition as a fixed factor, the rat and stimulus (pre or post) as within factors. When found significant, the component effects were further examined using the Tukey-Kramer (T-K) post-hoc test. Statistical analyses were performed using NCSS 2007 (NCSS, Kaysville UT).

RESULTS

Spike properties

Figure 21 displays an example of a raster plot of two responding units at each desflurane concentration level. In all desflurane levels, spike firing increased after flash. In 6 rats, a concentration-dependent decrease in the number of active units ($>1s^{-1}$) and overall spike rate (linear regression, $p<0.05$) was observed (Table 5). Across all conditions, the number of unique patterns and number of spikes for post-stimulus was greater than pre-stimulus conditions ($p<0.01$, RM-ANOVA). Desflurane significantly decreased both the number of unique patterns and spikes of pre- and post-stimulus components ($p<0.05$, linear regression, Table 5).

Figure 22 displays an example of the spike pattern distribution for one experiment for all anesthetic conditions. As the desflurane level increases, the pre-stimulus spike pattern distribution become sparse, however, the stimulus response remains (Figure 22B).

Information capacity

A significant difference between pre- and post-stimulus components were observed for integration, entropy and complexity, shown in Figure 24A ($p<0.01$, RM-ANOVA). A significant decrease in integration from wakefulness starting at 6%, (*$p<0.05$, T-K), entropy at 8% (*$p<0.5$, T-K), and gradual decrease in complexity (*$p<0.05$, T-K) was observed.

I considered the possibility that the significant difference between pre- and post-stimulus components could be due to the increased spike firing observed after the flash onset (Figure 21). A scatterplot of integration, entropy and complexity versus the spike count for pre- and post-stimulus components revealed a significant correlation between post-stimulus integration (R^2=0.72) and both pre- and post-stimulus components of complexity (R^2=0.92 and R^2=0.89, respectively) and is displayed in Figure 26.

To eliminate this effect, the post-stimulus number of spikes was decimated to approximately equal the pre-stimulus spike count as illustrated in Figure 23. As such, in order to maintain the temporal pattern and total duration while reducing the number of spikes occurrences, segments of spiking activity across all units were converted to 0 (indicating no spike is present) until the total spike count of the post-stimulus component was less than or equal to the pre-stimulus component. Measures of information capacity were once again calculated. Results showed a significant difference between the flash components for integration only (#p<0.01, RM-ANOVA, Figure 24B) that decreased in a concentration dependent manner (Figure 25). Upon loss of consciousness with desflurane (6%) integration and entropy was significantly suppressed (*p<0.05, T-K). A significant concentration-dependent decrease in complexity was also observed (*p<0.05, T-K) and displayed in Figure 24B.

Next, I investigated whether the concentration-dependent reduction of information capacity was due to the lower number of spike counts at the deepest anesthetic level. Once again segments of data from the post-stimulus component at each concentration was decimated to be approximately equivalent to the pre-stimulus number of spikes at 8% desflurane level. The effect of the decimation resulted in a significant reduction of integration at 6% from wakefulness (*p<0.05, T-K) and a significant difference in integration between both stimulus components (#p<0.01, RM-ANOVA), shown in Figure 24C and Figure 25. No effect of desflurane on entropy or complexity was observed (Figure 24 and Figure 25).

Additional dataset

In an additional 7 rats, a 49 pin rectangular (7x7, 400 μm spacing 400 μm) electrode array (Cyberkinetics Neurotechnology Systems, Salt Lake City, UT) was acutely implanted within V1M (7.0 mm posterior, 3-3.5mm lateral, relative to bregma) to a depth approximately within layer 5 (1.0-1.5 mm) and displayed in Figure 27. The cortical neuronal response to flash stimulus, presented every 5 seconds, at desflurane levels of 2, 4, 6, and 8% was recorded. Wakefulness was not examined and recording was performed under restrained conditions. Results showed that the increase in post-flash information capacity was accounted for by the change in spike rate (Figure 28A-B). Furthermore, when the influence of spike rate was removed from the measure of information capacity, a significant decrease from wakefulness in integration and entropy was observed at the deepest anesthetic level (8%) as shown in Figure 28C.

DISCUSSION

Here, I examined the concentration-dependent effects of desflurane anesthesia on the cortical information capacity of responding cells to flash stimuli. The cortical unit response to flash stimulation was compared to the pre-stimulus activity using three measures of information capacity. Our results showed a significant reduction of information integration at the anesthetic-induced unconsciousness level (6%), whereas changes to entropy and complexity was accounted for by the change in spike count. Furthermore, information integration of the cortical response to flash was higher than its pre-stimulus baseline. The results suggest that (1) information integration in the visual cortex is modulated by the presence of visual stimuli and (2) anesthetics reduce information capacity upon loss of consciousness by limiting the number of available states across all active units.

Increasing interest in the spatiotemporal dynamics of sensory processing in the cerebral cortex has been recently demonstrated. Information is thought to be conveyed by the integration of activity from specialized groups of neurons in order to guide behavior and actions (Tononi &

Edelman, 1998b). Furthermore, anesthesia is thought to suppress consciousness by blocking the brain's ability to process and integrate information (Alkire et al., 2008; Tononi, 2004). Interestingly, the significant reduction in information integration was observed at the desflurane concentration level known to produce unconsciousness (6%) as measured by the loss of righting reflex (LORR) (Imas et al., 2006).

Pre- versus post-stimulus information capacity

In general, the cortical unit response to flash in the visual cortex of the rat is composed of two main components, described as an initial (0-100 ms) and long-latency (>150 ms) response (Chapin, Waterhouse, & Woodward, 1981; Hudetz et al., 2009; Ikeda & Wright, 1974b; Robson, 1967). Desflurane anesthesia was found to attenuate the long-latency response to flash, whereas no significant change was observed for the early response (Hudetz et al., 2009). Here, the interval at which information capacity was calculated included both types of stimulus-induced response components (early and late). The higher capacity for information integration observed for the post-flash response compared to pre-stimulus activity may be due increased number of unique patterns reflecting a larger repertoire of available states. The significant drop in integration upon loss of consciousness may be associated with the anesthetic-induced suppression of the long-latency component, thought to reflect high order feedback processing of sensory information (Lamme & Roelfsema, 2000; Lamme et al., 1998) and consequently a reduced repertoire of independent states. Future studies to test this theory are warranted.

Decimation effect on information capacity

Most of the observed changes in information capacity were accounted for by the change in spike count. When the information capacity measure was corrected by decimating to the pre-stimulus spike count, the observed increase in entropy and complexity of the flash response component was removed. Integration however, remained resistant to the decimation. Next, when the flash component was decimated to the pre-stimulus spike count at the deepest anesthetic level,

the observed anesthetic-induced reduction in entropy and complexity was eliminated, indicating that the two measures may reflect changes to spike rate and not veritable effects of desflurane. The fact that integration remained impervious to decimation suggests latent effects of the network behavior itself that cannot be accounted for by changes in spike count.

Using surrogate datasets at which spike count remained constant but firing patterns were completely synchronized, a low complexity value was found (data not shown), consistent with previous findings (Crutchfield & Young, 1989; Tononi & Edelman, 1998b; Tononi, Sporns, & Edelman, 1994). The opposite effect was found with integration and interaction entropy of completely synchronized data. When data sets were randomized, integration and entropy decreased whereas CI was similar to the original data set. Furthermore, the changes in complexity were solely accounted for by the change in spike count. Interaction complexity is believed to related to the measure of neural complexity except the average values of integration and mutual information determined by all possible subsets in the network are not included in the calculation of CI (Tononi, Edelman, et al., 1998). The difference in how complexity is estimated may the reason for the discrepancy. Interaction entropy was found to be weakly correlated with the change in spike count. Decimation, however, removed the anesthetic-induced difference in entropy between post- and pre-flash activity and the desflurane induced reduction.

In order to further investigate the effect of decimation on information capacity, a surrogate dataset consisting of completely synchronized spike occurrences was decimated in two ways: by converting duration segments of spike occurrences to 0 or by removing segments across all units. The former reduced information capacity for all three measures, indicating that the number of available states is reduced. On the other hand, by completely removing segments of time and hence total duration, we saw a different effect. Reduction by removal either caused an increase of decrease in the three measures of information capacity. Hence, longer datasets may need to be acquired to eliminate the dependency of entropy measures on the distribution of spike patterns.

Inter- versus intra-laminar information capacity

Information capacity using the rectangular 49-pin array differed from the 64 pin multi-shank neural probe. With the rectangular array, a significant change in integration and entropy was observed at the deepest anesthetic level. Moreover, all differences in information capacity of pre- and post-stimulus components were mainly due to the increased spike count of responding units. The differences in the results between the two datasets may be due to several factors. With the 64 pin array, each electrode shank spanned the entire depth of the cortex, recording from eight equally-spaced depths and eight equally spaced positions of 250 μm. With the 49 pin rectangular microelectrode array, recording was obtained from 49 equally spaced electrodes (400 μm) approximately located in the output layer (V-VI). Furthermore, the experimental protocol differed. With the 49-pin array, animals were anesthetized, tracheotomized, paralyzed with gallamine triethiodide (80 mg, IV), and artificially ventilated using a rodent ventilator (SAR 830/P; CWE, Ardmore, PA). Femoral arterial and venous lines were placed for monitoring blood pressure and periodic check of blood gases.

Visual processing is thought to initiate in sugranular cortical layers (Felleman & Van Essen, 1991; van der Togt, Spekreijse, & Super, 2005) whereas secondary processing originates in infragranular layers (Mitzdorf, 1994). Thus, with the multi-shank electrode that spans several cortical depths, information integration includes both input and output processing. Furthermore, the distance between electrode contacts of the 64 pin array was shorter than the 49 pin array. Increased correlation among neighboring neurons have been previously reported (Bartho et al., 2004; Fujisawa et al., 2008) and hence the difference in the results could reflect distance dependent correlation and sensory processing in the neuronal network.

In summary, our results demonstrate that general anesthesia reduces integration at the concentration level associated with loss of consciousness. The reduction in integration may result from a smaller number of available states in the neuronal network. Understanding the state-

dependent effects on neuronal firing patterns will help elucidate how the network population processes information in the brain.

Figures

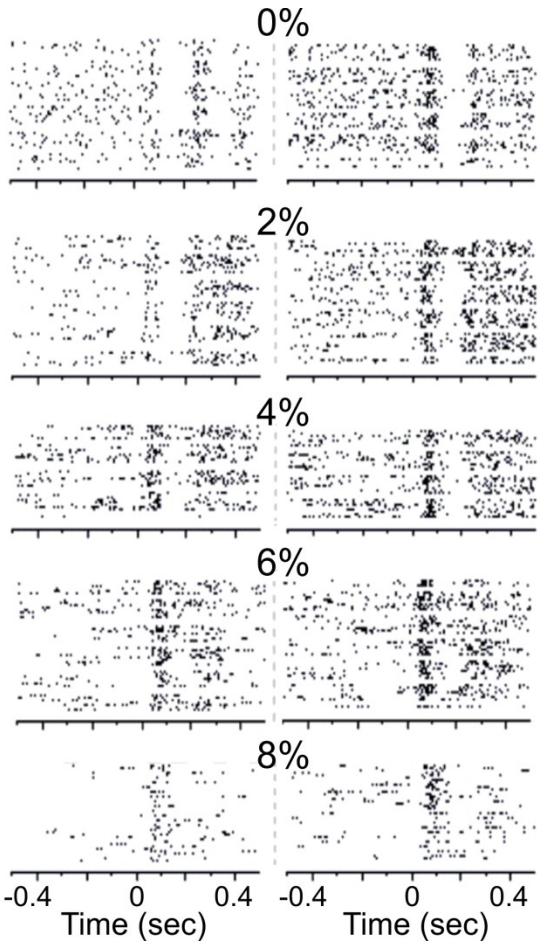

Figure 21. Raster plots two responding units at 5 desflurane levels.
Each row represents a flash trial with time 0 indicating the flash onset. Each tick in this raster plot represents the time of spike occurrence. At wakefulness (0%), an initial peak (<100 ms) followed by a secondary long-latency (>150 ms) peak is observed. As anesthesia level increases, the long-latency component is suppressed. Pre-stimulus component consisted of spike activity 250 ms before presentation of flash (-250 to 0 ms), whereas the post-stimulus component was composed of spiking activity 250 ms after flash (0 to 250 ms).

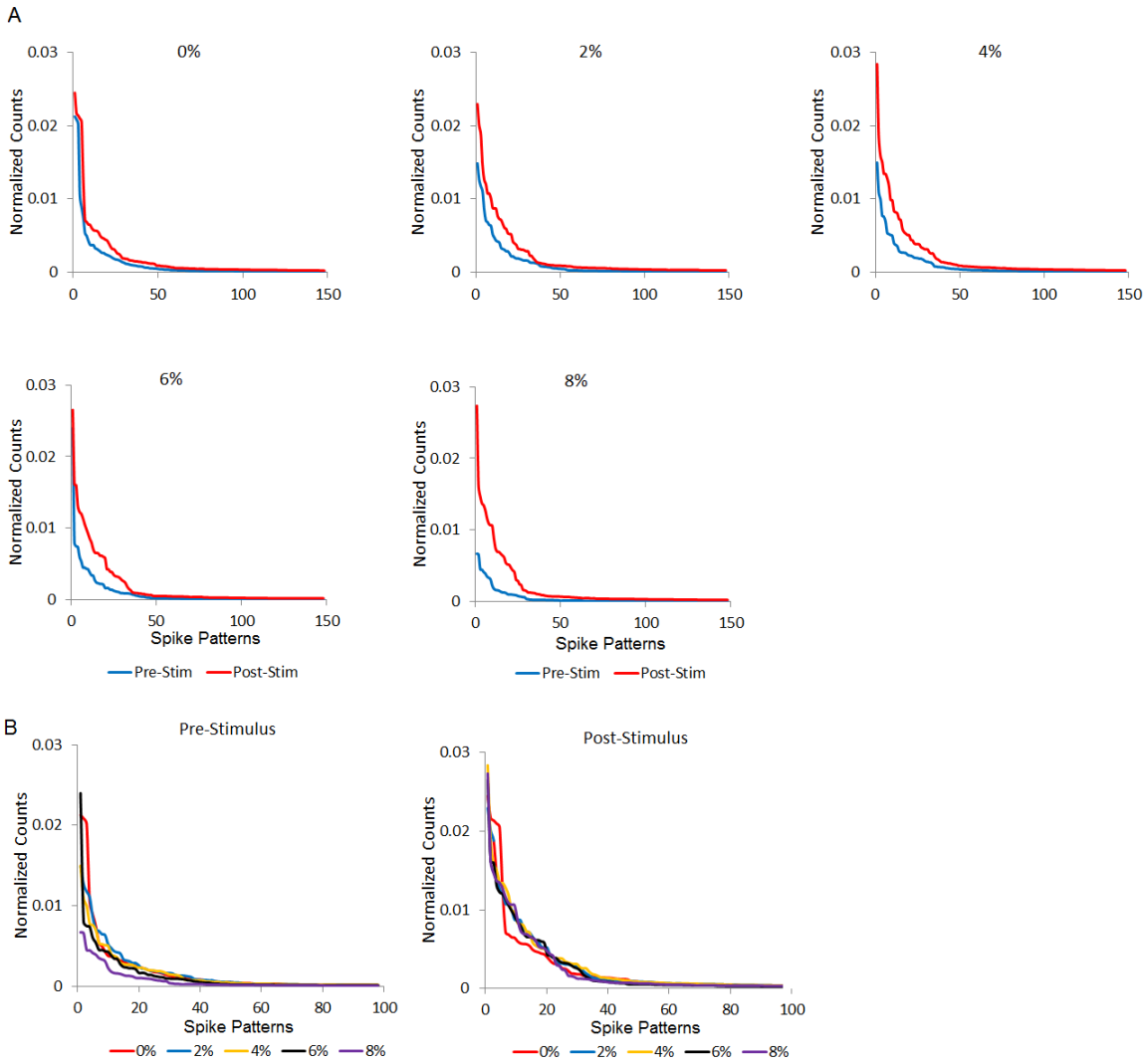

Figure 22. Example of spike pattern distribution from one experiment
(A) Top panels represent normalized distribution of pre-stimulus (blue) and post-stimulus (red) spike patterns at 5 desflurane levels for one experiment. For clarity, the number of counts of no firing represented as a spike pattern of 0 was removed from distribution. (B) Bottom panels display the spike pattern distribution for pre-stimulus (left) and post-stimulus (right) components at five anesthetic conditions. Pre-stimulus distribution is reduced with desflurane anesthesia whereas post-stimulus spike pattern distribution remains relatively stable.

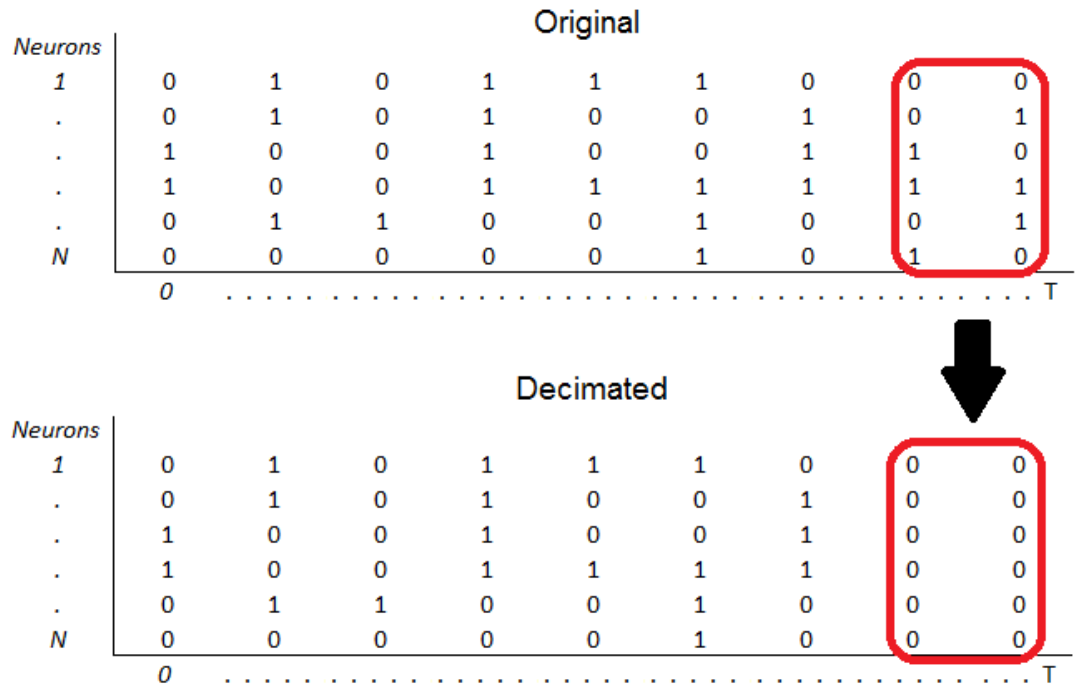

Figure 23. Illustration of decimation
Example of binarized spike train for N neurons over time (T). Decimation was performed by converting time segments of spike occurrences to zero.

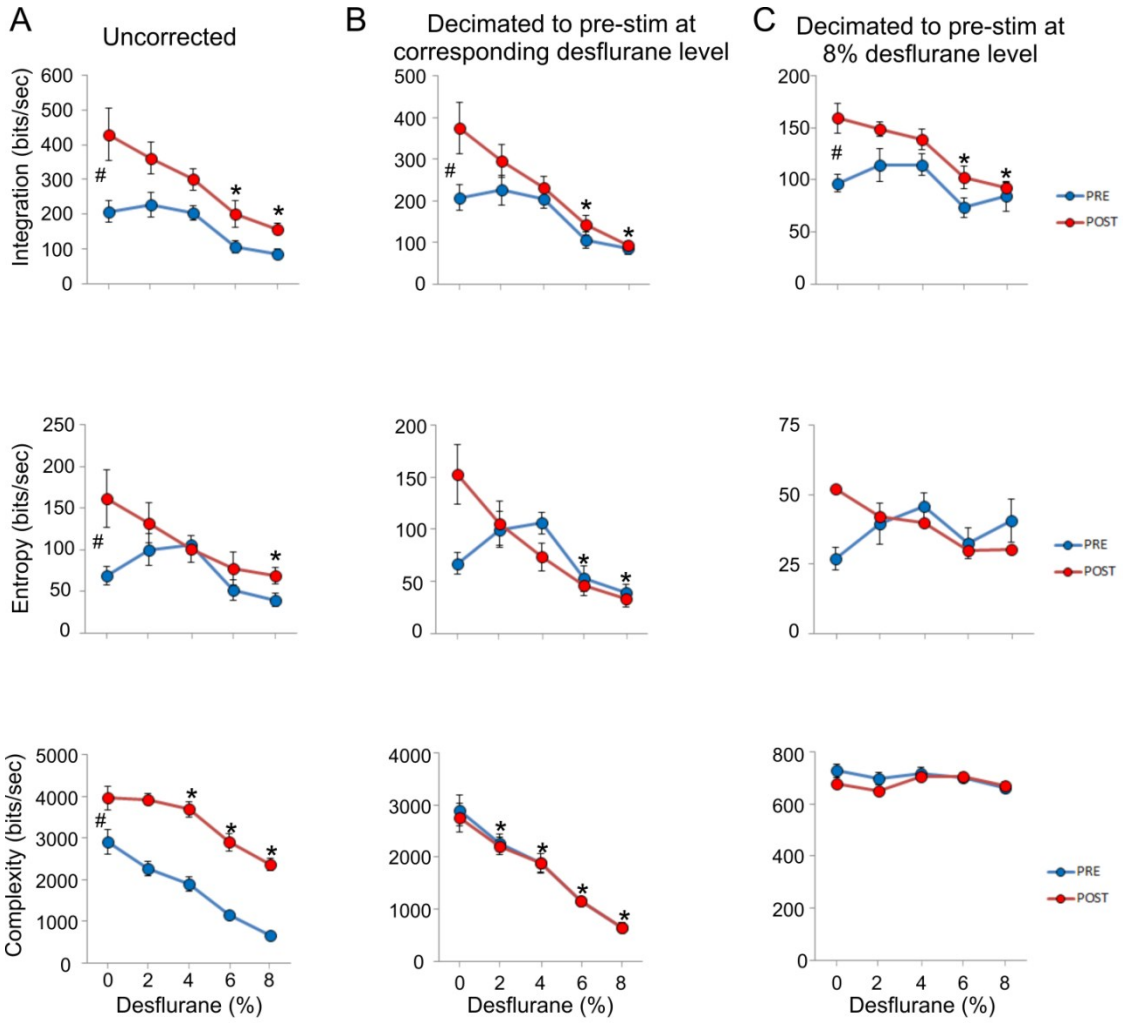

Figure 24. Desflurane effect on information capacity of multi-shank probe
(A) Concentration-dependent effects of desflurane anesthesia on integration (top), interaction entropy (middle) and interaction complexity (bottom). Overall information capacity was greater for flash response component than its baseline (#p<0.01, RM-ANOVA). Anesthesia reduced integration at 6-8% (*p<0.05, T-K), entropy at 8% (*p<0.05, T-K) and complexity from 4-8% (*p<0.05, T-K). (B) Time segments of spikes firing across all units were decimated to approximate the total number of spike in the pre-stimulus condition. Integration was insensitive to change in spike count and displayed increased integration of flash response (#p<0.01, T-K). Integration was significantly reduced from 6-8%, entropy from 6-8% and complexity from 2-8% (*p<0.05, T-K). The increase in post-stimulus entropy and complexity measure is accounted for by change in spike count. (C). Finally, time segments across all units were decimated to its baseline spike count at the deepest anesthetic level (8%). The change in information capacity for entropy and complexity could be accounted for by the reduction of spike counts, whereas integration was unaffected by the change in spike count. Integration for units response was greater than pre-stimulus baseline (#p<0.01, RM-ANOVA) and integration was significantly suppressed from 6-8% (*p<0.05, T-K).

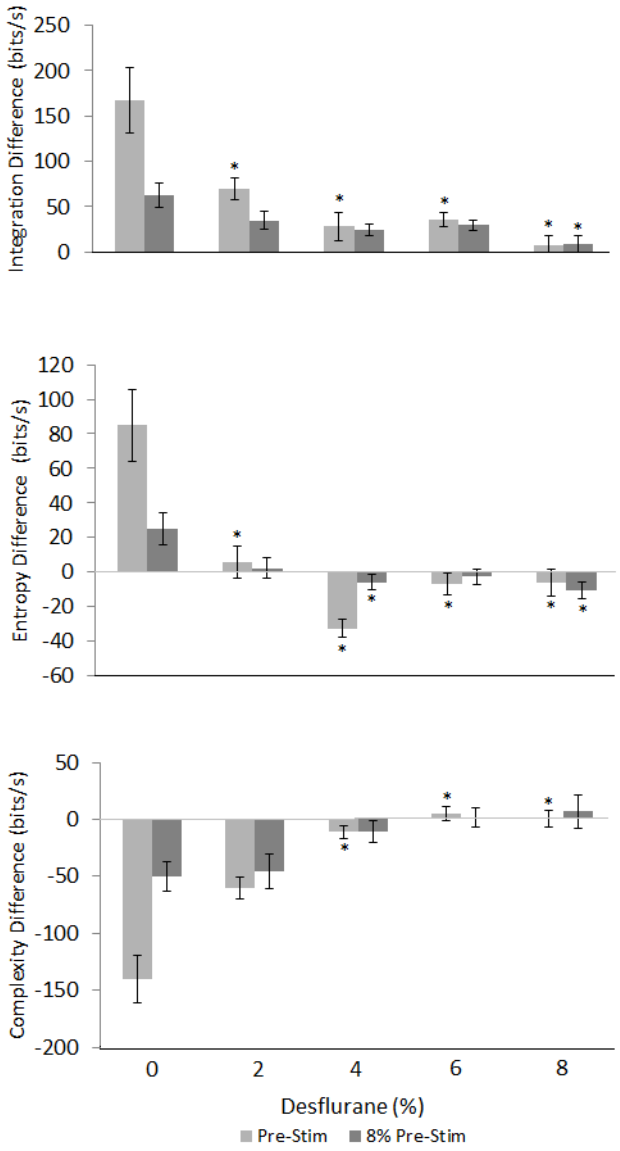

Figure 25. Concentration-dependent effects on the difference in information capacity between post-flash and pre-flash spiking activity

Desflurane reduces information capacity ($p<0.05$, T-K) of flash-component in integration (top), entropy (middle) and complexity (bottom).

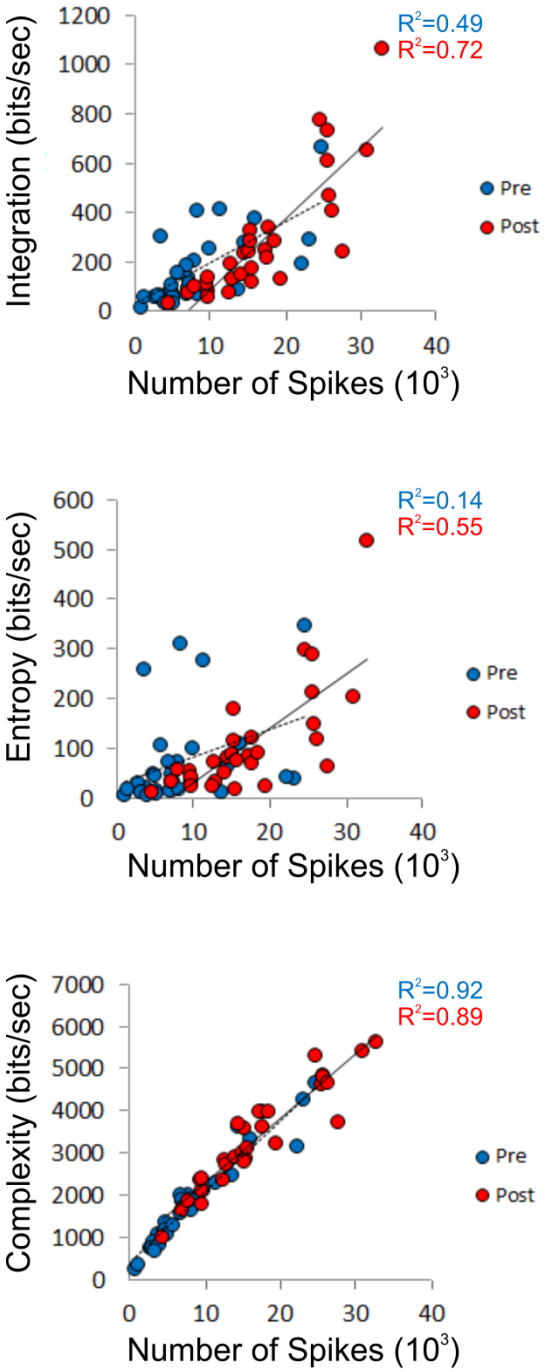

Figure 26. Scatterplot of information capacity and number of spikes across all concentrations.

A high correlation between integration (top) of post-stimulus number of spikes (R^2=0.72) is observed whereas a low correlation is present for pre-stimulus component (R^2=0.49). Interaction entropy (middle) is not correlated with increased number of spikes for both flash components (pre-stimulus: R^2=0.14, post-stimulus: R^2=0.55). Complexity (bottom) is highly correlated with the increased number of spikes of the pre-and post-stimulus components (R^2=0.92 and R^2=0.89, respectively).

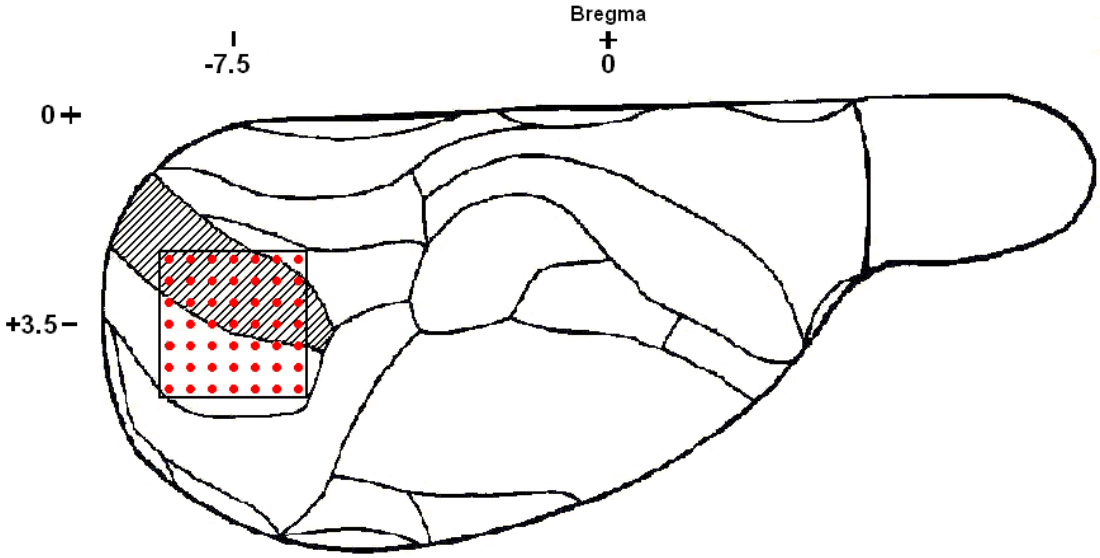

Figure 27. Electrode placement of 49-pin array.
Outline of electrode placement as viewed from the dorsal surface of the right hemisphere of the rat brain. Each dot represents an electrode penetrating at approximately a right angle to the brain surface. *Coordinates* indicate the location of the center of the electrode array relative to Bregma. *Shaded area* is the monocular region of the primary visual cortex. The region immediately lateral is the binocular region of the primary visual cortex. *Extracted from Hudetz et al. Anesthesiology 2009; 111:231–9.*

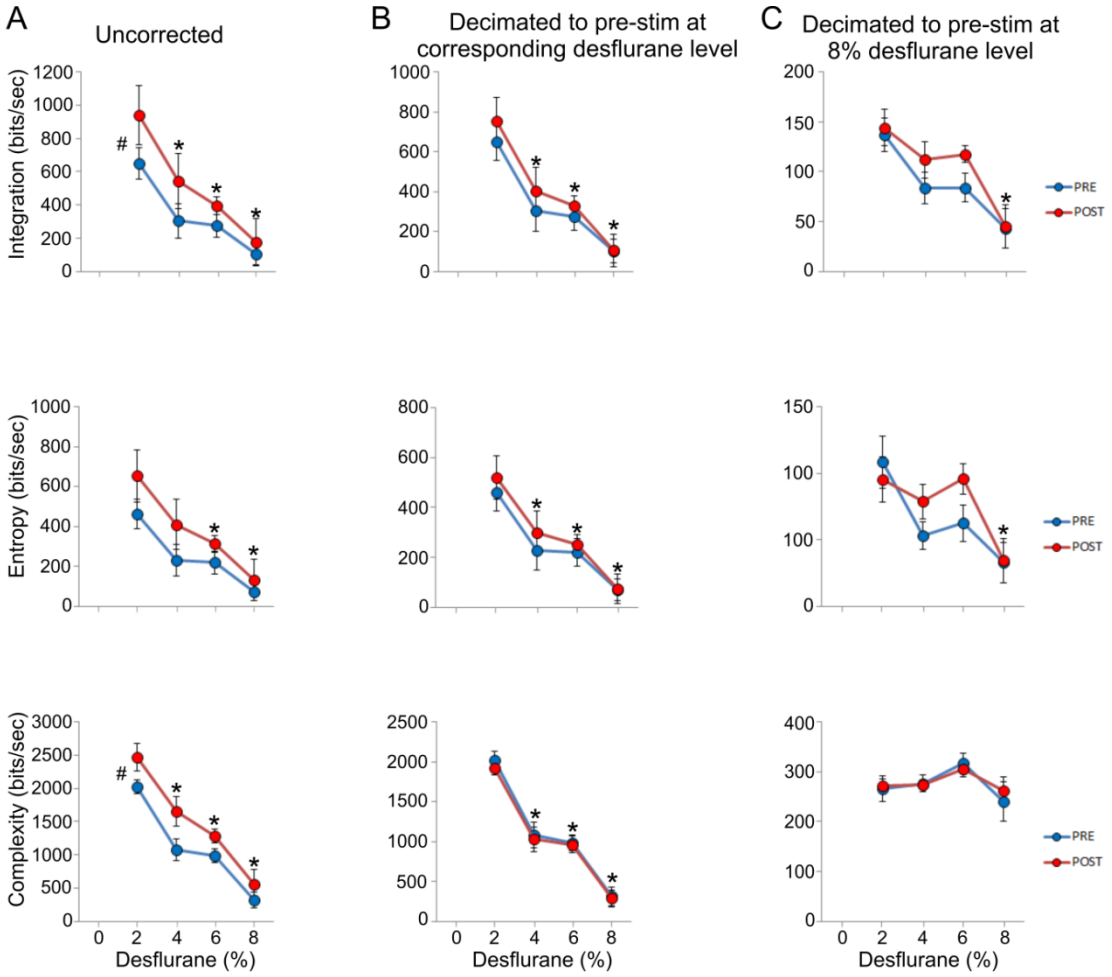

Figure 28. Desflurane effect on information capacity of 49 pin array implanted in layer 5 of visual cortex.

(A) Concentration-dependent effects of desflurane anesthesia on integration (top), interaction entropy (middle) and interaction complexity (bottom). Integration (top) and interaction complexity (bottom) was greater for flash response component than its baseline (#p<0.01, RM-ANOVA). Anesthesia reduced integration at 4-8% (*p<0.05, T-K), entropy at 6-8% (*p<0.05, T-K) and complexity at 4-8% (*p<0.05, T-K) from 2% control level. (B) Time segments of spikes firing across all units were decimated to approximate the total number of spike in the pre-stimulus condition. Decimation removed difference in information capacity between pre- and post-stimulus components. Information capacity was reduced from 4-8% from 2% control desflurane level (p<0.05, T-K). (C). Time segments across all units were decimated to its baseline spike count at the deepest anesthetic level (8%). The change in complexity was accounted for by the reduction of spike counts, whereas integration and entropy displayed significant reduction at 8% from control (*p<0.05, T-K). No difference between pre and post-stimulus components was observed.

	Desflurane (%)				
	0	2	4	6	8
*Number of Units**	50±17	50±15	49±12	39±11	29±10
*Overall Rate, 1/s**	6.1 (4.4,7.8)	4.4 (3.6,5.2)	3.5 (3.1,3.8)	2.9 (2.5,3.2)	2.3 (2.1,2.5)
Pre-stimulus					
*Unique Patterns**	1475±1061	1190±745	850±378	496±267	318±175
*Spikes (10^3)**	14±8	11±7	8±2	5±2	3±2
Post-stimulus					
*Unique Patterns **	2659±1819	2314±1154	1931±1220	1310±982	1023±566
*Spikes (10^3)**	21±9	21±7	18±7	14±6	12±4

Table 5. Properties of units and stimulus-response from 6 experiments.
A significant linear decrease in the number of active units and overall spike rates with desflurane was present. A concentration-dependent decrease in number of unique pattern and spike counts of pre-stimulus and flash-induced spiking activity was found. Rate is displayed as median with 95% confidence intervals. Number of units, patterns, spikes displayed as mean±S.D. *$p < 0.05$, linear trend

SUMMARY

Taken together, I have shown that the anesthetic-induced unconsciousness, as measured by LORR, is associated with altered functional interactions in the cortical neuronal network. Consequently, changes in network interactions with desflurane lead to a diminution of functional integration and complexity. Desflurane elevated the excitatory-inhibitory balance and reduced neuronal burst synchronization and information integration. Furthermore, anesthetic-induced unconsciousness may be associated with reduction of functional interactions across cortical layers indicating a suppression of laminar dependent local processing.

One theory suggests anesthetics work by enhancing inhibitory and suppressing excitatory synaptic transmission. While numerous studies have demonstrated enhanced inhibitory and suppressed excitatory synaptic transmission with *in vitro* studies, our results show an enhanced excitatory spike transmission probability in cortical neuronal networks, *in vivo*. This suggests that in intact neuronal networks, communication via the recurrent nature of excitatory and inhibitory interactions in local circuits are differentially affected by desflurane.

Another theory suggests the thalamus as a primary target of anesthetics leading to the theory of a "thalamic switch" of consciousness (Alkire et al., 2000). This suggests that hyperpolarization of thalamocortical neurons disrupt thalamocortical circuits necessary for consciousness. In previous studies in our lab, we have shown that anesthetics preferentially reduced long-latency spike responses to flash but had no significant effect on the early response component (Hudetz et al., 2009). The early component is thought to reflect the initial reactivity to stimuli produced by feed-forward transmission whereas the late component is thought to reflect top-down sensory processing through feedback connections. These results suggest that under anesthesia, the brain continues to process information and hence get through the thalamus. Therefore, although thalamus appears to be a common site of modulation by several anesthetics, this may be secondary to cortical effects.

Here we examined how the neuronal cells in a localized network interact under various conscious states. Our results support the hypothesis that anesthetics may work by altering functional interaction involved with information processing ultimately leading to loss-of-consciousness.

NOVEL APPROACHES

Although anesthetic effects on somatosensory, auditory, visual evoked responses have been extensively investigated, such effects on the functional neuronal networks of the brain have not been studied. Several novel approaches implemented in this study include:

Recordings done in freely behaving rats

All experiments were performed in freely-behaving rats. This approach is beneficial because it eliminates stress induced under restrained conditions that may influence data recordings.

Recordings done in steady state conditions from deep anesthesia to wakefulness

Previous studies examined neuronal functional connectivity in awake, asleep or deeply anesthetized conditions. Here we investigated the changes in functional connectivity at graded, steady-state levels at wakefulness and various levels of desflurane associated with unconsciousness. Hence our studies more readily test for changes associated with the anesthetic-induced LOC.

Recording of spontaneous as well as stimulus-induced neuronal activity

The effect of desflurane anesthesia was examined on spontaneously as well a flash-evoked spiking activity. Spontaneous activity has been increasingly studied with electrophysiological as well as fMRI modalities and are presumed to reflect intrinsic functional connections. External stimuli, such as the presentation of a flash, is useful for increasing neuronal excitability and facilitating the integration of sensory information.

Inverted Mexican hat

In Aim 2, in order to quantify bursting we To quantify ‘spike bursting’ (Ranck, 1973), the autocorrelogram or ACG of each neuron was fit with an inverted Mexican hat function between

the interval of -50 to +50 ms. Previous approaches have used an exponential (Bartho et al., 2004) or Gaussian fit to the positive phase of the cross- and auto-correlogram. We found that the inverted Mexican fit was a better estimator of the firing response probability distribution of cells.

Weighted ISI

With a typical interspike interval histogram, the scarcely occurring slower intervals between spikes are damped by the numerous high firing intervals between spikes. Therefore, in Aim 2 we used a duration weighted interspike interval (ISI) histogram to augment the secondary peak that corresponds to interburst periods. The unimodal distribution then transformed to a bimodal shape of which the discrimination between periods of bursting and non-bursting spike activity were more easily differentiated.

LED implantation

For visual stimulation which was used in Aim 3, an LED was then implanted subcutaneously between the tissue and bone in the opposite hemisphere behind the contralateral eye . The LED has a peak wavelength of ~650nm, therefore allowing the red light to penetrate through the tissue and directly stimulate the retina (Szabo-Salfay et al., 2001).

Some of the benefits of this technique include:

1. Can be used in freely-moving animals
2. Pupil size, animal behavior, and head-position does not influence the data;
3. Response to flash stimuli has been found to be highly reproducible and identical to commonly used methods of visual stimulation.

Patterns for entropy measure

In Aim 3, we measured information complexity using patterns of firing activity from binarized representations across all active units. We used the distribution of spike pattern across all units to represent the possible cortical states, thought to be highest at consciousness. Entropy

was then calculated using the normalized probability distributions at each anesthetic condition. As far as we know, this method has not been applied elsewhere.

LIMITATIONS

Rat model

These studies were conducted using albino Sprague-Dawley male rats. This species is docile and is readily available. A large number of anesthetic studies in this rodent species provide the most extensive background material for comparative purposes. Furthermore, because of the transparency of their iris, atropine dilation of the eye is unnecessary for albino rats compared to hooded rats. A comparison between albino and Long Evans rats (Kimura, 1962) found no difference in the photic evoked response between the two strains. We would reconsider the choice of species if we were to switch from flash to patterned visual stimulation.

Visual cortex

Extracellular neuronal recordings in this study were acquired from the primary visual cortex of the rat. We chose this cortical area to investigate the role of visual sensory integration as correlate of visual awareness. Although we agree that comparison of our results to other cortical areas is needed, the visual cortex is necessary first step for conscious perception. Without the activation of stimuli in the primary visual cortex, sensory information would not be consciously perceived.

Micro-electrode arrays

Although very useful, microelectrodes are invasive with only the conductive tip being capable of recording spikes. This damaging process caused by insertion of the electrode into the brain leads to inflammation which in return causes astrocytes and microglia to proliferate and form a glial scar which encapsulates the implant. In return, acquisition of recorded spikes is degraded, reducing signal-to-noise ratio. Various types of microelectrodes are now available with

variable sizes, substrates, spacing, length and geometries with each having certain advantages that may reduce these unwanted effects.

Pairwise analysis

The use of pairwise analysis to construct the neuronal network has several potential drawbacks. First, when considering only pairs of neurons, the effects of other unobserved or third-party cells cannot be accounted for with this analysis. Yet, several studies show that pairwise analysis may be sufficient to represent the correlated states (Schneidman et al., 2006) within a network and we believe that pairwise analysis served as a reasonable first approximation.

Sampling duration

How sampling duration effects the results observed in this study warrants further investigation. For example, using only an estimated 15 min recording duration for Aim 3, all possible number of spike patterns across all active units were not fully acquired. For example, in one unit sampled every 1 ms for 30 ms, the number of possible binary states is equal to 2^{30}, roughly one billion possibilities (Nemenman, Lewen, Bialek, & de Ruyter van Steveninck, 2008)! Furthermore, at least 10% of sampling duration is needed to obtain a 50% chance of sampling the most frequent events in a system. Hence, neurons can generate many more meaningfully distinguishable responses than the number that we can sample in realistic experiments, due to limited data storage and a computationally demanding process.

FUTURE DIRECTIONS

In this study, I showed that desflurane at concentrations that produce unconsciousness elevated the excitatory-inhibitory balance, reduced neuronal burst synchronization and functional integration in the visual cortex. The results agreed with the hypothesis that a disruption of cortical information exchange and integration is a correlate of the anesthetic-induced loss of consciousness. The following are just a few potential extensions of this study:

Location

Micro-electrode arrays will be used in future experiments to include additional cortical regions, associated with consciousness. Some potential candidates include the posterior parietal-cingulate-precuneus region and the nonspecific thalamus.

Multi-unit electrode arrays

Custom-designed electrodes will be used to investigate the anesthetic effect on the neuronal functional integration, as well as to search for the neurons that are selectively involved in the feedforward and feedback cortical information exchange, and to examine their role in the intra-regional integration. Various custom-designed electrode parameters will considered to minimize microglia proliferation and increase or decrease recording area to examine laminar and regional effects of anesthetics.

Higher-order measures

In this study we mainly applied pairwise analysis to assess the level of consciousness under desflurane anesthesia. Other proposed methods that include higher-order contributions such as previous spiking history and third-party cells may be incorporated into measures of connectivity. These include network likelihood model, Bayesian approaches and other information theoretic measures that will be compared to pairwise analysis in future studies.

Moreover, time-varying approaches to account for dynamic changes in connectivity will be examined.

Anesthetic agents

The effect of different anesthetic agents on cortical functional integration will be investigated. Inhalational anesthetics such as isoflurane and sevoflurane, as well as intravenous anesthetics propofol and midazolam, and perhaps α-chloralose (Garrett & Gan, 1998), primarily GABAA potentiators similar to desflurane, may produce comparable results. Generalization to other types of anesthetics, such as ketamine or urethane, with substantially different ionic mechanisms and targets (Hara & Harris, 2002; Harrison & Simmonds, 1985; Sceniak & Maciver, 2006) is not straightforward. Therefore, other anesthetics will also be compared to determine a unitary correlate of the anesthetic-induced unconsciousness.

Electrical and pharmacological modulation

Changes in functional integration will be assessed as a function of both electrical and pharmacological modulation of neuronal activity. Previously, in our lab we demonstrated that micro-infusion of the excitatory transmitter norepinephrine into the nucleus basalis of rats produced transient behavioral and EEG activation during desflurane anesthesia (Pillay et al., 2011). Cholinergic activation of the cerebral cortex under isoflurane produced similar results (Hudetz et al., 2003). The effect of electrical or pharmacologic stimulation in localized neuronal networks with spikes under anesthesia will be examined.

Functional integration theory

Our results support the hypothesis that the anesthetic-induced unconsciousness, as measured by LORR, is accompanied by changes in network interaction. Further investigations requiring (1) selective manipulation of neuronal features (connectivity, correlations, etc.) and (2) a direct assessment of consciousness, is needed to corroborate this theory.

BIBLIOGRAPHY

Aertsen, A. M., & Gerstein, G. L. (1985). Evaluation of neuronal connectivity: sensitivity of cross-correlation. [Research Support, Non-U.S. Gov't Research Support, U.S. Gov't, Non-P.H.S. Research Support, U.S. Gov't, P.H.S.]. *Brain Res, 340*(2), 341-354.

Alkire, M. T., Haier, R. J., Barker, S. J., Shah, N. K., Wu, J. C., & Kao, Y. J. (1995). Cerebral metabolism during propofol anesthesia in humans studied with positron emission tomography. *Anesthesiology, 82*(2), 393-403; discussion 327A.

Alkire, M. T., Haier, R. J., & Fallon, J. H. (2000). Toward a unified theory of narcosis: brain imaging evidence for a thalamocortical switch as the neurophysiologic basis of anesthetic-induced unconsciousness. *Conscious Cogn, 9*(3), 370-386.

Alkire, M. T., Haier, R. J., Fallon, J. H., & Barker, S. J. (1996). Pet imaging of conscious and unconscious verbal memory. *J Consciousness Studies, 3*(5-6), 448-462.

Alkire, M. T., Haier, R. J., Shah, N. K., & Anderson, C. T. (1997). Positron emission tomography study of regional cerebral metabolism in humans during isoflurane anesthesia. *Anesthesiology, 86*(3), 549-557.

Alkire, M. T., Hudetz, A. G., & Tononi, G. (2008). Consciousness and anesthesia. *Science, 322*(5903), 876-880.

Alkire, M. T., Pomfrett, C. J., Haier, R. J., Gianzero, M. V., Chan, C. M., Jacobsen, B. P., & Fallon, J. H. (1999). Functional brain imaging during anesthesia in humans: effects of halothane on global and regional cerebral glucose metabolism. *Anesthesiology, 90*(3), 701-709.

Amzica, F. (2009). Basic physiology of burst-suppression. [Review]. *Epilepsia, 50 Suppl 12*, 38-39. doi: 10.1111/j.1528-1167.2009.02345.x

Amzica, F., Neckelmann, D., & Steriade, M. (1997). Instrumental conditioning of fast (20- to 50-Hz) oscillations in corticothalamic networks. [Research Support, Non-U.S. Gov't]. *Proc Natl Acad Sci U S A, 94*(5), 1985-1989.

Amzica, F., & Steriade, M. (1998). Electrophysiological correlates of sleep delta waves. [Review]. *Electroencephalogr Clin Neurophysiol, 107*(2), 69-83.

Andrade, J. (1995). Learning during anaesthesia: a review. *Br J Psychol, 86*(Pt 4), 479-506.

Andrade, J. (1996). Investigations of hypesthesia: using anesthetics to explore relationships between consciousness, learning, and memory. *Conscious Cogn, 5*(4), 562-580.

Angel, A. (1991). The G. L. Brown lecture. Adventures in anaesthesia. *Exp Physiol, 76*(1), 1-38.

Antkowiak, B., & Kirschfeld, K. (2000). [Neural mechanisms of anesthesia]. [Review]. *Anasthesiol Intensivmed Notfallmed Schmerzther, 35*(12), 731-743. doi: 10.1055/s-2000-8935

Antognini, J. F., & Carstens, E. (1999). Increasing isoflurane from 0.9 to 1.1 minimum alveolar concentration minimally affects dorsal horn cell responses to noxious stimulation. *Anesthesiology, 90*(1), 208-214.

Antognini, J. F., & Carstens, E. (2002). In vivo characterization of clinical anaesthesia and its components. *Br J Anaesth, 89*(1), 156-166.

Antognini, J. F., Carstens, E., Sudo, M., & Sudo, S. (2000). Isoflurane depresses electroencephalographic and medial thalamic responses to noxious stimulation via an indirect spinal action. *Anesth Analg, 91*(5), 1282-1288.

Antognini, J. F., & Kien, N. D. (1995). Potency (minimum alveolar anesthetic concentration) of isoflurane is independent of peripheral anesthetic effects. *Anesth Analg, 81*(1), 69-72.

Balduzzi, D., & Tononi, G. (2008). Integrated information in discrete dynamical systems: motivation and theoretical framework. [Research Support, N.I.H., ExtramuralResearch Support, Non-U.S. Gov't]. *PLoS Comput Biol, 4*(6), e1000091. doi: 10.1371/journal.pcbi.1000091

Balduzzi, D., & Tononi, G. (2012). What can neurons do for their brain? Communicate selectivity with bursts. *Theory Biosci*. doi: 10.1007/s12064-012-0165-0

Banks, M. I., & Pearce, R. A. (1999). Dual actions of volatile anesthetics on GABA(A) IPSCs: dissociation of blocking and prolonging effects. [In Vitro Research Support, Non-U.S. Gov't Research Support, U.S. Gov't, P.H.S.]. *Anesthesiology, 90*(1), 120-134.

Bartho, P., Hirase, H., Monconduit, L., Zugaro, M., Harris, K. D., & Buzsaki, G. (2004). Characterization of neocortical principal cells and interneurons by network interactions and extracellular features. *J Neurophysiol, 92*(1), 600-608.

Berry, M. J., Warland, D. K., & Meister, M. (1997). The structure and precision of retinal spike trains. [In Vitro Research Support, U.S. Gov't, Non-P.H.S. Research Support, U.S. Gov't, P.H.S.]. *Proc Natl Acad Sci U S A, 94*(10), 5411-5416.

Bieda, M. C., & MacIver, M. B. (2004). Major role for tonic GABAA conductances in anesthetic suppression of intrinsic neuronal excitability. [In Vitro Research Support, U.S. Gov't, P.H.S.]. *J Neurophysiol, 92*(3), 1658-1667. doi: 10.1152/jn.00223.2004

Boly, M., Garrido, M. I., Gosseries, O., Bruno, M. A., Boveroux, P., Schnakers, C., . . . Friston, K. (2011). Preserved feedforward but impaired top-down processes in the vegetative state. [Research Support, N.I.H., Extramural Research Support, Non-U.S. Gov't]. *Science, 332*(6031), 858-862. doi: 10.1126/science.1202043

Boly, M., Moran, R., Murphy, M., Boveroux, P., Bruno, M. A., Noirhomme, Q., . . . Friston, K. (2012). Connectivity changes underlying spectral EEG changes during propofol-induced

loss of consciousness. [Clinical Trial Research Support, N.I.H., Extramural Research Support, Non-U.S. Gov't]. *J Neurosci, 32*(20), 7082-7090. doi: 10.1523/JNEUROSCI.3769-11.2012

Boly, M., Tshibanda, L., Vanhaudenhuyse, A., Noirhomme, Q., Schnakers, C., Ledoux, D., . . . Laureys, S. (2009). Functional connectivity in the default network during resting state is preserved in a vegetative but not in a brain dead patient. [Research Support, Non-U.S. Gov't]. *Hum Brain Mapp, 30*(8), 2393-2400. doi: 10.1002/hbm.20672

Bonhomme, V., Fiset, P., Meuret, P., Backman, S., Plourde, G., Paus, T., . . . Evans, A. C. (2001). Propofol anesthesia and cerebral blood flow changes elicited by vibrotactile stimulation: a positron emission tomography study. *J Neurophysiol, 85*(3), 1299-1308.

Brown, E. N., Kass, R. E., & Mitra, P. P. (2004). Multiple neural spike train data analysis: state-of-the-art and future challenges. [Research Support, U.S. Gov't, P.H.S. Review]. *Nat Neurosci, 7*(5), 456-461. doi: 10.1038/nn1228

Brown, E. N., Lydic, R., & Schiff, N. D. (2010). General anesthesia, sleep, and coma. [Research Support, N.I.H., Extramural Research Support, Non-U.S. Gov't Review]. *N Engl J Med, 363*(27), 2638-2650. doi: 10.1056/NEJMra0808281

Buzsaki, G. (2004). Large-scale recording of neuronal ensembles. *Nat Neurosci, 7*(5), 446-451.

Buzsaki, G. (2006). *Rhythms of the Brain*. New York: Oxford University Press.

Buzsaki, G. (2007). The structure of consciousness. *Nature, 446*(7133), 267.

Buzsáki, G. (2006). *Rhythms of the brain*. Oxford ; New York: Oxford University Press.

Buzsaki, G., Kaila, K., & Raichle, M. (2007). Inhibition and brain work. *Neuron, 56*(5), 771-783.

Chapin, J. K., Waterhouse, B. D., & Woodward, D. J. (1981). Differences in cutaneous sensory response properties of single somatosensory cortical neurons in awake and halothane anesthetized rats. [Research Support, Non-U.S. Gov't Research Support, U.S. Gov't, P.H.S.]. *Brain Res Bull, 6*(1), 63-70.

Ching, S., Purdon, P. L., Vijayan, S., Kopell, N. J., & Brown, E. N. (2012). A neurophysiological-metabolic model for burst suppression. [Research Support, N.I.H., Extramural Research Support, U.S. Gov't, Non-P.H.S.]. *Proc Natl Acad Sci U S A, 109*(8), 3095-3100. doi: 10.1073/pnas.1121461109

Cocatre-Zilgien, J. H., & Delcomyn, F. (1992). Identification of bursts in spike trains. [Research Support, Non-U.S. Gov't]. *J Neurosci Methods, 41*(1), 19-30.

Crick, F., & Koch, C. (1990). Some reflections on visual awareness. [Research Support, Non-U.S. Gov't Research Support, U.S. Gov't, Non-P.H.S. Review]. *Cold Spring Harb Symp Quant Biol, 55*, 953-962.

Crochet, S., & Petersen, C. C. (2009). Cortical dynamics by layers. *Neuron, 64*(3), 298-300.

Crutchfield, J. P., & Young, K. (1989). Inferring statistical complexity. *Phys Rev Lett, 63*(2), 105-108.

Csicsvari, J., Henze, D. A., Jamieson, B., Harris, K. D., Sirota, A., Bartho, P., . . . Buzsaki, G. (2003). Massively parallel recording of unit and local field potentials with silicon-based electrodes. [Research Support, U.S. Gov't, P.H.S.]. *J Neurophysiol, 90*(2), 1314-1323. doi: 10.1152/jn.00116.2003

Csicsvari, J., Hirase, H., Czurko, A., & Buzsaki, G. (1998). Reliability and state dependence of pyramidal cell-interneuron synapses in the hippocampus: an ensemble approach in the behaving rat. *Neuron, 21*(1), 179-189.

de Haan, W., Pijnenburg, Y. A., Strijers, R. L., van der Made, Y., van der Flier, W. M., Scheltens, P., & Stam, C. J. (2009). Functional neural network analysis in frontotemporal dementia and Alzheimer's disease using EEG and graph theory. *BMC Neurosci, 10*, 101. doi: 10.1186/1471-2202-10-101

Dean, P. (1990). Sensory Cortex: Visual Perceptual Functions. In B. Kolb & R. C. Tees (Eds.), *The Cerebral Cortex of the Rat* (pp. 275-307). Cambridge: MIT Press.

Deco, G., Jirsa, V. K., & McIntosh, A. R. (2011). Emerging concepts for the dynamical organization of resting-state activity in the brain. [Research Support, Non-U.S. Gov't Review]. *Nat Rev Neurosci, 12*(1), 43-56. doi: 10.1038/nrn2961

Deeprose, C., & Andrade, J. (2006). Is priming during anesthesia unconscious? *Conscious Cogn, 15*(1), 1-23.

Del Cul, A., Baillet, S., & Dehaene, S. (2007). Brain dynamics underlying the nonlinear threshold for access to consciousness. [Research Support, Non-U.S. Gov't]. *PLoS Biol, 5*(10), e260. doi: 10.1371/journal.pbio.0050260

Destexhe, A., Contreras, D., & Steriade, M. (1999). Spatiotemporal analysis of local field potentials and unit discharges in cat cerebral cortex during natural wake and sleep states. [Research Support, Non-U.S. Gov't]. *J Neurosci, 19*(11), 4595-4608.

Detsch, O., Kochs, E., Siemers, M., Bromm, B., & Vahle-Hinz, C. (2002). Increased responsiveness of cortical neurons in contrast to thalamic neurons during isoflurane-induced EEG bursts in rats. *Neurosci Lett, 317*(1), 9-12.

Detsch, O., Vahle-Hinz, C., Kochs, E., Siemers, M., & Bromm, B. (1999). Isoflurane induces dose-dependent changes of thalamic somatosensory information transfer. *Brain Res, 829*(1-2), 77-89.

Devor, M., & Zalkind, V. (2001). Reversible analgesia, atonia, and loss of consciousness on bilateral intracerebral microinjection of pentobarbital. *Pain, 94*(1), 101-112.

Disbrow, E., Buonocore, M., Antognini, J., Carstens, E., & Rowley, H. A. (1998). Somatosensory cortex: a comparison of the response to noxious thermal, mechanical, and electrical stimuli using functional magnetic resonance imaging. *Hum Brain Mapp, 6*(3), 150-159.

Dueck, M. H., Petzke, F., Gerbershagen, H. J., Paul, M., Hesselmann, V., Girnus, R., . . . Boerner, U. (2005). Propofol attenuates responses of the auditory cortex to acoustic stimulation in a dose-dependent manner: a FMRI study. *Acta Anaesthesiol Scand, 49*(6), 784-791.

Eger, E. I., 2nd, & Johnson, B. H. (1987). Rates of awakening from anesthesia with I-653, halothane, isoflurane, and sevoflurane: a test of the effect of anesthetic concentration and duration in rats. *Anesth Analg, 66*(10), 977-982.

Engel, A., Konig, P., Kreiter, A., & Singer, W. (1991). Interhemispheric synchronization of oscillatory neuronal responses in cat visual cortex. *Science, 252*(5009), 1177-1179. doi: 10.1126/science.252.5009.1177

Engel, A. K., Fries, P., Konig, P., Brecht, M., & Singer, W. (1999a). Does time help to understand consciousness? [Comment]. *Conscious Cogn, 8*(2), 260-268. doi: 10.1006/ccog.1999.0400

Engel, A. K., Fries, P., Konig, P., Brecht, M., & Singer, W. (1999b). Temporal binding, binocular rivalry, and consciousness. [Research Support, Non-U.S. Gov't]. *Conscious Cogn, 8*(2), 128-151. doi: 10.1006/ccog.1999.0389

Engel, A. K., Konig, P., Gray, C. M., & Singer, W. (1990). Stimulus-Dependent Neuronal Oscillations in Cat Visual Cortex: Inter-Columnar Interaction as Determined by Cross-Correlation Analysis. *Eur J Neurosci, 2*(7), 588-606.

Engel, A. K., & Singer, W. (2001). Temporal binding and the neural correlates of sensory awareness. *Trends Cogn Sci, 5*(1), 16-25.

Erchova, I. A., Lebedev, M. A., & Diamond, M. E. (2002). Somatosensory cortical neuronal population activity across states of anaesthesia. *Eur J Neurosci, 15*(4), 744-752.

Esser, S. K., Hill, S., & Tononi, G. (2009). Breakdown of effective connectivity during slow wave sleep: investigating the mechanism underlying a cortical gate using large-scale modeling. [Research Support, N.I.H., Extramural]. *J Neurophysiol, 102*(4), 2096-2111. doi: 10.1152/jn.00059.2009

Fahrenfort, I., Klooster, J., Sjoerdsma, T., & Kamermans, M. (2005). The involvement of glutamate-gated channels in negative feedback from horizontal cells to cones. [Review]. *Prog Brain Res, 147*, 219-229. doi: 10.1016/S0079-6123(04)47017-4

Fee, M. S., Mitra, P. P., & Kleinfeld, D. (1996). Automatic sorting of multiple unit neuronal signals in the presence of anisotropic and non-Gaussian variability. *J Neurosci Methods, 69*(2), 175-188.

Felleman, D. J., & Van Essen, D. C. (1991). Distributed hierarchical processing in the primate cerebral cortex. *Cereb Cortex, 1*(1), 1-47.

Ferrarelli, F., Massimini, M., Sarasso, S., Casali, A., Riedner, B. A., Angelini, G., . . . Pearce, R. A. (2010). Breakdown in cortical effective connectivity during midazolam-induced loss of consciousness. *Proc Natl Acad Sci U S A, 107*(6), 2681-2686.

Ferron, J. F., Kroeger, D., Chever, O., & Amzica, F. (2009). Cortical inhibition during burst suppression induced with isoflurane anesthesia. [Research Support, Non-U.S. Gov't]. *J Neurosci, 29*(31), 9850-9860. doi: 10.1523/JNEUROSCI.5176-08.2009

Fingelkurts, A. A., & Kahkonen, S. (2005). Functional connectivity in the brain--is it an elusive concept? [Research Support, U.S. Gov't, Non-P.H.S. Research Support, U.S. Gov't, P.H.S. Review]. *Neurosci Biobehav Rev, 28*(8), 827-836. doi: 10.1016/j.neubiorev.2004.10.009

Fiset, P., Paus, T., Daloze, T., Plourde, G., Meuret, P., Bonhomme, V., . . . Evans, A. C. (1999). Brain mechanisms of propofol-induced loss of consciousness in humans: a positron emission tomographic study. *J Neurosci, 19*(13), 5506-5513.

Forget, J., Buiatti, M., & Dehaene, S. (2010). Temporal integration in visual word recognition. *J Cogn Neurosci, 22*(5), 1054-1068. doi: 10.1162/jocn.2009.21300

Franks, N. P. (2006). Molecular targets underlying general anaesthesia. [Historical Article Review]. *Br J Pharmacol, 147 Suppl 1*, S72-81. doi: 10.1038/sj.bjp.0706441

Franks, N. P. (2008). General anaesthesia: from molecular targets to neuronal pathways of sleep and arousal. *Nat Rev Neurosci, 9*(5), 370-386.

Friedman, E. B., Sun, Y., Moore, J. T., Hung, H. T., Meng, Q. C., Perera, P., . . . Kelz, M. B. (2010). A conserved behavioral state barrier impedes transitions between anesthetic-induced unconsciousness and wakefulness: evidence for neural inertia. *PLoS One, 5*(7), e11903.

Fries, P. (2005). A mechanism for cognitive dynamics: neuronal communication through neuronal coherence. [Research Support, Non-U.S. Gov't Review]. *Trends Cogn Sci, 9*(10), 474-480. doi: 10.1016/j.tics.2005.08.011

Fujisawa, S., Amarasingham, A., Harrison, M. T., & Buzsaki, G. (2008). Behavior-dependent short-term assembly dynamics in the medial prefrontal cortex. *Nat Neurosci, 11*(7), 823-833.

Fujiwara, N., Higashi, H., Nishi, S., Shimoji, K., Sugita, S., & Yoshimura, M. (1988). Changes in spontaneous firing patterns of rat hippocampal neurones induced by volatile anaesthetics. *J Physiol, 402*, 155-175.

Fujiwara, S. E., Akema, T., & Izaki, Y. (2008). Cross-correlogram between rat hippocampal and prefrontal neuronal activities. *Neuroreport, 19*(18), 1777-1782. doi: 10.1097/WNR.0b013e328318edca

Gamez, D. (2010). Information integration based predictions about the conscious states of a spiking neural network. [Research Support, Non-U.S. Gov't]. *Conscious Cogn, 19*(1), 294-310. doi: 10.1016/j.concog.2009.11.001

Gamez, D., & Aleksander, I. (2011). Accuracy and performance of the state-based Phi and liveliness measures of information integration. [Research Support, Non-U.S. Gov't]. *Conscious Cogn, 20*(4), 1403-1424. doi: 10.1016/j.concog.2011.05.016

Garofalo, M., Nieus, T., Massobrio, P., & Martinoia, S. (2009). Evaluation of the performance of information theory-based methods and cross-correlation to estimate the functional connectivity in cortical networks. *PLoS One, 4*(8), e6482. doi: 10.1371/journal.pone.0006482

Garrett, K. M., & Gan, J. (1998). Enhancement of gamma-aminobutyric acidA receptor activity by alpha-chloralose. [Research Support, Non-U.S. Gov't]. *J Pharmacol Exp Ther, 285*(2), 680-686.

Gerstein, G. L., & Perkel, D. H. (1969). Simultaneously recorded trains of action potentials: analysis and functional interpretation. *Science, 164*(881), 828-830.

Ghoneim, M. M., & Block, R. I. (1997). Learning and memory during general anesthesia: an update. *Anesthesiology, 87*(2), 387-410.

Gourevitch, B., & Eggermont, J. J. (2007). A nonparametric approach for detection of bursts in spike trains. [Research Support, Non-U.S. Gov't]. *J Neurosci Methods, 160*(2), 349-358. doi: 10.1016/j.jneumeth.2006.09.024

Gray, C. M. (1999). The temporal correlation hypothesis of visual feature integration: still alive and well. [Research Support, U.S. Gov't, P.H.S. Review]. *Neuron, 24*(1), 31-47, 111-125.

Greenberg, D. S., Houweling, A. R., & Kerr, J. N. (2008). Population imaging of ongoing neuronal activity in the visual cortex of awake rats. [Research Support, Non-U.S. Gov't]. *Nat Neurosci, 11*(7), 749-751. doi: 10.1038/nn.2140

Grun, S., Diesmann, M., & Aertsen, A. (2002). Unitary events in multiple single-neuron spiking activity: I. Detection and significance. *Neural Comput, 14*(1), 43-80.

Grun, S., Diesmann, M., Grammont, F., Riehle, A., & Aertsen, A. (1999). Detecting unitary events without discretization of time. [Research Support, Non-U.S. Gov't]. *J Neurosci Methods, 94*(1), 67-79.

Gugino, L. D., Chabot, R. J., Prichep, L. S., John, E. R., Formanek, V., & Aglio, L. S. (2001). Quantitative EEG changes associated with loss and return of consciousness in healthy adult volunteers anaesthetized with propofol or sevoflurane. *Br J Anaesth, 87*(3), 421-428.

Haas, R. E. (1998). Learning during anesthesia: myth or reality? *Semin Perioper Nurs, 7*(1), 46-53.

Hara, K., & Harris, R. A. (2002). The anesthetic mechanism of urethane: the effects on neurotransmitter-gated ion channels. [Research Support, U.S. Gov't, P.H.S.]. *Anesth Analg, 94*(2), 313-318, table of contents.

Harrison, N. L., & Simmonds, M. A. (1985). Quantitative studies on some antagonists of N-methyl D-aspartate in slices of rat cerebral cortex. [In Vitro Research Support, Non-U.S. Gov't]. *Br J Pharmacol, 84*(2), 381-391.

Hartikainen, K., Rorarius, M., Makela, K., Perakyla, J., Varila, E., & Jantti, V. (1995). Visually evoked bursts during isoflurane anaesthesia. *Br J Anaesth, 74*(6), 681-685.

Heinke, W., & Koelsch, S. (2005). The effects of anesthetics on brain activity and cognitive function. *Curr Opin Anaesthesiol, 18*(6), 625-631.

Hemmings, H. C., Jr., Akabas, M. H., Goldstein, P. A., Trudell, J. R., Orser, B. A., & Harrison, N. L. (2005). Emerging molecular mechanisms of general anesthetic action. [Research Support, N.I.H., Extramural Research Support, U.S. Gov't, P.H.S. Review]. *Trends Pharmacol Sci, 26*(10), 503-510. doi: 10.1016/j.tips.2005.08.006

Hentschke, H., Schwarz, C., & Antkowiak, B. (2005). Neocortex is the major target of sedative concentrations of volatile anaesthetics: strong depression of firing rates and increase of GABAA receptor-mediated inhibition. [Comparative Study Research Support, Non-U.S. Gov't]. *Eur J Neurosci, 21*(1), 93-102. doi: 10.1111/j.1460-9568.2004.03843.x

Hudetz, A. G. (2002). Effect of volatile anesthetics on interhemispheric EEG cross-approximate entropy in the rat. *Brain Res, 954*(1), 123-131.

Hudetz, A. G., & Hemmings, H. C., Jr. (2012). Anaesthesia awareness: 3 years of progress. [Congresses Editorial]. *Br J Anaesth, 108*(2), 180-182. doi: 10.1093/bja/aer454

Hudetz, A. G., & Imas, O. A. (2007). Burst activation of the cerebral cortex by flash stimuli during isoflurane anesthesia in rats. [Comparative Study Research Support, N.I.H., Extramural]. *Anesthesiology, 107*(6), 983-991. doi: 10.1097/01.anes.0000291471.80659.55

Hudetz, A. G., Vizuete, J. A., & Imas, O. A. (2009). Desflurane selectively suppresses long-latency cortical neuronal response to flash in the rat. [Research Support, N.I.H., Extramural]. *Anesthesiology, 111*(2), 231-239. doi: 10.1097/ALN.0b013e3181ab671e

Hudetz, A. G., Wood, J. D., & Kampine, J. P. (2003). Cholinergic reversal of isoflurane anesthesia in rats as measured by cross-approximate entropy of the electroencephalogram. *Anesthesiology, 99*(5), 1125-1131.

Ikeda, H., & Wright, M. J. (1974a). Effect of halothane-nitrous oxide anaesthesia on the behaviour of 'sustained' and 'transient' visual cortical neurones. *J Physiol, 237*(2), 20P-21P.

Ikeda, H., & Wright, M. J. (1974b). Sensitivity of neurones in visual cortex (area 17) under different levels of anaesthesia. *Exp Brain Res, 20*(5), 471-484.

Imas, O. A., Ropella, K. M., Ward, B. D., Wood, J. D., & Hudetz, A. G. (2005a). Volatile anesthetics disrupt frontal-posterior recurrent information transfer at gamma frequencies in rat. *Neurosci Lett, 387*(3), 145-150.

Imas, O. A., Ropella, K. M., Ward, B. D., Wood, J. D., & Hudetz, A. G. (2005b). Volatile anesthetics enhance flash-induced gamma oscillations in rat visual cortex. *Anesthesiology, 102*(5), 937-947.

Imas, O. A., Ropella, K. M., Wood, J. D., & Hudetz, A. G. (2006). Isoflurane disrupts anterio-posterior phase synchronization of flash-induced field potentials in the rat. *Neurosci Lett, 402*(3), 216-221.

Iselin-Chaves, I. A., Flaishon, R., Sebel, P. S., Howell, S., Gan, T. J., Sigl, J., . . . Glass, P. S. (1998). The effect of the interaction of propofol and alfentanil on recall, loss of consciousness, and the Bispectral Index. *Anesth Analg, 87*(4), 949-955.

Iselin-Chaves, I. A., Willems, S. J., Jermann, F. C., Forster, A., Adam, S. R., & Van der Linden, M. (2005). Investigation of implicit memory during isoflurane anesthesia for elective surgery using the process dissociation procedure. *Anesthesiology, 103*(5), 925-933.

Izhikevich, E. M. (2002). Resonance and selective communication via bursts in neurons having subthreshold oscillations. [Research Support, Non-U.S. Gov't]. *Biosystems, 67*(1-3), 95-102.

Jirsa, V. K. (2008). Dispersion and time delay effects in synchronized spike-burst networks. *Cogn Neurodyn, 2*(1), 29-38. doi: 10.1007/s11571-007-9030-0

Jordan, M. I. (1999). *Learning in graphical models*. Cambridge, Mass.: MIT Press.

Judge, O., Hill, S., & Antognini, J. F. (2009). Modeling the effects of midazolam on cortical and thalamic neurons. [Research Support, N.I.H., Extramural]. *Neurosci Lett, 464*(2), 135-139. doi: 10.1016/j.neulet.2009.08.041

Kara, P., & Reid, R. C. (2003). Efficacy of retinal spikes in driving cortical responses. *J Neurosci, 23*(24), 8547-8557.

Kass, R. E., Ventura, V., & Brown, E. N. (2005). Statistical issues in the analysis of neuronal data. *J Neurophysiol, 94*(1), 8-25.

Kelly, R. C., Smith, M. A., Kass, R. E., & Lee, T. S. (2010). Local field potentials indicate network state and account for neuronal response variability. *J Comput Neurosci, 29*(3), 567-579.

Kerssens, C., Hamann, S., Peltier, S., Hu, X. P., Byas-Smith, M. G., & Sebel, P. S. (2005). Attenuated brain response to auditory word stimulation with sevoflurane: a functional magnetic resonance imaging study in humans. *Anesthesiology, 103*(1), 11-19.

Kim, U., & McCormick, D. A. (1998). The functional influence of burst and tonic firing mode on synaptic interactions in the thalamus. [Research Support, Non-U.S. Gov't Research Support, U.S. Gov't, P.H.S.]. *J Neurosci, 18*(22), 9500-9516.

Kimura, D. (1962). Multiple response of visual cortex of the rat to photic stimulation. *Electroencephalogr Clin Neurophysiol, 14*, 115-122.

Kiviniemi, K. (1994). Conscious awareness and memory during general anesthesia. *Aana J, 62*(5), 441-449.

Kiviniemi, K. (1997). Unexpected awareness and memory in the perianesthesia setting. *J Perianesth Nurs, 12*(1), 17-24.

Klausberger, T., & Somogyi, P. (2008). Neuronal diversity and temporal dynamics: the unity of hippocampal circuit operations. [Review]. *Science, 321*(5885), 53-57. doi: 10.1126/science.1149381

Kolb, B. (1990). Posterior Parietal and Temporal Association. In B. Kolb & R. C. Tees (Eds.), *The Cerbral Cortex of the Rat* (pp. 459-471). Cambridge: MIT Press.

Kreuzer, M., Hentschke, H., Antkowiak, B., Schwarz, C., Kochs, E. F., & Schneider, G. (2010). Cross-approximate entropy of cortical local field potentials quantifies effects of anesthesia--a pilot study in rats. *BMC Neurosci, 11*, 122.

Kroeger, D., & Amzica, F. (2007). Hypersensitivity of the anesthesia-induced comatose brain. [Research Support, Non-U.S. Gov't]. *J Neurosci, 27*(39), 10597-10607. doi: 10.1523/JNEUROSCI.3440-07.2007

Ku, S. W., Lee, U., Noh, G. J., Jun, I. G., & Mashour, G. A. (2011). Preferential inhibition of frontal-to-parietal feedback connectivity is a neurophysiologic correlate of general anesthesia in surgical patients. [Randomized Controlled Trial]. *PLoS One, 6*(10), e25155. doi: 10.1371/journal.pone.0025155

Lahti, K. M., Ferris, C. F., Li, F., Sotak, C. H., & King, J. A. (1999). Comparison of evoked cortical activity in conscious and propofol- anesthetized rats using functional MRI. *Magn Reson Med, 41*(2), 412-416.

Lamme, V. A., & Roelfsema, P. R. (2000). The distinct modes of vision offered by feedforward and recurrent processing. [Review]. *Trends Neurosci, 23*(11), 571-579.

Lamme, V. A., Super, H., & Spekreijse, H. (1998). Feedforward, horizontal, and feedback processing in the visual cortex. [Research Support, Non-U.S. Gov't Review]. *Curr Opin Neurobiol, 8*(4), 529-535.

Lamme, V. A., Zipser, K., & Spekreijse, H. (2002). Masking interrupts figure-ground signals in V1. [Research Support, Non-U.S. Gov't]. *J Cogn Neurosci, 14*(7), 1044-1053. doi: 10.1162/089892902320474490

Landsness, E., Bruno, M. A., Noirhomme, Q., Riedner, B., Gosseries, O., Schnakers, C., . . . Boly, M. (2011). Electrophysiological correlates of behavioural changes in vigilance in vegetative state and minimally conscious state. [Research Support, N.I.H., Extramural Research Support, Non-U.S. Gov't]. *Brain, 134*(Pt 8), 2222-2232. doi: 10.1093/brain/awr152

Langheim, F. J., Murphy, M., Riedner, B. A., & Tononi, G. (2011). Functional connectivity in slow-wave sleep: identification of synchronous cortical activity during wakefulness and sleep using time series analysis of electroencephalographic data. *J Sleep Res, 20*(4), 496-505.

Laureys, S. (2005). The neural correlate of (un)awareness: lessons from the vegetative state. *Trends Cogn Sci, 9*(12), 556-559.

Lawhern, V., Nikonov, A. A., Wu, W., & Contreras, R. J. (2011). Spike rate and spike timing contributions to coding taste quality information in rat periphery. *Front Integr Neurosci, 5*, 18.

Le Van Quyen, M., & Bragin, A. (2007). Analysis of dynamic brain oscillations: methodological advances. [Review]. *Trends Neurosci, 30*(7), 365-373. doi: 10.1016/j.tins.2007.05.006

Lee, U., Mashour, G. A., Kim, S., Noh, G. J., & Choi, B. M. (2009). Propofol induction reduces the capacity for neural information integration: implications for the mechanism of consciousness and general anesthesia. [Research Support, Non-U.S. Gov't]. *Conscious Cogn, 18*(1), 56-64. doi: 10.1016/j.concog.2008.10.005

Legendy, C. R., & Salcman, M. (1985). Bursts and recurrences of bursts in the spike trains of spontaneously active striate cortex neurons. [Comparative Study Research Support, U.S. Gov't, P.H.S.]. *J Neurophysiol, 53*(4), 926-939.

Lewicki, M. S. (1998). A review of methods for spike sorting: the detection and classification of neural action potentials. [Review]. *Network, 9*(4), R53-78.

Lidierth, M. (2009). sigTOOL: A MATLAB-based environment for sharing laboratory-developed software to analyze biological signals. *J Neurosci Methods, 178*(1), 188-196.

Liu, X., Lauer, K. K., Ward, B. D., Rao, S. M., Li, S. J., & Hudetz, A. G. (2012). Propofol disrupts functional interactions between sensory and high-order processing of auditory verbal memory. *Hum Brain Mapp, 33*(10), 2487-2498. doi: 10.1002/hbm.21385

Liu, X., Li, R., Yang, Z., Hudetz, A. G., & Li, S. J. (2012). Differential effect of isoflurane, medetomidine, and urethane on BOLD responses to acute levo-tetrahydropalmatine in the rat. [Research Support, N.I.H., Extramural]. *Magn Reson Med, 68*(2), 552-559. doi: 10.1002/mrm.23243

Luczak, A., Bartho, P., Marguet, S. L., Buzsaki, G., & Harris, K. D. (2007). Sequential structure of neocortical spontaneous activity in vivo. [Research Support, N.I.H., Extramural Research Support, Non-U.S. Gov't]. *Proc Natl Acad Sci U S A, 104*(1), 347-352. doi: 10.1073/pnas.0605643104

Lukatch, H. S., Kiddoo, C. E., & Maciver, M. B. (2005). Anesthetic-induced burst suppression EEG activity requires glutamate-mediated excitatory synaptic transmission. [In Vitro Research Support, N.I.H., Extramural Research Support, U.S. Gov't, Non-P.H.S. Research Support, U.S. Gov't, P.H.S.]. *Cereb Cortex, 15*(9), 1322-1331. doi: 10.1093/cercor/bhi015

Ma, J., Shen, B., Stewart, L. S., Herrick, I. A., & Leung, L. S. (2002). The septohippocampal system participates in general anesthesia. *J Neurosci, 22*(2), RC200.

Maclver, M. B., Mikulec, A. A., Amagasu, S. M., & Monroe, F. A. (1996). Volatile anesthetics depress glutamate transmission via presynaptic actions. [Comparative Study In Vitro Research Support, U.S. Gov't, P.H.S.]. *Anesthesiology, 85*(4), 823-834.

Maier, A., Adams, G. K., Aura, C., & Leopold, D. A. (2010). Distinct superficial and deep laminar domains of activity in the visual cortex during rest and stimulation. *Front Syst Neurosci, 4*. doi: 10.3389/fnsys.2010.00031

Maier, A., Aura, C. J., & Leopold, D. A. (2011). Infragranular sources of sustained local field potential responses in macaque primary visual cortex. [Research Support, N.I.H., Intramural]. *J Neurosci, 31*(6), 1971-1980. doi: 10.1523/JNEUROSCI.5300-09.2011

Mainen, Z. F., & Sejnowski, T. J. (1995). Reliability of spike timing in neocortical neurons. [In Vitro Research Support, Non-U.S. Gov't]. *Science, 268*(5216), 1503-1506.

Makela, K., Hartikainen, K., Rorarius, M., & Jantti, V. (1996). Suppression of F-VEP during isoflurane-induced EEG suppression. *Electroencephalogr Clin Neurophysiol, 100*(3), 269-272.

Marshall, L., Henze, D. A., Hirase, H., Leinekugel, X., Dragoi, G., & Buzsaki, G. (2002). Hippocampal pyramidal cell-interneuron spike transmission is frequency dependent and responsible for place modulation of interneuron discharge. [Research Support, Non-U.S. Gov't Research Support, U.S. Gov't, P.H.S.]. *J Neurosci, 22*(2), RC197.

McCormick, D. A., & Feeser, H. R. (1990). Functional implications of burst firing and single spike activity in lateral geniculate relay neurons. [In Vitro Research Support, Non-U.S. Gov't Research Support, U.S. Gov't, Non-P.H.S. Research Support, U.S. Gov't, P.H.S.]. *Neuroscience, 39*(1), 103-113.

McGaraughty, S., & Reinis, S. (1993). Simultaneous multi- and single-unit recordings in the rostral ventromedial medulla of ketamine-anaesthetized rats, and the cross-correlogram analysis of their interactions. *Exp Brain Res, 92*(3), 489-494.

McGaraughty, S., Reinis, S., & Tsoukatos, J. (1995). A correlogram analysis of the activity in the rostral ventromedial medulla of awake rats and in rats anesthetized with ketamine or pentobarbital following the administration of morphine. [Comparative Study]. *Exp Brain Res, 106*(2), 283-290.

Melloni, L., Molina, C., Pena, M., Torres, D., Singer, W., & Rodriguez, E. (2007). Synchronization of neural activity across cortical areas correlates with conscious perception. [Comparative Study Research Support, Non-U.S. Gov't]. *J Neurosci, 27*(11), 2858-2865. doi: 10.1523/JNEUROSCI.4623-06.2007

Miller, M. W., & Vogt, B. A. (1984). Direct connections of rat visual cortex with sensory, motor, and association cortices. *J Comp Neurol, 226*(2), 184-202.

Mitchell, B. D., & Cauller, L. J. (2001). Corticocortical and thalamocortical projections to layer I of the frontal neocortex in rats. *Brain Res, 921*(1-2), 68-77.

Mitzdorf, U. (1994). Properties of cortical generators of event-related potentials. *Pharmacopsychiatry, 27*(2), 49-51.

Moffitt, M. A., & McIntyre, C. C. (2005). Model-based analysis of cortical recording with silicon microelectrodes. *Clin Neurophysiol, 116*(9), 2240-2250.

Munglani, R., Andrade, J., Sapsford, D. J., Baddeley, A., & Jones, J. G. (1993). A measure of consciousness and memory during isoflurane administration: the coherent frequency. [Research Support, Non-U.S. Gov't]. *Br J Anaesth, 71*(5), 633-641.

Murrell, J. C., Waters, D., & Johnson, C. B. (2008). Comparative effects of halothane, isoflurane, sevoflurane and desflurane on the electroencephalogram of the rat. *Lab Anim, 42*(2), 161-170.

Nelson, L. E., Guo, T. Z., Lu, J., Saper, C. B., Franks, N. P., & Maze, M. (2002). The sedative component of anesthesia is mediated by GABA(A) receptors in an endogenous sleep pathway. *Nat Neurosci, 5*(10), 979-984.

Nemenman, I., Lewen, G. D., Bialek, W., & de Ruyter van Steveninck, R. R. (2008). Neural coding of natural stimuli: information at sub-millisecond resolution. [Research Support, Non-U.S. Gov't Research Support, U.S. Gov't, Non-P.H.S.]. *PLoS Comput Biol, 4*(3), e1000025. doi: 10.1371/journal.pcbi.1000025

Nir, Y., Staba, R. J., Andrillon, T., Vyazovskiy, V. V., Cirelli, C., Fried, I., & Tononi, G. (2011). Regional slow waves and spindles in human sleep. [Comparative Study Research Support, N.I.H., Extramural Research Support, Non-U.S. Gov't]. *Neuron, 70*(1), 153-169. doi: 10.1016/j.neuron.2011.02.043

Okatan, M., Wilson, M. A., & Brown, E. N. (2005). Analyzing functional connectivity using a network likelihood model of ensemble neural spiking activity. [Research Support, N.I.H., Extramural Research Support, U.S. Gov't, P.H.S.]. *Neural Comput, 17*(9), 1927-1961. doi: 10.1162/0899766054322973

Olavarria, J., & Montero, V. M. (1981). Reciprocal connections between the striate cortex and extrastriate cortical visual areas in the rat. *Brain Res, 217*(2), 358-363.

Olavarria, J., & Montero, V. M. (1984). Relation of callosal and striate-extrastriate cortical connections in the rat: morphological definition of extrastriate visual areas. *Exp Brain Res, 54*(2), 240-252.

Palm, G. (1981). Evidence, information, and surprise. *Biol Cybern, 42*(1), 57-68.

Paxinos, G., & Watson, C. (1998). *The Rat Brain in Stereotaxic Coordinates* (4th ed.). San Diego: Academic Press.

Pearce, R. A., Stringer, J. L., & Lothman, E. W. (1989). Effect of volatile anesthetics on synaptic transmission in the rat hippocampus. *Anesthesiology, 71*(4), 591-598.

Phelps, E. A., & LeDoux, J. E. (2005). Contributions of the amygdala to emotion processing: from animal models to human behavior. *Neuron, 48*(2), 175-187.

Pillay, S., Vizuete, J. A., McCallum, J. B., & Hudetz, A. G. (2011). Norepinephrine infusion into nucleus basalis elicits microarousal in desflurane-anesthetized rats. [Research Support, N.I.H., Extramural]. *Anesthesiology, 115*(4), 733-742. doi: 10.1097/ALN.0b013e31822c5ee1

Pillow, J. W., Shlens, J., Paninski, L., Sher, A., Litke, A. M., Chichilnisky, E. J., & Simoncelli, E. P. (2008). Spatio-temporal correlations and visual signalling in a complete neuronal population. [Research Support, N.I.H., Extramural Research Support, Non-U.S. Gov't Research Support, U.S. Gov't, Non-P.H.S.]. *Nature, 454*(7207), 995-999. doi: 10.1038/nature07140

Pittson, S., Himmel, A. M., & MacIver, M. B. (2004). Multiple synaptic and membrane sites of anesthetic action in the CA1 region of rat hippocampal slices. *BMC Neurosci, 5*, 52.

Plourde, G., Baribeau, J., & Bonhomme, V. (1997). Ketamine increases the amplitude of the 40-Hz auditory steady-state response in humans. *Br J Anaesth, 78*(5), 524-529.

Plourde, G., Belin, P., Chartrand, D., Fiset, P., Backman, S. B., Xie, G., & Zatorre, R. J. (2006). Cortical processing of complex auditory stimuli during alterations of consciousness with the general anesthetic propofol. *Anesthesiology, 104*(3), 448-457.

Plourde, G., & Boylan, J. F. (1991). The long-latency auditory evoked potential as a measure of the level of consciousness during sufentanil anesthesia. *J Cardiothorac Vasc Anesth, 5*(6), 577-583.

Populin, L. C. (2005). Anesthetics change the excitation/inhibition balance that governs sensory processing in the cat superior colliculus. *J Neurosci, 25*(25), 5903-5914.

Quilichini, P., Sirota, A., & Buzsaki, G. (2010). Intrinsic circuit organization and theta-gamma oscillation dynamics in the entorhinal cortex of the rat. *J Neurosci, 30*(33), 11128-11142.

Rabe, L. S., Moreno, L., Rigor, B. M., & Dafny, N. (1980). Effects of halothane on evoked field potentials recorded from cortical and subcortical nuclei. *Neuropharmacology, 19*(9), 813-825.

Ramcharan, E. J., Gnadt, J. W., & Sherman, S. M. (2000). Burst and tonic firing in thalamic cells of unanesthetized, behaving monkeys. *Vis Neurosci, 17*(1), 55-62.

Rampil, I. J. (1994). Anesthetic potency is not altered after hypothermic spinal cord transection in rats. *Anesthesiology, 80*(3), 606-610.

Rampil, I. J., & King, B. S. (1996). Volatile anesthetics depress spinal motor neurons. *Anesthesiology, 85*(1), 129-134.

Rampil, I. J., Mason, P., & Singh, H. (1993). Anesthetic potency (MAC) is independent of forebrain structures in the rat. *Anesthesiology, 78*(4), 707-712.

Rehberg, B., Bouillon, T., Zinserling, J., & Hoeft, A. (1999). Comparative pharmacodynamic modeling of the electroencephalography-slowing effect of isoflurane, sevoflurane, and desflurane. *Anesthesiology, 91*(2), 397-405.

Reinsel, R. A., Veselis, R. A., Dnistrian, A. M., Feshchenko, V. A., Beattie, B. J., & Duff, M. R. (2000). Midazolam decreases cerebral blood flow in the left prefrontal cortex in a dose-dependent fashion. *Int J Neuropsychopharmacol, 3*(2), 117-127.

Ries, C. R., & Puil, E. (1999a). Ionic mechanism of isoflurane's actions on thalamocortical neurons. *J Neurophysiol, 81*(4), 1802-1809.

Ries, C. R., & Puil, E. (1999b). Ionic mechanism of isoflurane's actions on thalamocortical neurons. *J Neurophysiol, 81*(4), 1802-1809.

Ries, C. R., & Puil, E. (1999c). Mechanism of anesthesia revealed by shunting actions of isoflurane on thalamocortical neurons. *J Neurophysiol, 81*(4), 1795-1801.

Robson, J. G. (1967). The effects of anesthetic drugs on cortical units. *Anesthesiology, 28*(1), 144-154.

Rubinov, M., & Sporns, O. (2010). Complex network measures of brain connectivity: uses and interpretations. [Research Support, Non-U.S. Gov't]. *Neuroimage, 52*(3), 1059-1069. doi: 10.1016/j.neuroimage.2009.10.003

Rudolph, U., & Antkowiak, B. (2004). Molecular and neuronal substrates for general anaesthetics. [Research Support, Non-U.S. Gov't Review]. *Nat Rev Neurosci, 5*(9), 709-720. doi: 10.1038/nrn1496

Sakata, S., & Harris, K. D. (2009). Laminar structure of spontaneous and sensory-evoked population activity in auditory cortex. *Neuron, 64*(3), 404-418.

Sanderson, K. J., Dreher, B., & Gayer, N. (1991). Prosencephalic connections of striate and extrastriate areas of rat visual cortex. *Exp Brain Res, 85*(2), 324-334.

Santarelli, R., Carraro, L., Conti, G., Capello, M., Plourde, G., & Arslan, E. (2003). Effects of isoflurane on auditory middle latency (MLRs) and steady-state (SSRs) responses recorded from the temporal cortex of the rat. *Brain Res, 973*(2), 240-251.

Sceniak, M. P., & Maciver, M. B. (2006). Cellular actions of urethane on rat visual cortical neurons in vitro. *J Neurophysiol, 95*(6), 3865-3874. doi: 10.1152/jn.01196.2005

Schiff, N. D., Ribary, U., Moreno, D. R., Beattie, B., Kronberg, E., Blasberg, R., . . . Plum, F. (2002). Residual cerebral activity and behavioural fragments can remain in the persistently vegetative brain. *Brain, 125*(Pt 6), 1210-1234.

Schneidman, E., Berry, M. J., 2nd, Segev, R., & Bialek, W. (2006). Weak pairwise correlations imply strongly correlated network states in a neural population. [Research Support, N.I.H., Extramural Research Support, Non-U.S. Gov't]. *Nature, 440*(7087), 1007-1012. doi: 10.1038/nature04701

Schrouff, J., Perlbarg, V., Boly, M., Marrelec, G., Boveroux, P., Vanhaudenhuyse, A., . . . Benali, H. (2011). Brain functional integration decreases during propofol-induced loss of consciousness. [Research Support, Non-U.S. Gov't]. *Neuroimage, 57*(1), 198-205. doi: 10.1016/j.neuroimage.2011.04.020

Schumacher, J. W., Schneider, D. M., & Woolley, S. M. (2011). Anesthetic state modulates excitability but not spectral tuning or neural discrimination in single auditory midbrain neurons. [Comparative Study Research Support, N.I.H., Extramural Research Support, U.S. Gov't, Non-P.H.S.]. *J Neurophysiol, 106*(2), 500-514. doi: 10.1152/jn.01072.2010

Schwender, D., Klasing, S., Madler, C., Poppel, E., & Peter, K. (1993). Mid-latency auditory evoked potentials during ketamine anaesthesia in humans. *Br J Anaesth, 71*(5), 629-632.

Seymour, J. P., & Kipke, D. R. (2007). Neural probe design for reduced tissue encapsulation in CNS. [Research Support, N.I.H., Extramural Research Support, U.S. Gov't, Non-P.H.S.]. *Biomaterials, 28*(25), 3594-3607. doi: 10.1016/j.biomaterials.2007.03.024

Sherman, S. M. (2001). Tonic and burst firing: dual modes of thalamocortical relay. [Research Support, U.S. Gov't, P.H.S. Review]. *Trends Neurosci, 24*(2), 122-126.

Shew, W. L., Yang, H., Petermann, T., Roy, R., & Plenz, D. (2009). Neuronal avalanches imply maximum dynamic range in cortical networks at criticality. [In Vitro Research Support, N.I.H., Intramural Research Support, Non-U.S. Gov't Research Support, U.S. Gov't, Non-P.H.S.]. *J Neurosci, 29*(49), 15595-15600. doi: 10.1523/JNEUROSCI.3864-09.2009

Shew, W. L., Yang, H., Yu, S., Roy, R., & Plenz, D. (2011). Information capacity and transmission are maximized in balanced cortical networks with neuronal avalanches. *J Neurosci, 31*(1), 55-63.

Shlens, J., Field, G. D., Gauthier, J. L., Grivich, M. I., Petrusca, D., Sher, A., . . . Chichilnisky, E. J. (2006). The structure of multi-neuron firing patterns in primate retina. *J Neurosci, 26*(32), 8254-8266.

Singer, W. (1999). Neuronal synchrony: a versatile code for the definition of relations? [Research Support, U.S. Gov't, P.H.S. Review]. *Neuron, 24*(1), 49-65, 111-125.

Singer, W., & Gray, C. M. (1995). Visual feature integration and the temporal correlation hypothesis. [Comparative Study Research Support, Non-U.S. Gov't Research Support, U.S.

Gov't, Non-P.H.S. Research Support, U.S. Gov't, P.H.S. Review]. *Annu Rev Neurosci, 18*, 555-586. doi: 10.1146/annurev.ne.18.030195.003011

Sleigh, J. W., Olofsen, E., Dahan, A., de Goede, J., & Steyn-Ross, A. (2001). Entropies of the EEG: The effects of general anaesthesia. *5th International Conference on Memory, Awareness and Consciousness*.

Sleigh, J. W., Vizuete, J. A., Voss, L., Steyn-Ross, A., Steyn-Ross, M., Marcuccilli, C. J., & Hudetz, A. G. (2009). The electrocortical effects of enflurane: experiment and theory. *Anesth Analg, 109*(4), 1253-1262.

Smith, T. L., & Zapala, D. (1998). The evolution of the auditory midlatency response in evaluating unconscious memory formation during general anesthesia. *Crna, 9*(2), 44-49.

Sporns, O., Tononi, G., & Edelman, G. M. (2000). Connectivity and complexity: the relationship between neuroanatomy and brain dynamics. *Neural Netw, 13*(8-9), 909-922.

Stam, C. J., Jones, B. F., Nolte, G., Breakspear, M., & Scheltens, P. (2007). Small-world networks and functional connectivity in Alzheimer's disease. *Cereb Cortex, 17*(1), 92-99. doi: 10.1093/cercor/bhj127

Steriade, M. (2004). Slow-wave sleep: serotonin, neuronal plasticity, and seizures. [Research Support, Non-U.S. Gov't Research Support, U.S. Gov't, P.H.S. Review]. *Arch Ital Biol, 142*(4), 359-367.

Steriade, M., Amzica, F., & Contreras, D. (1994). Cortical and thalamic cellular correlates of electroencephalographic burst-suppression. [Research Support, Non-U.S. Gov't]. *Electroencephalogr Clin Neurophysiol, 90*(1), 1-16.

Steriade, M., Amzica, F., & Contreras, D. (1996). Synchronization of fast (30-40 Hz) spontaneous cortical rhythms during brain activation. [Research Support, Non-U.S. Gov't]. *J Neurosci, 16*(1), 392-417.

Steriade, M., Contreras, D., & Amzica, F. (1994). Synchronized sleep oscillations and their paroxysmal developments. [Research Support, Non-U.S. Gov't Review]. *Trends Neurosci, 17*(5), 199-208.

Steriade, M., & Timofeev, I. (2003). Neuronal plasticity in thalamocortical networks during sleep and waking oscillations. [Research Support, Non-U.S. Gov't Research Support, U.S. Gov't, P.H.S. Review]. *Neuron, 37*(4), 563-576.

Stevenson, I. H., Rebesco, J. M., Hatsopoulos, N. G., Haga, Z., Miller, L. E., & Kording, K. P. (2009). Bayesian inference of functional connectivity and network structure from spikes. [Research Support, N.I.H., Extramural]. *IEEE Trans Neural Syst Rehabil Eng, 17*(3), 203-213. doi: 10.1109/TNSRE.2008.2010471

Stevenson, I. H., Rebesco, J. M., Miller, L. E., & Kording, K. P. (2008). Inferring functional connections between neurons. [Review]. *Curr Opin Neurobiol, 18*(6), 582-588. doi: 10.1016/j.conb.2008.11.005

Super, H., Spekreijse, H., & Lamme, V. A. (2001). Two distinct modes of sensory processing observed in monkey primary visual cortex (V1). [Research Support, Non-U.S. Gov't]. *Nat Neurosci, 4*(3), 304-310. doi: 10.1038/85170

Szabo-Salfay, O., Palhalmi, J., Szatmari, E., Barabas, P., Szilagyi, N., & Juhasz, G. (2001). The electroretinogram and visual evoked potential of freely moving rats. [Research Support, Non-U.S. Gov't]. *Brain Res Bull, 56*(1), 7-14.

Tamas, G., Buhl, E. H., & Somogyi, P. (1997). Fast IPSPs elicited via multiple synaptic release sites by different types of GABAergic neurone in the cat visual cortex. [Research Support, Non-U.S. Gov't]. *J Physiol, 500 (Pt 3)*, 715-738.

Tang, A., Jackson, D., Hobbs, J., Chen, W., Smith, J. L., Patel, H., . . . Beggs, J. M. (2008). A maximum entropy model applied to spatial and temporal correlations from cortical networks in vitro. *J Neurosci, 28*(2), 505-518.

Thomson, A. M., West, D. C., Hahn, J., & Deuchars, J. (1996). Single axon IPSPs elicited in pyramidal cells by three classes of interneurones in slices of rat neocortex. [In Vitro Research Support, Non-U.S. Gov't]. *J Physiol, 496 (Pt 1)*, 81-102.

Tigwell, D. A., & Sauter, J. (1992). On the use of isofluorane as an anaesthetic for visual neurophysiology. *Exp Brain Res, 88*(1), 224-228.

Tononi, G. (2004). An information integration theory of consciousness. *BMC Neurosci, 5*, 42. doi: 10.1186/1471-2202-5-42

Tononi, G. (2005). Consciousness, information integration, and the brain. [Review]. *Prog Brain Res, 150*, 109-126. doi: 10.1016/S0079-6123(05)50009-8

Tononi, G. (2010). Information integration: its relevance to brain function and consciousness. [Research Support, Non-U.S. Gov't]. *Arch Ital Biol, 148*(3), 299-322.

Tononi, G., & Edelman, G. M. (1998a). Consciousness and complexity. *Science, 282*(5395), 1846-1851.

Tononi, G., & Edelman, G. M. (1998b). Consciousness and the integration of information in the brain. *Adv Neurol, 77*, 245-279; discussion 279-280.

Tononi, G., Edelman, G. M., & Sporns, O. (1998). Complexity and coherency: integrating information in the brain. *Trends Cogn Sci, 2*(12), 474-484.

Tononi, G., & Massimini, M. (2008). Why does consciousness fade in early sleep? [Research Support, N.I.H., Extramural]. *Ann N Y Acad Sci, 1129*, 330-334. doi: 10.1196/annals.1417.024

Tononi, G., McIntosh, A. R., Russell, D. P., & Edelman, G. M. (1998). Functional clustering: identifying strongly interactive brain regions in neuroimaging data. [Clinical Trial Research Support, Non-U.S. Gov't]. *Neuroimage, 7*(2), 133-149. doi: 10.1006/nimg.1997.0313

Tononi, G., Sporns, O., & Edelman, G. M. (1994). A measure for brain complexity: relating functional segregation and integration in the nervous system. *Proc Natl Acad Sci U S A, 91*(11), 5033-5037.

Truccolo, W., Eden, U. T., Fellows, M. R., Donoghue, J. P., & Brown, E. N. (2005). A point process framework for relating neural spiking activity to spiking history, neural ensemble, and extrinsic covariate effects. [Research Support, Non-U.S. Gov't Research Support, U.S. Gov't, Non-P.H.S. Research Support, U.S. Gov't, P.H.S.]. *J Neurophysiol, 93*(2), 1074-1089. doi: 10.1152/jn.00697.2004

Usrey, W. M., Reppas, J. B., & Reid, R. C. (1998). Paired-spike interactions and synaptic efficacy of retinal inputs to the thalamus. *Nature, 395*(6700), 384-387.

Uzzell, V. J., & Chichilnisky, E. J. (2004). Precision of spike trains in primate retinal ganglion cells. *J Neurophysiol, 92*(2), 780-789.

van der Togt, C., Spekreijse, H., & Super, H. (2005). Neural responses in cat visual cortex reflect state changes in correlated activity. [Comparative Study]. *Eur J Neurosci, 22*(2), 465-475. doi: 10.1111/j.1460-9568.2005.04237.x

Van Hooff, J. C., De Beer, N. A., Brunia, C. H., Cluitmans, P. J., Korsten, H. H., Tavilla, G., & Grouls, R. (1995). Information processing during cardiac surgery: an event related potential study. *Electroencephalogr Clin Neurophysiol, 96*(5), 433-452.

Vanluchene, A. L., Struys, M. M., Heyse, B. E., & Mortier, E. P. (2004). Spectral entropy measurement of patient responsiveness during propofol and remifentanil. A comparison with the bispectral index. [Clinical Trial Comparative Study Randomized Controlled Trial Research Support, Non-U.S. Gov't]. *Br J Anaesth, 93*(5), 645-654. doi: 10.1093/bja/aeh251

Vanluchene, A. L., Vereecke, H., Thas, O., Mortier, E. P., Shafer, S. L., & Struys, M. M. (2004). Spectral entropy as an electroencephalographic measure of anesthetic drug effect: a comparison with bispectral index and processed midlatency auditory evoked response. [Clinical Trial Comparative Study Randomized Controlled Trial]. *Anesthesiology, 101*(1), 34-42.

Veselis, R., Reinsel, R., Feshchenko, V., Beattie, B., & Akhurst, T. (2004). Auditory rCBF covariation with word rate during drug-induced sedation and unresponsiveness: a H2015 PET study. *Brain Cogn, 54*(2), 142-144.

Veselis, R. A., Reinsel, R. A., Beattie, B. J., Mawlawi, O. R., Feshchenko, V. A., DiResta, G. R., . . . Blasberg, R. G. (1997). Midazolam changes cerebral blood flow in discrete brain regions: an H2(15)O positron emission tomography study. *Anesthesiology, 87*(5), 1106-1117.

Villeneuve, C., Caudrillier, A., Ordener, C., Pizzinat, N., Parini, A., & Mialet-Perez, J. (2009). Dose-dependent activation of distinct hypertrophic pathways by serotonin in cardiac cells. [Research Support, Non-U.S. Gov't]. *Am J Physiol Heart Circ Physiol, 297*(2), H821-828. doi: 10.1152/ajpheart.00345.2009

Villeneuve, M. Y., & Casanova, C. (2003). On the use of isoflurane versus halothane in the study of visual response properties of single cells in the primary visual cortex. *J Neurosci Methods, 129*(1), 19-31.

Vizuete, J. A., Pillay, S., Diba, K., Ropella, K. M., & Hudetz, A. G. (2012). Monosynaptic functional connectivity in cerebral cortex during wakefulness and under graded levels of anesthesia. [Original Research]. *Frontiers in Integrative Neuroscience, 6*. doi: 10.3389/fnint.2012.00090

von Stein, A., Chiang, C., & Konig, P. (2000). Top-down processing mediated by interareal synchronization. [Research Support, Non-U.S. Gov't]. *Proc Natl Acad Sci U S A, 97*(26), 14748-14753. doi: 10.1073/pnas.97.26.14748

Vyazovskiy, V. V., Cirelli, C., & Tononi, G. (2011). Electrophysiological correlates of sleep homeostasis in freely behaving rats. [Research Support, N.I.H., Extramural Research Support, Non-U.S. Gov't Review]. *Prog Brain Res, 193*, 17-38. doi: 10.1016/B978-0-444-53839-0.00002-8

Vyazovskiy, V. V., Olcese, U., Hanlon, E. C., Nir, Y., Cirelli, C., & Tononi, G. (2011). Local sleep in awake rats. [Research Support, N.I.H., Extramural Research Support, U.S. Gov't, Non-P.H.S.]. *Nature, 472*(7344), 443-447. doi: 10.1038/nature10009

Wang, J. X., & Zochowski, M. (2012). Interactions of excitatory and inhibitory feedback topologies in facilitating pattern separation and retrieval. *Neural Comput, 24*(1), 32-59.

Watanabe, S. (1960). Information Theoretical Analysis of Multivariate Correlation. *IBM Journal of Research and Development, 4*, 66-82.

Winslow, B. D., Christensen, M. B., Yang, W. K., Solzbacher, F., & Tresco, P. A. (2010). A comparison of the tissue response to chronically implanted Parylene-C-coated and uncoated planar silicon microelectrode arrays in rat cortex. [Research Support, N.I.H., Extramural]. *Biomaterials, 31*(35), 9163-9172. doi: 10.1016/j.biomaterials.2010.05.050

Yizhar, O., Fenno, L. E., Prigge, M., Schneider, F., Davidson, T. J., O'Shea, D. J., . . . Deisseroth, K. (2011). Neocortical excitation/inhibition balance in information processing and social dysfunction. *Nature, 477*(7363), 171-178.

Yoshitani, K., Kawaguchi, M., Takahashi, M., Kitaguchi, K., & Furuya, H. (2003). Plasma propofol concentration and EEG burst suppression ratio during normothermic cardiopulmonary bypass. [Clinical Trial Randomized Controlled Trial]. *Br J Anaesth, 90*(2), 122-126.

Yu, S., Huang, D., Singer, W., & Nikolic, D. (2008). A small world of neuronal synchrony. *Cereb Cortex, 18*(12), 2891-2901.

Zhou, J., Liu, X., Song, W., Yang, Y., Zhao, Z., Ling, F., . . . Li, S. J. (2011). Specific and nonspecific thalamocortical functional connectivity in normal and vegetative states. [Research Support, N.I.H., Extramural Research Support, Non-U.S. Gov't]. *Conscious Cogn, 20*(2), 257-268. doi: 10.1016/j.concog.2010.08.003

Zilles, K., & Wree, A. (1995). Cortex: Areal and Laminar Structure. In G. Paxinos (Ed.), *The Rat Nervous System* (2nd ed., pp. 649-685). San Diego: Academic Press.